

## Author's Response

### Response to Referee #1:

We are grateful for the reviewer's comments. Those comments are all valuable and helpful for improving our paper. Our response to the comments and changes to the manuscript are included below. We repeat the specific points raised by the reviewer in bold font, followed by our response in italic font. The pages numbers and lines mentioned below are consistent with those in the Atmospheric Chemistry and Physics Discussions (ACPD) paper.

**While this paper uses sound techniques, cites relevant literature, and is well written, it ultimately fails to address relevant scientific questions within the scope of ACP. The reviewer admits this work presents two new pieces of novel data. First, the ERH of the studied mixtures was dependent on the molar ratio of oxalic acid to ammonium sulfate. Second, aqueous reactions in drying droplets of OA and AS can produce nonhygroscopic products. This novel data, however, is not discussed within the framework of our current knowledge in the literature. Thus, it is not clear to the reviewer how atmospherically relevant or important this work is.**

**This reviewer suggests two pathways to increase the efficacy of this work. In one pathway, the authors would expand this work especially the discussion section. Currently, the discussion section contains no effort to frame the results of this study into the existing literature. In the second pathway, the authors could to submit to a technical journal that does not emphasize "studies with general implications for atmospheric science." In addition to this very general comment, several general comments and specific comments are outlined below. Technical comments, however, are omitted in this initial review.**

**Reply:** *According to the reviewer's suggestion, we expand relevant discussion on our results within the framework of the existing literature to highlight atmospheric relevance.*

*The observed efflorescence relative humidity (ERH) for mixed droplets was dependent on the molar ratio of oxalic acid to ammonium sulfate. The mixed OA/AS droplets with an OIR of 1:3 are observed to effloresce completely at  $34.4 \pm 2.0\%$  RH relative to ERH of pure AS ( $44.3 \pm 2.5\%$ ) or OA ( $77 \pm 2.5\%$ ). It can be seen that AS as a major fraction of the particle does not promote the heterogeneous nucleation of OA. Meanwhile, the crystallization of AS is also influenced due to the presence of OA. The similar phenomenon was also observed for malonic acid/ammonium sulfate*

1 mixtures with minor organic content (Braban and Abbatt, 2004; Parsons et al., 2004). Braban and  
2 Abbatt (2004) found that the ERH of malonic acid/ammonium sulfate mixed particles was  
3 considerably decreased compared to that of pure ammonium sulfate for mass fractions of malonic  
4 acid less than 0.3. They concluded that the presence of ammonium sulfate in the supersaturated  
5 droplet could exert the extra barrier to nucleation of malonic acid crystals rather than play the role  
6 of a heterogeneous nucleation site. As for 1:3 OA/AS mixed droplets, ammonium sulfate may also  
7 inhibit the nucleation of oxalic acid at relatively high RH. With decreasing RH, aqueous oxalic acid  
8 could enhance the viscosity of the droplet due to hydrogen bond interactions (Mikhailov et al.,  
9 2009), thus limiting the nucleation of ammonium sulfate and resulting in a lower ERH with respect  
10 to the value of pure AS (Parsons et al., 2004). In the case of mixed OA/AS droplets with an OIR of  
11 1:1 and 3:1, the  $\text{NH}_4\text{HC}_2\text{O}_4$  formed at ~75% RH upon dehydration likely acts as a heterogeneous  
12 nucleus for crystallization of other components, which increases full efflorescence point of mixed  
13 particles. One study indicated that Aldrich humic acid sodium salt (NaHA) could also promote the  
14 ERH of ammonium sulfate (Badger et al., 2006). Similar to oxalic acid, succinic acid and adipic  
15 acid have a high deliquescence point and low solubility. However, it has been found that the  
16 efflorescence point of ammonium sulfate in mixed particles is not elevated even when the content of  
17 succinic acid or adipic acid is not less than 50% by mass or mole fractions (Ling and Chan, 2008;  
18 Yeung et al., 2009; Laskina et al., 2015). In contrast to ammonium sulfate particles containing  
19 succinic acid or adipic acid, our results suggest that the addition of oxalic acid into ammonium  
20 sulfate droplets may trigger partial and full crystallisation of aerosols at relatively higher RH upon  
21 dehydration due to  $\text{NH}_4\text{HC}_2\text{O}_4$  product acting as an effective nucleus.

22 During the deliquescence process, the OA/AS mixed particles with an OIR of 1:3 and 1:1 exhibit  
23 a slightly lower deliquescence point than that of pure ammonium sulfate, consistent with previous  
24 observations of effects of crystalline oxalic acid on deliquescence transition of ammonium sulfate  
25 (Brooks et al., 2002; Wise et al., 2003; Jing et al., 2016). It should be noted that prior literature  
26 result also showed that continuous or smooth water uptake from low RH was observed for particles  
27 composed of AS and OA with a mass ratio of 1.5:1 due to the fact that after drying processing  
28 oxalic acid existing in an amorphous or liquid-like state prevented nucleation of ammonium sulfate  
29 even under dry conditions (Prenni et al., 2003). In the present study, water uptake by the OA/AS  
30 mixed particles at high RH upon hydration is dramatically lower than that upon dehydration and

1 significantly decreased with elevated OA content. This phenomenon distinguishes from hygroscopic  
2 characteristic of typical water-soluble mixtures in literatures. It has been found that hydration  
3 growth curve and dehydration growth curve are typically merged above deliquescence point for  
4 mixed systems containing inorganic salts and water-soluble organic compounds (Choi and Chan,  
5 2002; Chan and Chan, 2003; Gysel et al., 2004; Clegg and Seinfeld, 2006; Sjogren et al., 2007;  
6 Pope et al., 2010; Ghorai et al., 2014; Estillore et al., 2016). In this study, Raman spectra and  
7 micrograph (Figure R2 (d)) suggest the presence of solid  $\text{NH}_4\text{HC}_2\text{O}_4$  and residual solid OA at high  
8 RH should be responsible for the decreased water uptake during the hydration process. In contrast,  
9 Prenni et al. (2003) reported that the hygroscopic growth of OA/AS mixed particles remained  
10 unchanged at 90% RH with OA mass fraction ranging from 0.01 to 0.4. In addition, they also found  
11 that water uptake after deliquescence was well described by the model method assuming complete  
12 dissolution of OA in aqueous phase as well as no interactions between OA and AS, which was also  
13 observed by Jing et al. (2016) using the HTDMA. The previous HTDMA studies for OA/AS mixed  
14 particles indicate no composition change and no specific interactions existing between OA and AS  
15 (Prenni et al., 2003; Jing et al., 2016). However, it should be noted that the HTDMA studies did not  
16 perform measurements for the dehydration process such that aerosols underwent rapid drying on  
17 the time scale of seconds, i.e., the total residence time for transformation of droplets into dry  
18 particles in the drying section of HTDMA is typically tens of seconds (Prenni et al., 2003; Jing et al.,  
19 2016), much shorter than that (10 ~ 12 h) in our study. In the HTDMA experiments, the  
20 combination of faster drying and smaller particles with submicron size implies that the aqueous  
21 phase obtained higher supersaturations than in our present study (Rosenoern et al., 2008), leading  
22 to less dissociation of oxalic acid and thus less  $\text{HC}_2\text{O}_4^-$  formed in the droplets as well as the  
23 inhibited formation of  $\text{NH}_4\text{HC}_2\text{O}_4$ . The fast evaporation of water from the surface of an aqueous  
24 droplet upon rapid drying could result in a higher surface concentration of solutes than the slow  
25 drying process (Treuel et al., 2011). The higher surface concentration of oxalic acid corresponds to  
26 less formation and hence decreased supersaturation of  $\text{HC}_2\text{O}_4^-$ . Due to the dependence of  
27 nucleation rate on the extent of supersaturation, it can be expected that the nucleation of  
28  $\text{NH}_4\text{HC}_2\text{O}_4$  is suppressed within OA/AS mixed droplets undergoing rapid drying.

29 The prior hygroscopic studies suggest that crystallization of internally mixed ammonium  
30 sulfate/dicarboxylic acid particles may lead to the formation of trace organic salt. Lightstone et al.

1 (2000) estimated that approximately 2% of the initial succinic acid may form ammoniated succinate  
2 within mixed ammonium nitrate/succinic acid particles during the efflorescence process. Ling and  
3 Chan (2008) inferred that crystallization of ammonium sulfate/succinic acid droplets likely  
4 generated metastable organic salt based on change in the Raman peak form of succinic acid.  
5 Braban and Abbatt (2004) reported that  $\text{NH}_4\text{HSO}_4$  and ammoniated malonate were likely generated  
6 upon crystallization of mixed ammonium sulfate/malonic acid particles. However, due to the trace  
7 amount of organic salt below Raman or infrared detection limit, they found no apparent influence of  
8 organic salt formed upon dehydration on the water uptake or phase change of mixed particles. In  
9 contrast, our results indicate that the chemical processing upon drying of droplets containing OA  
10 and AS influences efflorescence transition and water uptake of mixed aerosols during the humidity  
11 cycle by modifying particulate component.

12 Our results highlight the atmospheric importance of dicarboxylic acid–ammonium sulfate  
13 interactions in aerosol aqueous chemistry. Such chemical processing upon drying of aerosols  
14 comprised of organic acid/ $(\text{NH}_4)_2\text{SO}_4$  mixtures may enhance the acidity of aqueous phase in the  
15 intermediate RH due to the transformation of  $(\text{NH}_4)_2\text{SO}_4$  into  $\text{NH}_4\text{HSO}_4$ . These experiments also  
16 imply that the chemical reaction between aqueous  $(\text{NH}_4)_2\text{SO}_4$  and oxalic acid upon slow  
17 dehydration is a possible formation pathway for the low-volatility oxalate in ambient particles,  
18 which could enhance partitioning of dicarboxylic acids to aqueous particles with the presence of  
19 ammonium sulfate (Yli-Juuti et al., 2013; Hakkinen et al., 2014). It has been reported that the  
20 aerosol aqueous processing within organic acid/AS mixtures partly contributes to enhanced  
21 loadings of secondary organic aerosol (SOA) from biogenic precursors (Hoyle et al., 2011).  
22 Compared to aqueous processing such as condensed phase acid-catalyzed reactions relevant to  
23 formation of organosulfates, the contribution of other aerosol processing containing organic salt  
24 formation to SOA burden likely becomes important under less acidic condition. Formation of  
25 low-solubility organic salts from aqueous processing within aerosols alters particle-phase  
26 component and thus modifies aerosol's hygroscopicity, optical properties and chemical reactivity.  
27 Our findings provide fundamental insight into effects of drying conditions (drying rate or time) on  
28 formation of organic salt from reactions of organic acids with inorganic salts in particle phase  
29 under ambient RH conditions. Overall, a better understanding of the chemical interactions between  
30 species in a multicomponent system during the humidity cycle is critical for the accurate modeling

1 *efforts of aerosol phase behavior in thermodynamic models.*

2 ***Related changes in the revised manuscript:***

3 ***Page 11 line 18-29: The sentences from line 18 to 29 are replaced by “The observed efflorescence***  
4 *relative humidity (ERH) for mixed droplets was dependent on the molar ratio of oxalic acid to*  
5 *ammonium sulfate. The mixed OA/AS droplets with an OIR of 1:3 are observed to effloresce*  
6 *completely at  $34.4 \pm 2.0\%$  RH relative to ERH of pure AS ( $44.3 \pm 2.5\%$ ) or OA ( $77 \pm 2.5\%$ ). It can*  
7 *be seen that AS as a major fraction of the particle does not promote the heterogeneous nucleation of*  
8 *OA. Meanwhile, the crystallization of AS is also influenced due to the presence of OA. The similar*  
9 *phenomenon was also observed for malonic acid/ammonium sulfate mixtures with minor organic*  
10 *content (Braban and Abbatt, 2004; Parsons et al., 2004). Braban and Abbatt (2004) found that the*  
11 *ERH of malonic acid/ammonium sulfate mixed particles was considerably decreased compared to*  
12 *that of pure ammonium sulfate for mass fractions of malonic acid less than 0.3. They concluded that*  
13 *the presence of ammonium sulfate in the supersaturated droplet could exert the extra barrier to*  
14 *nucleation of malonic acid crystals rather than play the role of a heterogeneous nucleation site. As*  
15 *for 1:3 OA/AS mixed droplets, ammonium sulfate may also inhibit the nucleation of oxalic acid at*  
16 *relatively high RH. With decreasing RH, aqueous oxalic acid could enhance the viscosity of the*  
17 *droplet due to hydrogen bond interactions (Mikhailov et al., 2009), thus limiting the nucleation of*  
18 *ammonium sulfate and resulting in a lower ERH with respect to the value of pure AS (Parsons et al.,*  
19 *2004). In the case of mixed OA/AS droplets with an OIR of 1:1 and 3:1, the  $\text{NH}_4\text{HC}_2\text{O}_4$  formed at*  
20  *$\sim 75\%$  RH upon dehydration likely acts as a heterogeneous nucleus for crystallization of other*  
21 *components, which increases full efflorescence point of mixed particles. One study indicated that*  
22 *Aldrich humic acid sodium salt (NaHA) could also promote the ERH of ammonium sulfate (Badger*  
23 *et al., 2006). Similar to oxalic acid, succinic acid and adipic acid have a high deliquescence point*  
24 *and low solubility. However, it has been found that the efflorescence point of ammonium sulfate in*  
25 *mixed particles is not elevated even when the content of succinic acid or adipic acid is not less than*  
26 *50% by mass or mole fractions (Ling and Chan, 2008; Yeung et al., 2009; Laskina et al., 2015). In*  
27 *contrast to ammonium sulfate particles containing succinic acid or adipic acid, our results suggest*  
28 *that the addition of oxalic acid into ammonium sulfate droplets may trigger partial and full*  
29 *crystallisation of aerosols at relatively higher RH upon dehydration due to  $\text{NH}_4\text{HC}_2\text{O}_4$  product*  
30 *acting as an effective nucleus.*

1 During the deliquescence process, the OA/AS mixed particles with an OIR of 1:3 and 1:1 exhibit a  
2 slightly lower deliquescence point than that of pure ammonium sulfate, consistent with previous  
3 observations of effects of crystalline oxalic acid on deliquescence transition of ammonium sulfate  
4 (Brooks et al., 2002; Wise et al., 2003; Jing et al., 2016). It should be noted that prior literature  
5 result also showed that continuous or smooth water uptake from low RH was observed for particles  
6 composed of AS and OA with a mass ratio of 1.5:1 due to the fact that after drying processing  
7 oxalic acid existing in an amorphous or liquid-like state prevented nucleation of ammonium sulfate  
8 even under dry conditions (Prenni et al., 2003). In the present study, water uptake by the OA/AS  
9 mixed particles at high RH upon hydration is dramatically lower than that upon dehydration and  
10 significantly decreased with elevated OA content. This phenomenon distinguishes from hygroscopic  
11 characteristic of typical water-soluble mixtures in literatures. It has been found that hydration  
12 growth curve and dehydration growth curve are typically merged above deliquescence point for  
13 mixed systems containing inorganic salts and water-soluble organic compounds (Choi and Chan,  
14 2002; Chan and Chan, 2003; Gysel et al., 2004; Clegg and Seinfeld, 2006; Sjogren et al., 2007;  
15 Pope et al., 2010; Ghorai et al., 2014; Estillore et al., 2016). In this study, Raman spectra and  
16 micrograph suggest the presence of solid  $\text{NH}_4\text{HC}_2\text{O}_4$  and residual solid OA at high RH should be  
17 responsible for the decreased water uptake during the hydration process. In contrast, Prenni et al.  
18 (2003) reported that the hygroscopic growth of OA/AS mixed particles remained unchanged at 90%  
19 RH with OA mass fraction ranging from 0.01 to 0.4. In addition, they also found that water uptake  
20 after deliquescence was well described by the model method assuming complete dissolution of OA  
21 in aqueous phase as well as no interactions between OA and AS, which was also observed by Jing  
22 et al. (2016) using the HTDMA. The previous HTDMA studies for OA/AS mixed particles indicate  
23 no composition change and no specific interactions existing between OA and AS (Prenni et al.,  
24 2003; Jing et al., 2016). However, it should be noted that the HTDMA studies did not perform  
25 measurements for the dehydration process such that aerosols underwent rapid drying on the time  
26 scale of seconds, i.e., the total residence time for transformation of droplets into dry particles in the  
27 drying section of HTDMA is typically tens of seconds (Prenni et al., 2003; Jing et al., 2016), much  
28 shorter than that (10 ~ 12 h) in our study. In the HTDMA experiments, the combination of faster  
29 drying and smaller particles with submicron size implies that the aqueous phase obtained higher  
30 supersaturations than in our present study (Rosenoern et al., 2008), leading to less dissociation of

1 oxalic acid and thus less  $\text{HC}_2\text{O}_4^-$  formed in the droplets as well as the inhibited formation of  
2  $\text{NH}_4\text{HC}_2\text{O}_4$ . The fast evaporation of water from the surface of an aqueous droplet upon rapid drying  
3 could result in a higher surface concentration of solutes than the slow drying process (Treuel et al.,  
4 2011). The higher surface concentration of oxalic acid corresponds to less formation and hence  
5 decreased supersaturation of  $\text{HC}_2\text{O}_4^-$ . Due to the dependence of nucleation rate on the extent of  
6 supersaturation, it can be expected that the nucleation of  $\text{NH}_4\text{HC}_2\text{O}_4$  is suppressed within OA/AS  
7 mixed droplets undergoing rapid drying.”.

8 **Page 12 line 20: “4 Conclusions” is changed into “4 Conclusions and atmospheric implications”.**

9 **Page 13 line 9-20: This paragraph is replaced by** “The prior hygroscopic studies suggest that  
10 crystallization of internally mixed ammonium sulfate/dicarboxylic acid particles may lead to the  
11 formation of trace organic salt. Lightstone et al. (2000) estimated that approximately 2% of the  
12 initial succinic acid may form ammoniated succinate within mixed ammonium nitrate/succinic acid  
13 particles during the efflorescence process. Ling and Chan (2008) inferred that crystallization of  
14 ammonium sulfate/succinic acid droplets likely generated metastable organic salt based on change  
15 in the Raman peak form of succinic acid. Braban and Abbatt (2004) reported that  $\text{NH}_4\text{HSO}_4$  and  
16 ammoniated malonate were likely generated upon crystallization of mixed ammonium  
17 sulfate/malonic acid particles. However, due to the trace amount of organic salt below Raman or  
18 infrared detection limit, they found no apparent influence of organic salt formed upon dehydration  
19 on the water uptake or phase change of mixed particles. In contrast, our results indicate that the  
20 chemical processing upon drying of droplets containing OA and AS influences efflorescence  
21 transition and water uptake of mixed aerosols during the humidity cycle by modifying particulate  
22 component.

23 Our results highlight the atmospheric importance of dicarboxylic acid–ammonium sulfate  
24 interactions in aerosol aqueous chemistry. Such chemical processing upon drying of aerosols  
25 comprised of organic acid/ $(\text{NH}_4)_2\text{SO}_4$  mixtures may enhance the acidity of aqueous phase in the  
26 intermediate RH due to the transformation of  $(\text{NH}_4)_2\text{SO}_4$  into  $\text{NH}_4\text{HSO}_4$ . These experiments also  
27 imply that the chemical reaction between aqueous  $(\text{NH}_4)_2\text{SO}_4$  and oxalic acid upon slow  
28 dehydration is a possible formation pathway for the low-volatility oxalate in ambient particles,  
29 which could enhance partitioning of dicarboxylic acids to aqueous particles with the presence of  
30 ammonium sulfate (Yli-Juuti et al., 2013; Hakkinen et al., 2014). It has been reported that the

1 aerosol aqueous processing within organic acid/AS mixtures partly contributes to enhanced  
2 loadings of secondary organic aerosol (SOA) from biogenic precursors (Hoyle et al., 2011).  
3 Compared to aqueous processing such as condensed phase acid-catalyzed reactions relevant to  
4 formation of organosulfates, the contribution of other aerosol processing containing organic salt  
5 formation to SOA burden likely becomes important under less acidic condition. Formation of  
6 low-solubility organic salts from aqueous processing within aerosols alters particle-phase  
7 component and thus modifies aerosol's hygroscopicity, optical properties and chemical reactivity.  
8 Our findings provide fundamental insight into effects of drying conditions (drying rate or time) on  
9 formation of organic salt from reactions of organic acids with inorganic salts in particle phase  
10 under ambient RH conditions. Overall, a better understanding of the chemical interactions between  
11 species in a multicomponent system during the humidity cycle is critical for the accurate modeling  
12 efforts of aerosol phase behavior in thermodynamic models.”

13

#### 14 **General Comments:**

15 **Page 5, line 15: In general, the reviewer feels that the authors did not take advantage of the**  
16 **microscope in their experiment. Do the authors know the contact angle of water on their**  
17 **Raman substrate? If so, the physical growth factor of a spherically equivalent drop could be**  
18 **determined; this measurement would greatly increase confidence in the spectroscopic growth**  
19 **factor measurement. A physical growth factor measurement could also help explain the**  
20 **low-RH results in Figure 4b, where it is unclear if OA shrinks when it transitions from its**  
21 **dihydrate form to its anhydrous form.**

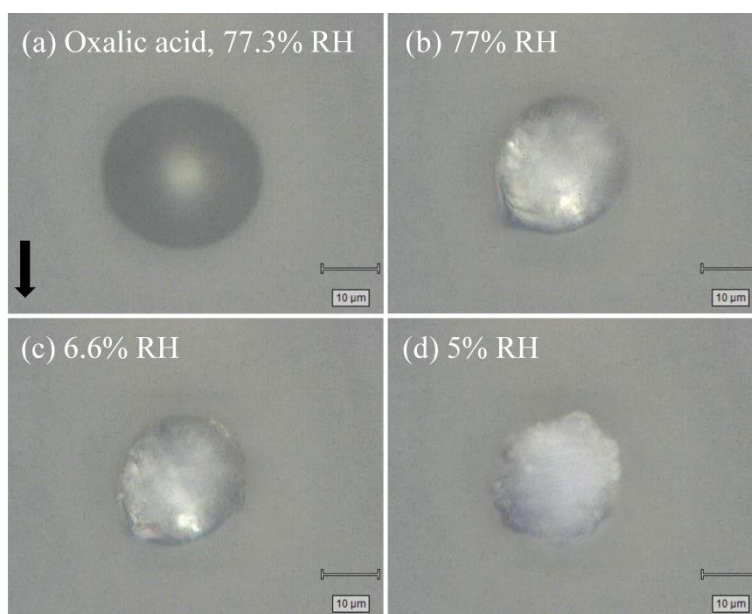
22 **Reply:** *We thank the reviewer for the suggestion. We have no contact angle data for droplets on our*  
23 *substrate. In fact, the spectra methods have been proved to be sensitive and reliable for study of*  
24 *aerosol hygroscopicity including phase transition and water uptake (Cziczo et al., 1997; Cziczo and*  
25 *Abbatt, 2000; Braban et al., 2003; Brooks et al., 2003; Braban and Abbatt, 2004; Garland et al.,*  
26 *2005; Badger et al., 2006; Liu et al., 2008a; Liu et al., 2008b; Yeung et al., 2009; Minambres et al.,*  
27 *2010; Yeung and Chan, 2010; Ghorai et al., 2014; Laskina et al., 2015; Zawadowicz et al., 2015).*  
28 *As shown in Figure R1, the size of an effloresced oxalic acid particle remains almost unchanged*  
29 *when oxalic acid dihydrate is transformed into anhydrous form. However, the corresponding Raman*  
30 *spectra indicate the changes in crystal water of OA particles. The other studies using infrared*



1 spectrometer and vapor sorption analyzer also observed the transition between anhydrous oxalic  
2 acid and dihydrate based on water mass changes in solid OA particles (Braban et al., 2003; Ma et  
3 al., 2013). Since size-based hygroscopicity is sensitive to particle geometry, the size growth factor of  
4 particles without a compact structure may not reflect the actual changes in water mass due to  
5 morphology effects (Piens et al., 2016). It seems that the structure of anhydrous OA particle is not  
6 as compact as that of dihydrate, seen in Figure R1. Thus, the loss of crystal water results in no  
7 obvious change in particle size. Overall, the spectra method is advantageous for probing the  
8 hygroscopic behavior of atmospheric particles with irregular morphologies.

9 **Related changes included in the revised manuscript:**

10 Figure R1 is supplemented in the main text. **Page 9, Line 5:** “As shown in Fig. 4b, the measured  
11 ERH of OA is  $77 \pm 2.5\%$  RH” is revised to “As shown in Fig. 6b and 8, the measured ERH of OA is  
12  $77 \pm 2.5\%$  RH”. **Page 9, Line 26:** We add “It seems that the structure of anhydrous OA particle is  
13 not as compact as that of dihydrate, seen in Fig. 8. Thus, the loss of crystal water results in no  
14 obvious change in particle size.”.



15  
16 **Figure R1.** Optical micrographs of the oxalic acid particle at (a) 77.3% RH, (b) 77% RH, (c) 6.6% RH and  
17 (d) 5% RH during the dehydration process, respectively.

18

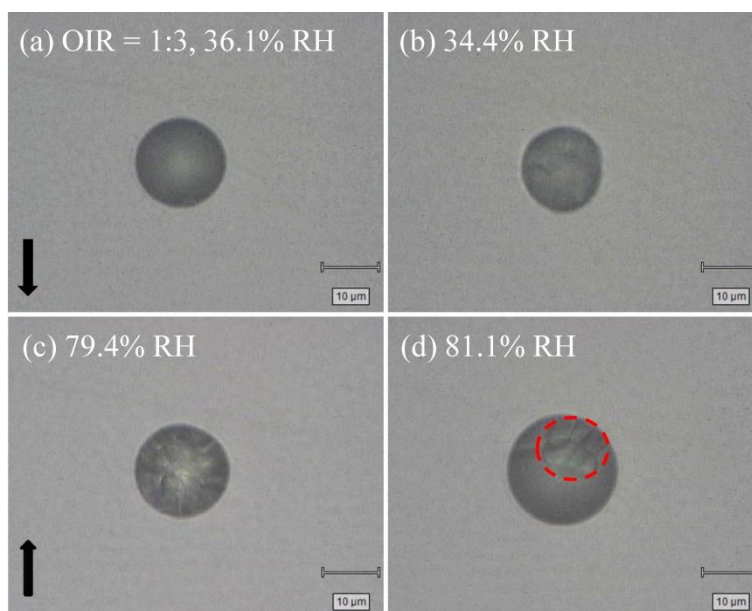
19 **Page 7, Line 1: Do the authors have an image of the effloresced particle to affirm that the**  
20  **$\nu(\text{SO}_4^{2-})$  peak shift corresponds with a hygroscopic phase change?**

21 **Reply:** As seen in Figure R2, the crystallization of OA/AS particles ( $\text{OIR} = 1:3$ ) occurs at 34.4% RH,

1 corresponding with the Raman peak shift of  $\nu_s(\text{SO}_4^{2-})$  from  $979\text{ cm}^{-1}$  to  $974\text{ cm}^{-1}$  at the same RH.  
2 The previous studies have also applied the abrupt shift in characteristic peak position to indicate  
3 phase transition of ammonium sulfate during the hygroscopic process (Braban and Abbatt, 2004;  
4 Ling and Chan, 2008; Yeung et al., 2009; Yeung and Chan, 2010).

5 **Related changes in the revised manuscript:**

6 Figure R2 is supplemented in the main text. **Page 7, Line 1: The sentence “At 34.4% RH, the shift**  
7 **of  $\nu_s(\text{SO}_4^{2-})$  peak from  $979\text{ cm}^{-1}$  to  $974\text{ cm}^{-1}$  indicates the crystallization of AS.” is revised to “At**  
8 **34.4% RH, the shift of  $\nu_s(\text{SO}_4^{2-})$  peak from  $979\text{ cm}^{-1}$  to  $974\text{ cm}^{-1}$  indicates the crystallization of AS,**  
9 **as also seen in Fig. 10b.”. **Page 8, Line 6: We add “The previous studies have also applied the**  
10 **abrupt shift in characteristic peak position to indicate phase transition of ammonium sulfate during**  
11 **the hygroscopic process (Braban and Abbatt, 2004; Ling and Chan, 2008; Yeung et al., 2009).”.****



12  
13 **Figure R2.** Optical micrographs of mixed oxalic acid/ammonium sulfate particles (OIR = 1:3) at phase  
14 change points. Dehydration: (a) 36.1% RH and (b) 34.4% RH. Hydration: (c) 79.4% RH and (d) 81.1% RH.  
15 In the image (d), the visual solid in aqueous phase is marked with a red dashed circle.

16

17 **Page 8, Line 2: Since multiple components are crystallizing, can the authors take advantage of**  
18 **the high spatial resolution of Raman microscopy to tell if there is a spatial distribution of**  
19 **chemicals? These results would explain if components are efflorescing in specific order and,**  
20 **consequently, if effloresced components are heterogeneously nucleating other components.**

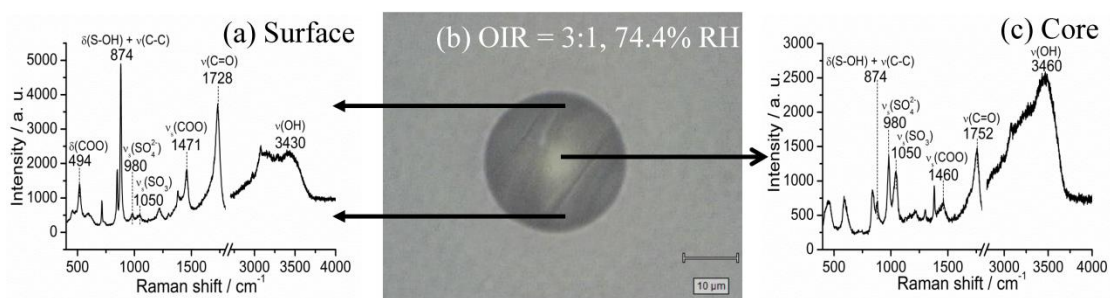
21 **Reply:** We appreciate the reviewer’s suggestion. Figure R3 presents the spatial distribution of

1 chemicals within mixed OA/AS (OIR = 3:1) particles at 74.4% RH. The characteristic peak of 980  
 2  $\text{cm}^{-1}$ , 1050  $\text{cm}^{-1}$  and 1471  $\text{cm}^{-1}$  is assigned to  $\text{SO}_4^{2-}$ ,  $\text{HSO}_4^-$  and  $\text{HC}_2\text{O}_4^-$ , respectively. The sharp  
 3 absorption at 874  $\text{cm}^{-1}$  and obvious peak at 1471  $\text{cm}^{-1}$  indicate the abundant content of  $\text{NH}_4\text{HC}_2\text{O}_4$ .  
 4 The comparison of characteristic peaks between inner and outer phase reveals that the major  
 5 component on the surface of a mixed OA/AS (OIR = 3:1) particle is  $\text{NH}_4\text{HC}_2\text{O}_4$ . In contrast to the  
 6 surface, the obvious features of 980  $\text{cm}^{-1}$  and 1050  $\text{cm}^{-1}$  at the core of the particle suggest that  
 7  $(\text{NH}_4)_2\text{SO}_4$  and  $\text{NH}_4\text{HSO}_4$  mainly exist in the inner aqueous phase. During the dehydration process,  
 8 crystalline  $\text{NH}_4\text{HC}_2\text{O}_4$  in the outer phase acts as heterogeneous nucleus, leading to the  
 9 crystallization of oxalic acid dihydrate,  $(\text{NH}_4)_2\text{SO}_4$  and  $\text{NH}_4\text{HSO}_4$  in the inner phase.

10 **Related changes in the revised manuscript:**

11 Figure R3 is added into the text. **Page 11, Line 4: The sentence “The crystallization of  $\text{NH}_4\text{HC}_2\text{O}_4$**   
 12 **may act as crystallization nuclei for  $\text{NH}_4^+$ ,  $\text{HSO}_4^-$  and OA in the mixed droplets to form  $\text{NH}_4\text{HSO}_4$**   
 13 **crystal and oxalic acid dihydrate.” is changed into “Figure 12 presents the spatial distribution of**  
 14 **chemicals within mixed OA/AS (OIR = 3:1) particles at 74.4% RH. The characteristic peak of 980**  
 15  **$\text{cm}^{-1}$ , 1050  $\text{cm}^{-1}$  and 1471  $\text{cm}^{-1}$  is assigned to  $\text{SO}_4^{2-}$ ,  $\text{HSO}_4^-$  and  $\text{HC}_2\text{O}_4^-$ , respectively. The sharp**  
 16 **absorption at 874  $\text{cm}^{-1}$  and obvious peak at 1471  $\text{cm}^{-1}$  indicate the abundant content of  $\text{NH}_4\text{HC}_2\text{O}_4$ .**  
 17 **The comparison of characteristic peaks between inner and outer phase reveals that the major**  
 18 **component on the surface of a mixed OA/AS (OIR = 3:1) particle is  $\text{NH}_4\text{HC}_2\text{O}_4$ . In contrast to the**  
 19 **surface, the obvious features of 980  $\text{cm}^{-1}$  and 1050  $\text{cm}^{-1}$  at the core of the particle suggest that**  
 20  **$(\text{NH}_4)_2\text{SO}_4$  and  $\text{NH}_4\text{HSO}_4$  mainly exist in the inner aqueous phase. During the dehydration process,**  
 21 **crystalline  $\text{NH}_4\text{HC}_2\text{O}_4$  in the outer phase acts as the heterogeneous nucleus, leading to the**  
 22 **crystallization of oxalic acid dihydrate,  $(\text{NH}_4)_2\text{SO}_4$  and  $\text{NH}_4\text{HSO}_4$  in the inner phase.”.**

23



24

25 **Figure R3.** The spatial distribution of chemicals within the mixed oxalic acid/ammonium sulfate (OIR = 3:1)  
 26 particle at 74.4% RH upon dehydration. (a) Raman spectrum acquired on the surface showing the shell  
 27 mainly consisting of  $\text{NH}_4\text{HC}_2\text{O}_4$ . (b) Optical micrograph of a partially effloresced droplet composed of oxalic

1 acid/ammonium sulfate (OIR = 3:1) mixtures at 74.4% RH upon dehydration. (c) Raman spectrum obtained  
2 at the core of the droplet showing the liquid phase dominated by oxalic acid and ammonium sulfate.

3

4 **Specific Comments:**

5 **Page 3, Line 16: Is there a reference for the reactions of organic acids with mineral salts,  
6 chloride salts, nitrate salts, and ammonium and amines?**

7 **Reply:** We add several references for the reactions of organic acids with mineral salts, chloride  
8 salts, nitrate salts, and ammonium and amines.

9 **Related changes in the revised manuscript:**

10 **Page 3, Line 13:** The sentence “Field measurements have observed the formation of low-volatility  
11 organic salts in atmospheric particles due to the reactions of organic acids with mineral salts,  
12 chloride salts, nitrate salts, ammonium and amines.” is revised to “Field measurements have  
13 observed the formation of low-volatility organic salts in atmospheric particles due to the reactions  
14 of organic acids with mineral salts, chloride salts, nitrate salts, ammonium and amines (Sullivan  
15 and Prather, 2007; Laskin et al., 2012; Wang and Laskin, 2014; Smith et al., 2010).”

16

17 **Page 4, Line 21: What was the dry diameter of these particles?**

18 **Reply:** The dry diameter of these particles after efflorescence ranged from 10 to 20  $\mu\text{m}$ .

19 **Related changes in the revised manuscript:**

20 **Page 4, Line 21:** We add the sentence “The dry size of these particles after efflorescence ranged  
21 from 10 to 20  $\mu\text{m}$ .”

22

23 **Page 5, Line 8: What is the numerical aperture of the 50x objective?**

24 **Reply:** The numerical aperture of the 50 $\times$  objective is 0.75.

25 **Related changes in the revised manuscript:**

26 **Page 5, Line 8:** The sentence “Then, spectroscopic measurements were made on droplets observed  
27 by using the Leica DMLM microscope with a 50 $\times$  objective lens.” is revised to “Then,  
28 spectroscopic measurements were made on droplets observed by using the Leica DMLM microscope  
29 with a 50 $\times$  objective (0.75 numerical aperture).”

30

1 **Page 5, Line 12: Why was 40 minutes chosen for the equilibration time? Do the authors have**  
2 **spectral evidence of this equilibration (perhaps from the area under the OH water peak?)**

3 **Reply:** *We used intensity ratios of the water peak ( $3430\text{ cm}^{-1}$ ) to the sulfate peak ( $980\text{ cm}^{-1}$ ) to test*  
4 *the equilibration time of droplets at the given RH. Our results indicate that the intensity ratios*  
5 *remain almost unchanged after 20 min for a  $30\text{ }\mu\text{m}$  droplet. To achieve the full equilibration for*  
6 *particles with size range studied, the droplets were equilibrated with water vapor at an ambient*  
7 *relative humidity for about 40 min. After 40 min, the Raman spectra in our experiment remain*  
8 *constant. Yeung et al. (2009) determined the equilibration time of at least 15 min for a  $20\text{-}30\text{ }\mu\text{m}$*   
9 *ammonium sulfate droplet based on the intensity ratio of the water peak ( $3430\text{ cm}^{-1}$ ) to the sulfate*  
10 *peak ( $980\text{ cm}^{-1}$ ) obtained by micro-Raman spectroscopy. They also found the equilibration time was*  
11 *longer for the same-sized particles containing organics.*

12 **Related changes in the revised manuscript:**

13 **Page 5, Line 11:** *The sentence “The particles were equilibrated with water vapor at a given RH for*  
14 *about 40 min.” is revised to “The particles were equilibrated with water vapor at a given RH for*  
15 *about 40 min, during which the intensity ratios of the water peak ( $3430\text{ cm}^{-1}$ ) to the sulfate peak*  
16 *( $980\text{ cm}^{-1}$ ) remained constant.”.*

17  
18 **Page 7, Line 3: It is unclear from the text if  $874\text{ cm}^{-1}$  corresponds to only  $\text{HSO}_4^-$  or both  $\text{HSO}_4^-$**   
19 **and  $\text{HC}_2\text{O}_4^-$ . The reviewer suggests this be clarified.**

20 **Reply:** *The band centred at  $874\text{ cm}^{-1}$  is contributed by both  $\text{HSO}_4^-$  and  $\text{HC}_2\text{O}_4^-$ . Dawson et al. (1986)*  
21 *reported the absorption of vibrational mode ( $\delta(\text{S-OH})$ ) of  $\text{HSO}_4^-$  ion from  $\text{NH}_4\text{HSO}_4$  occurred at*  
22  *$869\text{ cm}^{-1}$ . The absorption of  $\nu(\text{C-C})$  of  $\text{HC}_2\text{O}_4^-$  in crystal was observed at  $879\text{ cm}^{-1}$  by Shippey*  
23 *(1979). Thus, the peak centred at  $874\text{ cm}^{-1}$  corresponds to both  $\text{HSO}_4^-$  and  $\text{HC}_2\text{O}_4^-$ .*

24 **Related changes in the revised manuscript:**

25 **Page 7, Line 3:** *The sentence “A new band centered at  $874\text{ cm}^{-1}$  corresponds to the vibrational*  
26 *mode ( $\delta(\text{S-OH})$ ) of  $\text{HSO}_4^-$  ion from  $\text{NH}_4\text{HSO}_4$  and the  $\text{HC}_2\text{O}_4^-$  ion vibrating (Irish and Chen, 1970;*  
27 *Dawson et al., 1986; Villepin and Novak, 1971; Shippey, 1979),” is revised to “A new band*  
28 *centered at  $874\text{ cm}^{-1}$  corresponds to combination bands of the vibrational mode ( $\delta(\text{S-OH})$ ) of  $\text{HSO}_4^-$*   
29 *ion from  $\text{NH}_4\text{HSO}_4$  (Dawson et al., 1986) and  $\text{HC}_2\text{O}_4^-$  ion vibrating (Shippey, 1979)”.*

30

1 **Page 9, Line 11: The statement “likely due to drop size, substrate, and experimental methods”**  
2 **is vague. Can the authors be more specific about the cause of OA’s high ERH in this study?**

3 **Reply:** *We thank the reviewer for the helpful suggestion. After revisiting our explanation carefully,*  
4 *we give a more specific one as follows. The discrepancy on the ERH of OA compared to that*  
5 *reported by Peng et al. (2001) is likely due to the effects of substrate and sample purity. The size of*  
6 *dry particles ranging from 10 to 20  $\mu\text{m}$  in our experiment is consistent with observation using EDB*  
7 *by Peng et al. (2001), which eliminates the influence of particle size. The substrate supporting*  
8 *droplets may promote the heterogeneous nucleation of oxalic acid while the levitated droplets in*  
9 *EDB study can avoid induced nucleation by the substrate. Ghorai et al. (2014) also reported the*  
10 *potential effects of substrate on the efflorescence transition of NaCl/dicarboxylic acid mixed*  
11 *particles. In addition, The OA purity in our study is 99.0% lower than that of 99.5% in study by*  
12 *Peng et al. (2001). Thus, trace amounts of impurities in OA droplets acting as a heterogeneous*  
13 *nucleus could contribute to crystallization and result in a higher ERH of OA. Due to the effects of*  
14 *substrate and sample purity, the heterogeneous nucleation should be responsible for the*  
15 *discrepancy on the observed ERH of OA.*

16 **Corresponding changes in the revised manuscript:**

17 **Page 9, Line 10-17:** *the sentence “The discrepancies between this study and that by Peng et al.*  
18 *(2001) is likely due to the effects of droplet size, substrate and experimental method. According to*  
19 *classical nucleation theory, the probability of the formation of the critical nucleus is proportional to*  
20 *the particle volume (Martin, 2000; Parsons et al., 2006). Considering that the droplet size in our*  
21 *study was approximately 1-2 times larger than that observed by Peng et al. (2001), the droplets*  
22 *deposited on the substrate in our experiment may promote the heterogeneous nucleation while the*  
23 *levitated droplets using EDB can dispel the heterogeneous nucleation. Thus, the ERH of OA*  
24 *obtained in our study is higher than the observation of Peng et al. (2001).” is revised to “The*  
25 *discrepancy on the ERH of OA compared to that reported by Peng et al. (2001) is likely due to the*  
26 *effects of substrate and sample purity. The size of dry particles ranging from 10 to 20  $\mu\text{m}$  in our*  
27 *experiment is consistent with observation using EDB by Peng et al. (2001), which eliminates the*  
28 *influence of particle size. The substrate supporting droplets may promote the heterogeneous*  
29 *nucleation of oxalic acid while the levitated droplets in EDB study can avoid induced nucleation by*  
30 *the substrate. Ghorai et al. (2014) also reported the potential effects of substrate on the*

1 *efflorescence transition of NaCl/dicarboxylic acid mixed particles. In addition, The OA purity in our*  
2 *study is 99.0% lower than that of 99.5% in study by Peng et al. (2001). Thus, trace amounts of*  
3 *impurities in OA droplets acting as a heterogeneous nucleus could contribute to crystallization and*  
4 *result in a higher ERH of OA. Due to the effects of substrate and sample purity, the heterogeneous*  
5 *nucleation should be responsible for the discrepancy on the observed ERH of OA.”.*

6  
7 **Page 9, Line 16: Do the authors believe that 77% is the true ERH of OA, or that**  
8 **heterogeneous nucleation is occurring? If the latter, the reviewer suggests that the authors**  
9 **refrain from using the phrase “ERH of OA” hereafter.**

10 **Reply:** *Yes, we determine that 77% is the true ERH of pure OA from the Raman spectra. As stated in*  
11 *the initial manuscript, the Raman spectra indicated OA droplet was converted into oxalic acid*  
12 *dihydrate at 77% RH during the dehydration process. In addition, the images of OA particles upon*  
13 *dehydration also show the full efflorescence of OA occurs at 77% RH, seen in Figure R1.*

14 **Related changes in the revised manuscript:**

15 *Figure R1 is supplemented in the main text. Page 9, Line 5: “As shown in Fig. 4b, the measured*  
16 *ERH of OA is  $77 \pm 2.5\%$  RH” is revised to “As shown in Fig. 6b and 8, the measured ERH of OA is*  
17  *$77 \pm 2.5\%$  RH”.*

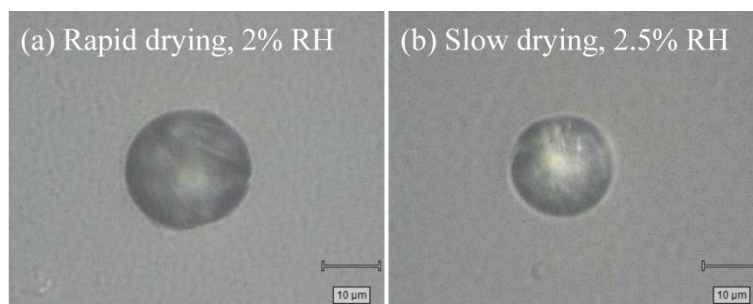
18  
19 **Page 12, Line 8: Do the “rapidly-dried” particles look physically different than the**  
20 **“regularly-dried” particles? Furthermore, do the rapidly-dried particles have a different**  
21 **ERH? This could help discern the underlying mechanism of efflorescence.**

22 **Reply:** *As shown in Figure R4, the morphology of rapidly-dried OA/AS particles with equal molar*  
23 *ratio could not be obviously distinguished from that of regularly-dried particles. However, the*  
24 *spectra evidence has shown significant compositional difference between the two kinds of particles.*  
25 *We observed one-step efflorescence of rapidly-dried particles (1:1, molar ratio) occurred at  $47\% \pm$*   
26  *$2.5\%$  RH, compared to the two-step efflorescence of slowly-dried particles occurring at 75% and*  
27 *44.3% RH, respectively.*

28 **Related changes in the revised manuscript:**

29 **Page 12, line 2: We add “We observed one-step efflorescence of rapidly-dried particles (1:1, molar**  
30 **ratio) occurred at  $47\% \pm 2.5\%$  RH, compared to the two-step efflorescence of slowly-dried particles**

1 occurring at 75% and 44.3% RH, respectively.”



2

3 **Figure R4.** Optical micrographs of equal molar mixed oxalic acid/ammonium sulfate particles after (a)  
4 rapid drying at 2% RH and (b) slow drying at 2.5% RH, respectively.

5

## 6 **References**

- 7 Badger, C. L., George, I., Griffiths, P. T., Braban, C. F., Cox, R. A., and Abbatt, J. P. D.: Phase transitions and  
8 hygroscopic growth of aerosol particles containing humic acid and mixtures of humic acid and ammonium  
9 sulphate, *Atmos. Chem. Phys.*, 6, 755-768, 2006.
- 10 Braban, C. F., Carroll, M. F., Styler, S. A., and Abbatt, J. P. D.: Phase transitions of malonic and oxalic acid  
11 aerosols, *J. Phys. Chem. A*, 107, 6594-6602, 10.1021/jp034483f, 2003.
- 12 Braban, C. F., and Abbatt, J. P. D.: A study of the phase transition behavior of internally mixed ammonium  
13 sulfate-malonic acid aerosols, *Atmos. Chem. Phys.*, 4, 1451-1459, 2004.
- 14 Brooks, S. D., Wise, M. E., Cushing, M., and Tolbert, M. A.: Deliquescence behavior of organic/ammonium  
15 sulfate aerosol, *Geophys. Res. Lett.*, 29, 10.1029/2002gl014733, 2002.
- 16 Brooks, S. D., Garland, R. M., Wise, M. E., Prenni, A. J., Cushing, M., Hewitt, E., and Tolbert, M. A.: Phase  
17 changes in internally mixed maleic acid/ammonium sulfate aerosols, *J. Geophys. Res.- Atmos.*, 108,  
18 10.1029/2002jd003204, 2003.
- 19 Chan, M. N., and Chan, C. K.: Hygroscopic properties of two model humic-like substances and their  
20 mixtures with inorganics of atmospheric importance, *Environ. Sci. Technol.*, 37, 5109-5115,  
21 10.1021/es034272o, 2003.
- 22 Choi, M. Y., and Chan, C. K.: The effects of organic species on the hygroscopic behaviors of inorganic  
23 aerosols, *Environ. Sci. Technol.*, 36, 2422-2428, 10.1021/es0113293, 2002.
- 24 Clegg, S. L., and Seinfeld, J. H.: Thermodynamic models of aqueous solutions containing inorganic  
25 electrolytes and dicarboxylic acids at 298.15 K. 1. The acids as nondissociating components, *J. Phys. Chem.*  
26 *A*, 110, 5692-5717, 10.1021/jp056149k, 2006.



1 Cziczo, D. J., Nowak, J. B., Hu, J. H., and Abbatt, J. P. D.: Infrared spectroscopy of model tropospheric  
2 aerosols as a function of relative humidity: Observation of deliquescence and crystallization, *J. Geophys.*  
3 *Res.- Atmos.*, 102, 18843-18850, 10.1029/97jd01361, 1997.

4 Cziczo, D. J., and Abbatt, J. P. D.: Infrared observations of the response of NaCl, MgCl<sub>2</sub>, NH<sub>4</sub>HSO<sub>4</sub>, and  
5 NH<sub>4</sub>NO<sub>3</sub> aerosols to changes in relative humidity from 298 to 238 K, *J. Phys. Chem. A*, 104, 2038-2047,  
6 10.1021/jp9931408, 2000.

7 Dawson, B. S. W., Irish, D. E., and Toogood, G. E.: Vibrational spectral studies of solutions at elevated  
8 temperatures and pressures. 8. A Raman spectral study of ammonium hydrogen sulfate solutions and the  
9 HSO<sub>4</sub><sup>-</sup>-SO<sub>4</sub><sup>2-</sup> equilibrium, *J. Phys. Chem.*, 90, 334-341, doi: 10.1021/j100274a027, 1986.

10 Estillore, A. D., Hettiyadura, A. P. S., Qin, Z., Leckrone, E., Wombacher, B., Humphry, T., Stone, E. A., and  
11 Grassian, V. H.: Water uptake and hygroscopic growth of organosulfate aerosol, *Environ. Sci. Technol.*, 50,  
12 4259-4268, 10.1021/acs.est.5b05014, 2016.

13 Garland, R. M., Wise, M. E., Beaver, M. R., DeWitt, H. L., Aiken, A. C., Jimenez, J. L., and Tolbert, M. A.:  
14 Impact of palmitic acid coating on the water uptake and loss of ammonium sulfate particles, *Atmos. Chem.*  
15 *Phys.*, 5, 1951-1961, 2005.

16 Ghorai, S., Wang, B., Tivanski, A., and Laskin, A.: Hygroscopic properties of internally mixed particles  
17 composed of NaCl and water-soluble organic acids, *Environ. Sci. Technol.*, 48, 2234-2241,  
18 10.1021/es404727u, 2014.

19 Gysel, M., Weingartner, E., Nyeki, S., Paulsen, D., Baltensperger, U., Galambos, I., and Kiss, G.:  
20 Hygroscopic properties of water-soluble matter and humic-like organics in atmospheric fine aerosol, *Atmos.*  
21 *Chem. Phys.*, 4, 35-50, 2004.

22 Hakkinen, S. A. K., McNeill, V. F., and Riipinen, I.: Effect of Inorganic Salts on the Volatility of Organic  
23 Acids, *Environ. Sci. Technol.*, 48, 13718-13726, 10.1021/es5033103, 2014.

24 Hoyle, C. R., Boy, M., Donahue, N. M., Fry, J. L., Glasius, M., Guenther, A., Hallar, A. G., Hartz, K. H.,  
25 Petters, M. D., Petaja, T., Rosenoern, T., and Sullivan, A. P.: A review of the anthropogenic influence on  
26 biogenic secondary organic aerosol, *Atmos. Chem. Phys.*, 11, 321-343, 10.5194/acp-11-321-2011, 2011.

27 Jing, B., Tong, S., Liu, Q., Li, K., Wang, W., Zhang, Y., and Ge, M.: Hygroscopic behavior of  
28 multicomponent organic aerosols and their internal mixtures with ammonium sulfate, *Atmos. Chem. Phys.*,  
29 16, 4101-4118, 10.5194/acp-16-4101-2016, 2016.

30 Laskin, A., Moffet, R. C., Gilles, M. K., Fast, J. D., Zaveri, R. A., Wang, B., Nigge, P., and Shutthanandan,

1 J.: Tropospheric chemistry of internally mixed sea salt and organic particles: Surprising reactivity of NaCl  
2 with weak organic acids, *J. Geophys. Res.*, 117, D15302, doi: 10.1029/2012jd017743, 2012.

3 Laskina, O., Morris, H. S., Grandquist, J. R., Qiu, Z., Stone, E. A., Tivanski, A. V., and Grassian, V. H.: Size  
4 matters in the water uptake and hygroscopic growth of atmospherically relevant multicomponent aerosol  
5 particles, *J. Phys. Chem. A*, 119, 4489-4497, 10.1021/jp510268p, 2015.

6 Lightstone, J. M., Onasch, T. B., Imre, D., and Oatis, S.: Deliquescence, efflorescence, and water activity in  
7 ammonium nitrate and mixed ammonium nitrate/succinic acid microparticles, *J. Phys. Chem. A*, 104,  
8 9337-9346, 10.1021/jp002137h, 2000.

9 Ling, T. Y., and Chan, C. K.: Partial crystallization and deliquescence of particles containing ammonium  
10 sulfate and dicarboxylic acids, *Journal of Geophysical Research: Atmospheres*, 113, 1-15, doi:  
11 10.1029/2008JD009779, 2008.

12 Liu, Y., Yang, Z., Desyaterik, Y., Gassman, P. L., Wang, H., and Laskin, A.: Hygroscopic behavior of  
13 substrate-deposited particles studied by micro-FT-IR spectroscopy and complementary methods of particle  
14 analysis, *Anal. Chem.*, 80, 633-642, 10.1021/ac701638r, 2008a.

15 Liu, Y. J., Zhu, T., Zhao, D. F., and Zhang, Z. F.: Investigation of the hygroscopic properties of  $\text{Ca}(\text{NO}_3)_2$   
16 and internally mixed  $\text{Ca}(\text{NO}_3)_2/\text{CaCO}_3$  particles by micro-Raman spectrometry, *Atmos. Chem. Phys.*, 8,  
17 7205-7215, 2008b.

18 Ma, Q., Ma, J., Liu, C., Lai, C., and He, H.: Laboratory study on the hygroscopic behavior of external and  
19 internal C2-C4 dicarboxylic acid-NaCl mixtures, *Environ. Sci. Technol.*, 47, 10381-10388, doi:  
20 10.1021/es4023267, 2013.

21 Mikhailov, E., Vlasenko, S., Martin, S. T., Koop, T., and Pöschl, U.: Amorphous and crystalline aerosol  
22 particles interacting with water vapor: conceptual framework and experimental evidence for restructuring,  
23 phase transitions and kinetic limitations, *Atmos. Chem. Phys.*, 9, 9491-9522, 2009.

24 Minambres, L., Sanchez, M. N., Castano, F., and Basterretxea, F. J.: Hygroscopic Properties of Internally  
25 Mixed Particles of Ammonium Sulfate and Succinic Acid Studied by Infrared Spectroscopy, *J. Phys. Chem.*  
26 *A*, 114, 6124-6130, 10.1021/jp101149k, 2010.

27 Parsons, M. T., Knopf, D. A., and Bertram, A. K.: Deliquescence and crystallization of ammonium sulfate  
28 particles internally mixed with water-soluble organic compounds, *J. Phys. Chem. A*, 108, 11600-11608,  
29 10.1021/jp0462862, 2004.

30 Pope, F. D., Dennis-Smith, B. J., Griffiths, P. T., Clegg, S. L., and Cox, R. A.: Studies of Single Aerosol

1 Particles Containing Malonic Acid, Glutaric Acid, and Their Mixtures with Sodium Chloride. I. Hygroscopic  
2 Growth, *J. Phys. Chem. A*, 114, 5335-5341, 10.1021/jp100059k, 2010.

3 Prenni, A. J., De Mott, P. J., and Kreidenweis, S. M.: Water uptake of internally mixed particles containing  
4 ammonium sulfate and dicarboxylic acids, *Atmos. Environ.*, 37, 4243-4251,  
5 10.1016/s1352-2310(03)00559-4, 2003.

6 Rosenoern, T., Schlenker, J. C., and Martin, S. T.: Hygroscopic growth of multicomponent aerosol particles  
7 influenced by several cycles of relative humidity, *J. Phys. Chem. A*, 112, 2378-2385, 10.1021/jp0771825,  
8 2008.

9 Shippey, T. A.: Very strong hydrogen bonding: single crystal raman studies of potassium hydrogen oxalate  
10 and sodium hydrogen oxalate monohydrate, *J. Mol. Struct.*, 57, 1-11, doi: 10.1016/0022-2860(79)80227-6,  
11 1979.

12 Sjogren, S., Gysel, M., Weingartner, E., Baltensperger, U., Cubison, M. J., Coe, H., Zardini, A. A., Marcolli,  
13 C., Krieger, U. K., and Peter, T.: Hygroscopic growth and water uptake kinetics of two-phase aerosol  
14 particles consisting of ammonium sulfate, adipic and humic acid mixtures, *J. Aerosol Sci.*, 38, 157-171,  
15 10.1016/j.jaerosci.2006.11.005, 2007.

16 Smith, J. N., Barsanti, K. C., Friedli, H. R., Ehn, M., Kulmala, M., Collins, D. R., Scheckman, J. H.,  
17 Williams, B. J., and McMurry, P. H.: Observations of ammonium salts in atmospheric nanoparticles and  
18 possible climatic implications, *Proc. Nat. Acad. Sci. U. S. A*, 107, 6634-6639, 10.1073/pnas.0912127107,  
19 2010.

20 Sullivan, R. C., and Prather, K. A.: Investigations of the diurnal cycle and mixing state of oxalic acid in  
21 individual particles in Asian aerosol outflow, *Environ. Sci. Technol.*, 41, 8062-8069, 10.1021/es071134g,  
22 2007.

23 Treuel, L., Sandmann, A., and Zellner, R.: Spatial separation of individual substances in effloresced crystals  
24 of ternary ammonium sulphate/dicarboxylic acid/water aerosols, *ChemPhysChem*, 12, 1109-1117, doi:  
25 10.1002/cphc.201000738, 2011.

26 Wang, B., and Laskin, A.: Reactions between water-soluble organic acids and nitrates in atmospheric  
27 aerosols: Recycling of nitric acid and formation of organic salts, *J. Geophys. Res.*, 119, 3335-3351, doi:  
28 10.1002/2013jd021169, 2014.

29 Wise, M. E., Surratt, J. D., Curtis, D. B., Shilling, J. E., and Tolbert, M. A.: Hygroscopic growth of  
30 ammonium sulfate/dicarboxylic acids, *J. Geophys. Res.- Atmos.*, 108, doi 10.1029/2003jd003775, 2003.

1 Yeung, M. C., Lee, A. K. Y., and Chan, C. K.: Phase transition and hygroscopic properties of internally  
2 mixed ammonium sulfate and adipic acid (AS-AA) particles by optical microscopic imaging and Raman  
3 spectroscopy, *Aerosol Sci. Technol.*, 43, 387–399, doi: 10.1080/02786820802672904, 2009.

4 Yeung, M. C., and Chan, C. K.: Water content and phase transitions in particles of inorganic and organic  
5 species and their mixtures using micro-Raman spectroscopy, *Aerosol Sci. Technol.*, 44, 269-280, doi:  
6 10.1080/02786820903583786, 2010.

7 Yli-Juuti, T., Zardini, A. A., Eriksson, A. C., Hansen, A. M. K., Pagels, J. H., Swietlicki, E., Svenningsson,  
8 B., Glasius, M., Worsnop, D. R., Riipinen, I., and Bilde, M.: Volatility of Organic Aerosol: Evaporation of  
9 Ammonium Sulfate/Succinic Acid Aqueous Solution Droplets, *Environ. Sci. Technol.*, 47, 12123-12130,  
10 10.1021/es401233c, 2013.

11 Zawadowicz, M. A., Proud, S. R., Seppalainen, S. S., and Cziczo, D. J.: Hygroscopic and phase separation  
12 properties of ammonium sulfate/organics/water ternary solutions, *Atmos. Chem. Phys.*, 15, 8975-8986,  
13 10.5194/acp-15-8975-2015, 2015.

14

1  
2  
3  
4  
5  
6  
7  
8  
9  
10  
11  
12  
13  
14  
15  
16  
17  
18  
19  
20  
21  
22  
23  
24  
25  
26  
27  
28  
29  
30  
31

**Response to Referee #2:**

We are grateful for the reviewer's comments. Those comments are all valuable and helpful for improving our paper. Our response to the comments and changes to the manuscript are included below. We repeat the specific points raised by the reviewer in bold font, followed by our response in italic font. The pages numbers and lines mentioned below are consistent with those in the Atmospheric Chemistry and Physics Discussions (ACPD) paper.

**I have many of the same comments as Reviewer #1. In particular revising the discussion section to include atmospheric relevance is crucial before final publication. After revision, I believe the manuscript represents a contribution to scientific progress within the scope of ACP. The scientific approach and methods are valid. I recommend publication in ACP after the authors address the concerns of the reviewers.**

*Reply: We thank the reviewer for the comments. We have supplemented atmospheric relevance as follows.*

***Related changes in the revised manuscript:***

***Page 12 line 20: "4 Conclusions" is changed into "4 Conclusions and atmospheric implications".***

***Page 13 line 9-20: This paragraph is replaced by "The prior hygroscopic studies suggest that crystallization of internally mixed ammonium sulfate/dicarboxylic acid particles may lead to the formation of trace organic salt. Lightstone et al. (2000) estimated that approximately 2% of the initial succinic acid may form ammoniated succinate within mixed ammonium nitrate/succinic acid particles during the efflorescence process. Ling and Chan (2008) inferred that crystallization of ammonium sulfate/succinic acid droplets likely generated metastable organic salt based on change in the Raman peak form of succinic acid. Braban and Abbatt (2004) reported that NH<sub>4</sub>HSO<sub>4</sub> and ammoniated malonate were likely generated upon crystallization of mixed ammonium sulfate/malonic acid particles. However, due to the trace amount of organic salt below Raman or infrared detection limit, they found no apparent influence of organic salt formed upon dehydration on the water uptake or phase change of mixed particles. In contrast, our results indicate that the chemical processing upon drying of droplets containing OA and AS influences efflorescence transition and water uptake of mixed aerosols during the humidity cycle by modifying particulate component.***

*Our results highlight the atmospheric importance of dicarboxylic acid–ammonium sulfate*

1 *interactions in aerosol aqueous chemistry. Such chemical processing upon drying of aerosols*  
2 *comprised of organic acid/(NH<sub>4</sub>)<sub>2</sub>SO<sub>4</sub> mixtures may enhance the acidity of aqueous phase in the*  
3 *intermediate RH due to the transformation of (NH<sub>4</sub>)<sub>2</sub>SO<sub>4</sub> into NH<sub>4</sub>HSO<sub>4</sub>. These experiments also*  
4 *imply that the chemical reaction between aqueous (NH<sub>4</sub>)<sub>2</sub>SO<sub>4</sub> and oxalic acid upon slow*  
5 *dehydration is a possible formation pathway for the low-volatility oxalate in ambient particles,*  
6 *which could enhance partitioning of dicarboxylic acids to aqueous particles with the presence of*  
7 *ammonium sulfate (Yli-Juuti et al., 2013; Hakkinen et al., 2014). It has been reported that the*  
8 *aerosol aqueous processing within organic acid/AS mixtures partly contributes to enhanced*  
9 *loadings of secondary organic aerosol (SOA) from biogenic precursors (Hoyle et al., 2011).*  
10 *Compared to aqueous processing such as condensed phase acid-catalyzed reactions relevant to*  
11 *formation of organosulfates, the contribution of other aerosol processing containing organic salt*  
12 *formation to SOA burden likely becomes important under less acidic condition. Formation of*  
13 *low-solubility organic salts from aqueous processing within aerosols alters particle-phase*  
14 *component and thus modifies aerosol's hygroscopicity, optical properties and chemical reactivity.*  
15 *Our findings provide fundamental insight into effects of drying conditions (drying rate or time) on*  
16 *formation of organic salt from reactions of organic acids with inorganic salts in particle phase*  
17 *under ambient RH conditions. Overall, a better understanding of the chemical interactions between*  
18 *species in a multicomponent system during the humidity cycle is critical for the accurate modeling*  
19 *efforts of aerosol phase behavior in thermodynamic models.”.*

20

21 **1) I was wondering if the authors considered referencing and discussing Amundson et al.**  
22 **(2007) which provides a sulfate/ammonium/oxalic acid phase diagram.**

23 **Reply:** *Thanks for the reviewer's suggestion. Amundson et al. (2007) presented a phase partitioning*  
24 *model (UHAERO) for mixtures of inorganic electrolytes and dicarboxylic acids. They assumed that*  
25 *solid oxalic acid was the only organic solid that could occur in the sulfate/ammonium/oxalic acid*  
26 *system. The limitations on the simple assumption for this system were a result of the lack of*  
27 *available thermodynamic data. Amundson et al. (2007) considered the incorporation of organic*  
28 *salts was crucial in the modeling of hygroscopic properties as well as multistage growth of*  
29 *organic/inorganic mixtures.*

30 **Related changes in the revised manuscript:**

1 **P4, L2: We add** “Due to the lack of available thermodynamic data, the aerosol thermodynamic  
2 models typically assume that upon dehydration dicarboxylic acid could only form organic solid  
3 without the organic salt in the inorganic electrolyte/dicarboxylic acid system (Clegg and Seinfeld,  
4 2006; Amundson et al., 2007). Thus, the incorporation of organic salts formed from interactions  
5 between inorganic salts and organic acids is crucial in the modeling of hygroscopic properties of  
6 mixed organic/inorganic particles.”.

7  
8 **2) Page 4, line 19: How did the authors create 30-40 micron particles with a syringe? This  
9 procedure needs to be explained better. Also, how was the environment of the particles  
10 maintained at 95% RH after injection? Aren't the particles subjected to the environment in  
11 the room which is surely less than 95% RH? Are 30-40 micron particles relevant in the  
12 atmosphere?**

13 **Reply:** *The sample solution was discharged from a syringe. Then, residual solution in the syringe  
14 was pushed rapidly to generate aerosol droplets spraying onto a PTFE substrate fixed to the bottom  
15 of the sample cell. Then, the sample cell was promptly sealed by a transparent polyethylene film.  
16 The RH in the sample cell was regulated by nitrogen streams consisting of a mixture of  
17 water-saturated N<sub>2</sub> and dry N<sub>2</sub> at controlled flow rates. At ~ 95% RH, the droplets with a diameter  
18 of 30~40 microns detected by an optical microscope (50× objective, 0.75 numerical aperture) were  
19 selected to acquire the Raman spectra. The droplet size of 30-40 micron in our study falls into the  
20 size range of cloud droplets (less than 50 μm).*

21 **Related changes in the revised manuscript:**

22 **P4, L19: the sentence** “Using a syringe, droplets from the solutions were injected onto the  
23 polytetrafluorethylene (PTFE) film fixed to the bottom of the sample cell. The diameters of these  
24 droplets ranged from 30 to 40 μm at ~ 95% RH. Then, the sample cell was sealed by a transparent  
25 polyethylene film and the RH in the sample cell was regulated by nitrogen streams consisting of a  
26 mixture of water-saturated N<sub>2</sub> and dry N<sub>2</sub> at controlled flow rates.” **is revised to** “The sample  
27 solution was discharged from a syringe. Then, residual solution in the syringe was pushed rapidly  
28 to generate aerosol droplets spraying onto a polytetrafluorethylene (PTFE) substrate fixed to the  
29 bottom of the sample cell. Then, the sample cell was promptly sealed by a transparent polyethylene  
30 film. The RH in the sample cell was regulated by nitrogen streams consisting of a mixture of

1 water-saturated  $N_2$  and dry  $N_2$  at controlled flow rates. At  $\sim 95\%$  RH, the droplets with a diameter  
2 of 30~40 microns detected by an optical microscope ( $50\times$  objective, 0.75 numerical aperture) were  
3 selected to acquire the Raman spectra. The dry size of these particles after efflorescence ranged  
4 from 10 to 20  $\mu\text{m}$ .”.

5

6 **3) Page 5, line 11: The authors state that the particles were equilibrated with water vapor for**  
7 **40 minutes at a given RH value and they state that the slow dehydration process occurred in**  
8 **the time scale of hours. Why was the time scale of 40 minutes chosen? Why not 30 minutes or**  
9 **60 minutes? Is 40 minutes the amount of time for the Raman spectrum to remain constant?**

10 **Reply:** We used intensity ratios of the water peak ( $3430\text{ cm}^{-1}$ ) to the sulfate peak ( $980\text{ cm}^{-1}$ ) to test  
11 the equilibration time of droplets at the given RH. Our results indicate that the intensity ratios  
12 remain almost unchanged after 20 min for a 30  $\mu\text{m}$  droplet. To achieve the full equilibration for  
13 particles with size range studied, the droplets were equilibrated with water vapor at an ambient  
14 relative humidity for about 40 min. After 40 min, the Raman spectra in our experiment remain  
15 constant. Yeung et al. (2009) determined the equilibration time of at least 15 min for a 20-30  $\mu\text{m}$   
16 ammonium sulfate droplet based on the intensity ratio of the water peak ( $3430\text{ cm}^{-1}$ ) to the sulfate  
17 peak ( $980\text{ cm}^{-1}$ ) obtained by micro-Raman spectroscopy. They also found the equilibration time was  
18 longer for the same-sized particles containing organics.

19 **Related changes in the revised manuscript:**

20 **Page 5, Line 11:** The sentence “The particles were equilibrated with water vapor at a given RH for  
21 about 40 min.” is revised to “The particles were equilibrated with water vapor at a given RH for  
22 about 40 min, during which the intensity ratios of the water peak ( $3430\text{ cm}^{-1}$ ) to the sulfate peak  
23 ( $980\text{ cm}^{-1}$ ) remained constant.”.

24

25 **4) Page 5, equation 1: I understand the equation for the growth factor but when the authors**  
26 **create the hygroscopic growth curve is the growth factor an average of many particles or only**  
27 **1 particle?**

28 **Reply:** Multiple particles (three or four) were selected to acquire the Raman spectra through each  
29 humidity cycle. Thus, the hygroscopic growth curve is derived from average growth factors of  
30 multiple particles. Each measurement for one particle was also repeated at least three times.



1 ***Related changes in the revised manuscript:***

2 ***Page 5, Line 13: We add the sentence “Multiple particles (three or four) were selected to acquire***  
3 ***the Raman spectra through each humidity cycle.”***

4 ***Page 5, Line 20: The sentence “Hygroscopic growth curves are acquired by plotting the Raman***  
5 ***growth factor as a function of RH.” is changed into “Hygroscopic growth curves are acquired by***  
6 ***plotting the average Raman growth factor of duplicate particles as a function of RH.”.***

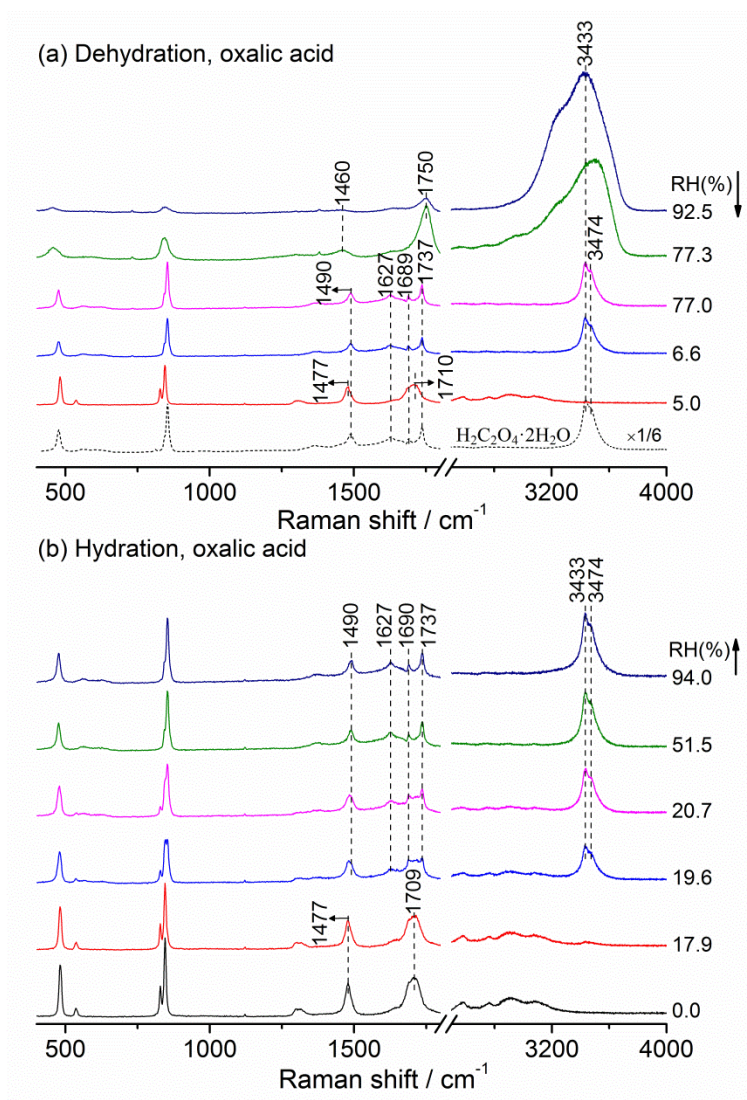
7

8 **5) Figure 1a: This is actually a problem I have with all the figures showing Raman spectra.**  
9 **There are just too many peak assignments and it clutters the figures up. Can the authors**  
10 **remove any peak assignments that don't illustrate the point of the figure? For example, in the**  
11 **OA dehydration process the peak at 1689 cm<sup>-1</sup> is obviously important because that's the peak**  
12 **associated with the dihydrate. That peak should clearly be highlighted. Also can the authors**  
13 **remove any of the Raman spectra that don't highlight something interesting happening? All**  
14 **that's happening is the water peaks are getting smaller. Also, the oxalic acid dihydrate**  
15 **spectrum at the bottom of Figure 1a looks like it is part of the dehydration process. It took me**  
16 **a little bit of time to figure out that the spectrum wasn't part of the dehydration process in the**  
17 **figure. I understand the importance of this spectrum but can it be boxed in or something so**  
18 **the reader doesn't think it is part of the dehydration process?**

19 ***Reply: Thanks for the reviewer's suggestion. We remove some minor peak assignments in the figures.***  
20 ***To avoid misunderstanding, the oxalic acid dihydrate spectrum at the bottom of Figure 1a is***  
21 ***indicated by a black dash line in the modified figure.***

22 ***Related changes in the revised manuscript:***

23 ***Figure R1 is the modified Figure 1 (i.e., Fig. 2 in the new version). The other figures are also***  
24 ***modified according to the reviewer's suggestion.***



1

2 **Figure R1.** Raman spectra of oxalic acid droplets during the (a) dehydration process and (b) hydration  
 3 process. In panel (a), the black dashed line indicates the spectrum of pure  $\text{H}_2\text{C}_2\text{O}_4 \cdot 2\text{H}_2\text{O}$  particles with the  
 4 peak height of  $\nu(\text{OH})$  located at  $3433 \text{ cm}^{-1}$  scaled by a factor of  $1/6$ .

5

6 **6) Page 6, line 5: This comment is associated with the comment above. Again, there are too**  
 7 **many peak assignments in the text. It clutters the paragraph up. Focus on the most important**  
 8 **peaks.**

9 **Reply:** According to reviewer's suggestion, we remove some minor peak assignments in the text.

10 **Related changes in the revised manuscript:**

11 **Page 6, line 5:** "As seen in Fig. 1a, the feature bands for OA droplets are observed at 457, 845,  
 12 1460, 1636, 1750 and  $3433 \text{ cm}^{-1}$  at 92.5% RH. At lower RH around 77% (Fig. 1a, magenta line),  
 13 these bands shift to 477, 855, 1490, 1627, 1737, 3433 and  $3474 \text{ cm}^{-1}$ , and a new band at  $1689 \text{ cm}^{-1}$

1 occurs, which is entirely consistent with the spectrum of oxalic acid dihydrate (Fig. 1a, black line).”  
2 **is changed into** “As seen in Fig. 2a, the feature bands for OA droplets are observed at 1460, 1750  
3 and 3433  $\text{cm}^{-1}$  at 92.5% RH. At lower RH around 77% (Fig. 2a, magenta line), these bands shift to  
4 1490, 1737, 3433 and 3474  $\text{cm}^{-1}$ , and a new band at 1689  $\text{cm}^{-1}$  occurs, which is entirely consistent  
5 with the spectrum of oxalic acid dihydrate (Fig. 2a, black dashed line).”  
6 Similar modifications in other places are also made.

7  
8 **7) General comment: I think it would be interesting to see pictures of the particles during the**  
9 **hydration and the dehydration process. Do the authors have pictures of the particles they**  
10 **could associate with the Raman spectra? The reason I bring this up is Wise et al. (2012) found**  
11 **that when aqueous sodium chloride particles effloresced at low temperatures the dihydrate**  
12 **formed. The morphology of those particles was different than the morphology of the**  
13 **dehydrated form. I am also wondering if the authors could physically see evidence of**  
14  **$\text{NH}_4\text{HSO}_4$  or  $\text{NH}_4\text{HC}_2\text{O}_4$  they claim to see spectral evidence of on page 7, line 4. Additionally**  
15 **can the authors see any coatings they argue are present on page 11, line 11?**

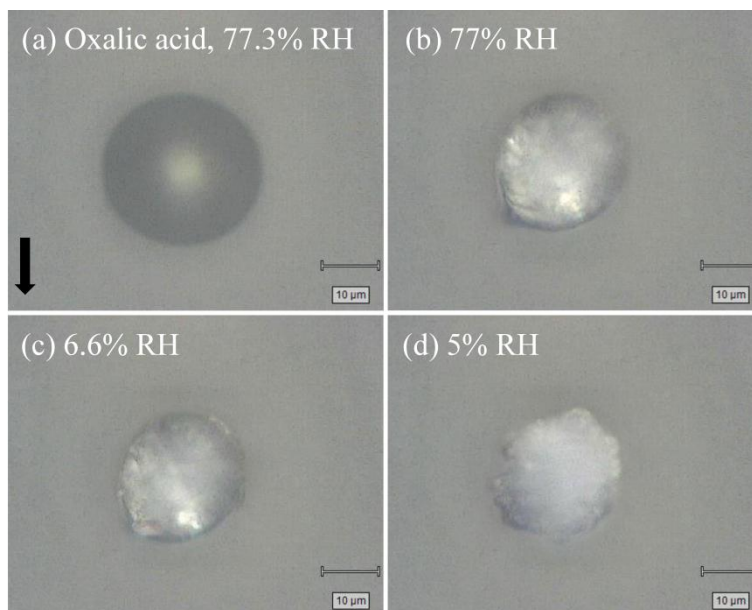
16 **Reply:** We thank for the reviewer’s suggestion. Although we have pictures of the particles associated  
17 with the Raman spectra, we could not distinguish the morphology of dry particles between  
18 dihydrate form and anhydrous one except for oxalic acid particles (Figure R2). Also, on page 7, line  
19 4,  $\text{NH}_4\text{HSO}_4$  or  $\text{NH}_4\text{HC}_2\text{O}_4$  could not be identified from the solid phase by visual inspection, seen in  
20 Figure R3 (b). On page 11, line 11,  $\text{NH}_4\text{HC}_2\text{O}_4$  coatings on 3:1 OA/AS particles were formed during  
21 the dehydration process, seen in Figure R4.

22 **Related changes in the revised manuscript:**

23 Some important pictures of the particles during the humidity cycle are supplemented into the  
24 modified version.

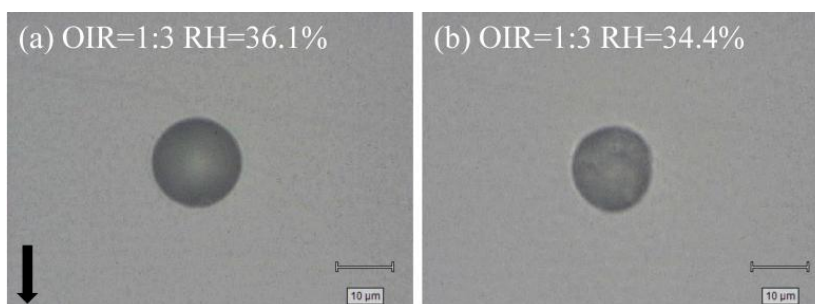
25 The picture of 3:1 OA/AS particles with  $\text{NH}_4\text{HC}_2\text{O}_4$  coatings formed during the dehydration process  
26 is added in the main text.

27



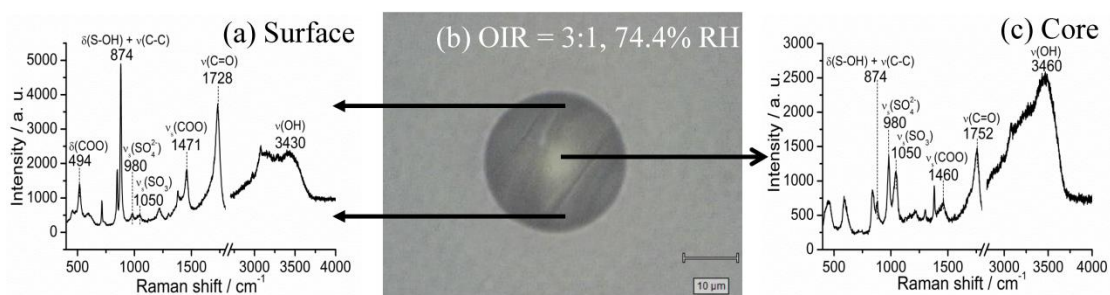
1  
2  
3  
4

**Figure R2.** Optical micrographs of the oxalic acid particle at (a) 77.3% RH, (b) 77% RH, (c) 6.6% RH and (d) 5% RH during the dehydration process, respectively.



5  
6  
7  
8

**Figure R3.** Optical micrographs of the mixed oxalic acid/ammonium sulfate particle (OIR = 1:3) upon dehydration: (a) 36.1% RH and (b) 34.4% RH.



9  
10  
11  
12  
13

**Figure R4.** The spatial distribution of chemicals within mixed oxalic acid/ammonium sulfate (OIR = 3:1) particles at 74.4% RH upon dehydration. (a) Raman spectrum acquired on the surface showing the shell mainly consisting of  $\text{NH}_4\text{HC}_2\text{O}_4$ . (b) Optical micrograph of a partially effloresced droplet composed of oxalic acid/ammonium sulfate (OIR = 3:1) mixtures at 74.4% RH upon dehydration. (c) Raman spectrum obtained

1 *at the core of the droplet showing the liquid phase dominated by oxalic acid and ammonium sulfate.*

2

3 **8) Page 7, line 10: There needs to be an arrow in the equation not an equal sign.**

4 ***Reply: P7, L10, we replace an equal sign with an arrow for the reaction.***

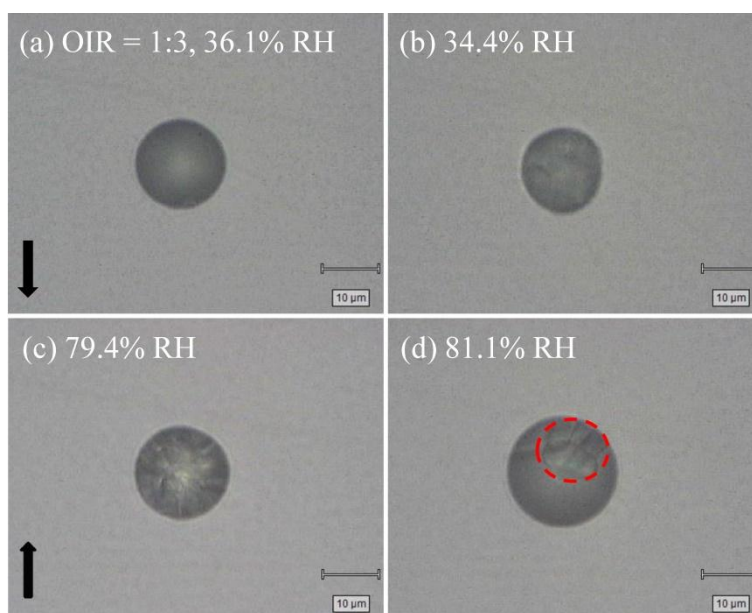
5

6 **9) Page 10, line 5: Again, I think pictures of the particles might help strengthen the case for**  
7 **water uptake prior to deliquescence. The authors should be able to see the particles gain water**  
8 **prior to full deliquescence. I am now wondering if the authors could create hygroscopic**  
9 **growth curves utilizing the physical size of the particles and if that correlates with the Raman**  
10 **growth factors.**

11 ***Reply: Page 10, line 5, the picture of mixed OA/AS particles with an OIR of 1:3 prior to full***  
12 ***deliquescence is given in Figure R5 (c). It can be seen that the size of 1:3 mixed OA/AS particle at***  
13 ***79.4% RH prior to deliquescence appears to be larger than that after complete efflorescence***  
14 ***(Figure R5 (b)), suggesting slight water uptake, as also confirmed by the Raman spectrum. Due to***  
15 ***the limitation of instrument, the picture resolution is not high enough to help identify distinct liquid***  
16 ***water. In addition, the slight water content may exist in the veins and cavities of the particle.***  
17 ***Since size-based hygroscopicity is sensitive to particle geometry, physical size of the particles may***  
18 ***not reflect the additions of water mass due to morphology effects (Piens et al., 2016). Due to the***  
19 ***lack of contact angle data, we cannot create hygroscopic growth curves based on the physical size***  
20 ***of the particles. In fact, the spectra method is advantageous for probing the hygroscopic behavior***  
21 ***and water content of atmospheric particles with regular or irregular morphologies.***

22 ***Related changes in the revised manuscript:***

23 ***Figure R5 and corresponding descriptions have been supplemented in the text.***



1  
2 **Figure R5.** Optical micrographs of the mixed oxalic acid/ammonium sulfate particle (OIR = 1:3) at phase  
3 change points. Dehydration: (a) 36.1% RH and (b) 34.4% RH. Hydration: (c) 79.4% RH and (d) 81.1% RH.  
4 In the image (d), the visual solid in aqueous phase is marked with a red dashed circle.

5  
6 **10) General comment:** Can the authors comment on the applicability of the data at  
7 temperatures lower than room temperature. Obviously, in the atmosphere the particles are  
8 going to experience temperatures much lower than room temperature.

9 **Reply:** Zobrist et al. (2006) investigated the heterogeneous freezing points of the aqueous oxalic  
10 acid/ammonium sulfate solutions. They found that oxalic acid precipitated as  $\text{NH}_4\text{H}_3(\text{C}_2\text{O}_4)_2 \cdot 2\text{H}_2\text{O}$   
11 in the mixed solution to act as a heterogeneous ice nucleus. The crystallization of oxalic  
12 acid/ammonium sulfate mixed systems at low temperature may show distinct behaviors relative to  
13 room temperature. Thus, we cannot give effective suggestions on applicability of our data at low  
14 temperatures.

15  
16 **11) Page 5, line 25:** Why did the authors decide to put the mixed hydration Raman spectra in  
17 the supplemental section? Surely, this data is important to the findings described in the paper.

18 **Reply:** According to the reviewer's suggestion, we move the mixed hydration Raman spectra in the  
19 supplemental section to the text.

20 **Related changes in the revised manuscript:**

21 **P6, L24:** The sentence: "The Raman spectra of mixed OA/AS droplets with OIRs of 1:3, 1:1 and 3:1

1 *at various RHs during the dehydration process are depicted in Fig. 2. The corresponding spectra*  
2 *for hydration process are given in Fig. S2 in the Supplement.” is revised to “The Raman spectra of*  
3 *mixed OA/AS droplets with OIRs of 1:3, 1:1 and 3:1 at various RHs during the dehydration and*  
4 *hydration process are depicted in Fig. 3 and 4, respectively.”.*

5

## 6 **References**

7 Amundson, N. R., Caboussat, A., He, J. W., Martynenko, A. V., and Seinfeld, J. H.: A phase equilibrium  
8 model for atmospheric aerosols containing inorganic electrolytes and organic compounds (UHAERO), with  
9 application to dicarboxylic acids, *J. Geophys. Res.: Atmos.*, 112, D24S13, 2007.

10 Braban, C. F., and Abbatt, J. P. D.: A study of the phase transition behavior of internally mixed ammonium  
11 sulfate-malonic acid aerosols, *Atmos. Chem. Phys.*, 4, 1451-1459, 2004.

12 Clegg, S. L., and Seinfeld, J. H.: Thermodynamic models of aqueous solutions containing inorganic  
13 electrolytes and dicarboxylic acids at 298.15 K. 1. The acids as nondissociating components, *J. Phys. Chem.*  
14 *A*, 110, 5692-5717, 10.1021/jp056149k, 2006.

15 Hakkinen, S. A. K., McNeill, V. F., and Riipinen, I.: Effect of Inorganic Salts on the Volatility of Organic  
16 Acids, *Environ. Sci. Technol.*, 48, 13718-13726, 10.1021/es5033103, 2014.

17 Hoyle, C. R., Boy, M., Donahue, N. M., Fry, J. L., Glasius, M., Guenther, A., Hallar, A. G., Hartz, K. H.,  
18 Petters, M. D., Petaja, T., Rosenoern, T., and Sullivan, A. P.: A review of the anthropogenic influence on  
19 biogenic secondary organic aerosol, *Atmos. Chem. Phys.*, 11, 321-343, 10.5194/acp-11-321-2011, 2011.

20 Lightstone, J. M., Onasch, T. B., Imre, D., and Oatis, S.: Deliquescence, efflorescence, and water activity in  
21 ammonium nitrate and mixed ammonium nitrate/succinic acid microparticles, *J. Phys. Chem. A*, 104,  
22 9337-9346, 10.1021/jp002137h, 2000.

23 Ling, T. Y., and Chan, C. K.: Partial crystallization and deliquescence of particles containing ammonium  
24 sulfate and dicarboxylic acids, *Journal of Geophysical Research: Atmospheres*, 113, 1-15, doi:  
25 10.1029/2008JD009779, 2008.

26 Piens, D. S., Kelly, S. T., Harder, T. H., Petters, M. D., O'Brien, R. E., Wang, B., Teske, K., Dowell, P.,  
27 Laskin, A., and Gilles, M. K.: Measuring mass-based hygroscopicity of atmospheric particles through in situ  
28 imaging, *Environ. Sci. Technol.*, 50, 5172-5180, doi: 10.1021/acs.est.6b00793, 2016.

29 Yeung, M. C., Lee, A. K. Y., and Chan, C. K.: Phase transition and hygroscopic properties of internally  
30 mixed ammonium sulfate and adipic acid (AS-AA) particles by optical microscopic imaging and Raman

1 spectroscopy, *Aerosol Sci. Technol.*, 43, 387–399, doi: 10.1080/02786820802672904, 2009.

2 Yli-Juuti, T., Zardini, A. A., Eriksson, A. C., Hansen, A. M. K., Pagels, J. H., Swietlicki, E., Svenningsson,  
3 B., Glasius, M., Worsnop, D. R., Riipinen, I., and Bilde, M.: Volatility of Organic Aerosol: Evaporation of  
4 Ammonium Sulfate/Succinic Acid Aqueous Solution Droplets, *Environ. Sci. Technol.*, 47, 12123-12130,  
5 10.1021/es401233c, 2013.

6 Zobrist, B., Marcolli, C., Koop, T., Luo, B. P., Murphy, D. M., Lohmann, U., Zardini, A. A., Krieger, U. K.,  
7 Corti, T., Cziczo, D. J., Fueglistaler, S., Hudson, P. K., Thomson, D. S., and Peter, T.: Oxalic acid as a  
8 heterogeneous ice nucleus in the upper troposphere and its indirect aerosol effect, *Atmos. Chem. Phys.*, 6,  
9 3115-3129, 2006.

10



1  
2  
3  
4  
5  
6  
7  
8  
9  
10  
11  
12  
13  
14  
15  
16  
17  
18  
19  
20  
21  
22  
23  
24  
25  
26  
27  
28  
29  
30  
31

**Response to Referee #3:**

We are grateful for the reviewer's comments. Those comments are all valuable and helpful for improving our paper. Our response to the comments and changes to the manuscript are included below. We repeat the specific points raised by the reviewer in bold font, followed by our response in italic font. The pages numbers and lines mentioned below are consistent with those in the Atmospheric Chemistry and Physics Discussions (ACPD) paper.

**The authors presented a laboratory work on the hygroscopic growth and phase transitions of oxalic acid (OA), ammonium sulfate (AS), and their mixed particles. The growth factor and the phase transition of deliquescence and efflorescence were determined using the spectra collected by confocal Raman spectroscopy at room temperature. It is showing that the particles with different mixing ratios showed different hygroscopicity during the hydration and dehydration cycles. At higher OA/AS ratio, the dehydration process produced less hygroscopic organic salt, such as  $\text{NH}_4\text{HC}_2\text{O}_2$ , from in particle phase reaction within the aqueous droplet as it loses water. In addition, the manuscript shows the possible effects on the growth factor by the different drying rates. The manuscript also provides explanation for the discrepancy on the ERH of OA compared to the previous studies. This study provides a set of valuable data for the hygroscopicity of model particles generated in the lab. This work demonstrates the effects of aqueous phase reaction on particle hygroscopicity during dehydration which was overlooked in the past. There is a quite important implication to atmospheric chemistry. It is recommended for publication after a minor revision. Please see the following comments which the authors may want to consider in the revision.**

**Minor comments:**

**1. P1, L17, L18, "aerosol" refers to the mixture of particle and gases. It is suggested to change the "aerosol" to "particle".**

*Reply: Thanks for your suggestion. P1, L17, L18, "aerosol" is changed into "particle" in the revised version.*

**2. P1, L28, how do you define "the partial deliquescence relative humidity"?**

*Reply: The partial deliquescence relative humidity is used to indicate the RH at which AS deliquesces while other coexisting components in the mixed particles remain solid during the*

1 hydration process.

2 **Related changes in the revised manuscript:**

3 **P1, L28, to avoid the misunderstanding, “the partial deliquescence relative humidity (DRH) for**  
4 **mixed OA/AS particles” is revised to “the deliquescence relative humidity (DRH) of AS in mixed**  
5 **OA/AS particles”.**

6

7 **3. P3, L23, this statement is not clear, in the previous sentences the authors showed that there**  
8 **are several studies on the OA/AS system. Please provide additional information or references**  
9 **to support this statement.**

10 **Reply:** P3, L23, this statement means that the effects of OA on **deliquescence behaviors** of AS have  
11 been extensively investigated (Brooks et al., 2002; Prenni et al., 2003; Wise et al., 2003; Miñambres  
12 et al., 2013; Jing et al., 2016), while there is still lack of study on influence of OA on **efflorescence**  
13 **behaviors** of AS. In the original version, we have used the term “**deliquescence process**” or  
14 “**efflorescence process**” to distinguish the studies on hygroscopicity of the OA/AS mixed system.

15

16 **4. P4, L19, it is not clear how the authors would be able to prepare the 30-40 μm aqueous**  
17 **particles with a syringe.**

18 **Reply:** The sample solution was discharged from a syringe. Then, residual solution in the syringe  
19 was pushed rapidly to generate aerosol droplets spraying onto a PTFE substrate fixed to the bottom  
20 of the sample cell. At ~ 95% RH, the droplets with a diameter of 30~40 microns detected by an  
21 optical microscope (50× objective, 0.75 numerical aperture) were selected to acquire the Raman  
22 spectra.

23 **Related changes in the revised manuscript:**

24 **P4, L19: The sentence “Using a syringe, droplets from the solutions were injected onto the**  
25 **polytetrafluorethylene (PTFE) film fixed to the bottom of the sample cell. The diameters of these**  
26 **droplets ranged from 30 to 40 μm at ~ 95% RH. Then, the sample cell was sealed by a transparent**  
27 **polyethylene film and the RH in the sample cell was regulated by nitrogen streams consisting of a**  
28 **mixture of water-saturated N<sub>2</sub> and dry N<sub>2</sub> at controlled flow rates.” is revised to “The sample**  
29 **solution was discharged from a syringe. Then, residual solution in the syringe was pushed rapidly**  
30 **to generate aerosol droplets spraying onto a polytetrafluorethylene (PTFE) substrate fixed to the**

1 bottom of the sample cell. Then, the sample cell was promptly sealed by a transparent polyethylene  
2 film. The RH in the sample cell was regulated by nitrogen streams consisting of a mixture of  
3 water-saturated N<sub>2</sub> and dry N<sub>2</sub> at controlled flow rates. At ~ 95% RH, the droplets with a diameter  
4 of 30~40 microns detected by an optical microscope (50× objective, 0.75 numerical aperture) were  
5 selected to acquire the Raman spectra. The dry size of these particles after efflorescence ranged  
6 from 10 to 20 μm.”.

7  
8 **5. P4, L25, If the temperature accuracy is 0.7 K, the uncertainty of RH at 297 K and 95%**  
9 **should be 4%. How the sample temperature is controlled during the experiments?**

10 **Reply:** We thank for the reviewer’s comment. Below 90% RH, the uncertainty of RH at 297 K was  
11 less than ±2.5%. We agree that the temperature accuracy of 0.7 K could result in uncertainty of 4%  
12 at RH of 95%. The temperature of the sample was maintained at 297 ± 0.5 K by using an automatic  
13 thermostat. We would like to add some changes to make it clear.

14 **Related changes in the revised manuscript:**

15 **P4, L24:** The sentence “The RH and temperature of the outflow from the sample cell was measured  
16 by a humidity/temperature meter (Centertek Center 313) with an accuracy of ± 2.5% and ± 0.7 K  
17 placed near the exit of the sample cell.” **is changed into** “The RH and temperature of the outflow  
18 from the sample cell was measured by a humidity/temperature meter (Centertek Center 313) with an  
19 accuracy of ± 2.5% below 90% RH and ± 0.7 K placed near the exit of the sample cell.”.

20 **P4, L26:** We **add** “The temperature accuracy of 0.7 K could result in uncertainty of 4% at RH of  
21 95%. The temperature of the sample was maintained at 297 ± 0.5 K by using an automatic  
22 thermostat.”.

23  
24 **6. P5, L25, I also suggested to move the Raman spectra to the main text.**

25 **Reply:** Thanks for your suggestion. The Raman spectra of AS droplets are moved to the main text.

26 **Related changes in the revised manuscript:**

27 **P5, L24,** the sentence “The Raman spectra of AS droplets during the dehydration and hydration  
28 process as a function of RH can be found in Fig. S1 (a) and (b) in the supplement, respectively.” **is**  
29 **revised to** “The Raman spectra of AS droplets during the dehydration and hydration process can be  
30 found in Fig. 1a and 1b, respectively.”.

1

2 **7. P6, L11-12, it is not clear to me that how oxalic acid dihydrate can be converted to**  
3 **anhydrous form at these experimental conditions? How long it will take for such process and**  
4 **is it atmospheric relevant?**

5 ***Reply:** In our experiments, oxalic acid particles after efflorescence exist in the form of dihydrate*  
6 *until 6.6% RH, at which the Raman spectrum of dihydrate remains unchanged for 40 min. Once RH*  
7 *decreases to 5%, oxalic acid dihydrate is **promptly** converted to anhydrous oxalic acid, as seen in*  
8 *Fig. 2a. This conversion only takes a few seconds during our observations. Our results indicate*  
9 *extremely dry conditions may favor the conversion of oxalic acid dihydrate into anhydrous form in*  
10 *the atmospheric environment.*

11 ***Related changes in the revised manuscript:***

12 ***To make it clear, P6, L9, we add** “Oxalic acid particles after efflorescence exist in the form of*  
13 *dihydrate until 6.6% RH, at which the Raman spectrum of dihydrate remains unchanged for 40*  
14 *min.”. **P6, L9, the sentence** “As RH further decreases to ~5.0%, the peaks shift to 482, 828, 845,*  
15 *1477, 1710, 2587, 2760 and 2909 cm<sup>-1</sup>,” **is changed into** “Once RH decreases to ~5.0%, the peaks*  
16 *promptly shift to 1477, 1710, 2587, 2760 and 2909 cm<sup>-1</sup>,”.*

17

18 **8. P7, L10, it is the reaction, not an equation.**

19 ***Reply:** P7, L10, we replace the equal sign with an arrow for the reaction.*

20

21 **9. P9, L6-11, the explanation for the discrepancy on the ERH of OA compared to the previous**  
22 **studies should be carefully addressed.**

23 ***Reply:** We thank the reviewer for the helpful suggestion. After revisiting our explanation carefully,*  
24 *we give a more specific one as follows. The discrepancy on the ERH of OA compared to that*  
25 *reported by Peng et al. (2001) is likely due to the effects of substrate and sample purity. The size of*  
26 *dry particles ranging from 10 to 20 μm in our experiment is consistent with observation using EDB*  
27 *by Peng et al. (2001), which eliminates the influence of particle size. The substrate supporting*  
28 *droplets may promote the heterogeneous nucleation of oxalic acid while the levitated droplets in*  
29 *EDB study can avoid induced nucleation by the substrate. Ghorai et al. (2014) also reported the*  
30 *potential effects of substrate on the efflorescence transition of NaCl/dicarboxylic acid mixed*

1 particles. In addition, The OA purity in our study is 99.0% lower than that of 99.5% in study by  
2 Peng et al. (2001). Thus, trace amounts of impurities in OA droplets acting as a heterogeneous  
3 nucleus could contribute to crystallization and result in a higher ERH of OA. Due to the effects of  
4 substrate and sample purity, the heterogeneous nucleation should be responsible for the  
5 discrepancy on the observed ERH of OA.

6 **Corresponding changes in the revised manuscript:**

7 **Page 9, Line 10-17:** The sentence “The discrepancies between this study and that by Peng et al.  
8 (2001) is likely due to the effects of droplet size, substrate and experimental method. According to  
9 classical nucleation theory, the probability of the formation of the critical nucleus is proportional to  
10 the particle volume (Martin, 2000; Parsons et al., 2006). Considering that the droplet size in our  
11 study was approximately 1-2 times larger than that observed by Peng et al. (2001), the droplets  
12 deposited on the substrate in our experiment may promote the heterogeneous nucleation while the  
13 levitated droplets using EDB can dispel the heterogeneous nucleation. Thus, the ERH of OA  
14 obtained in our study is higher than the observation of Peng et al. (2001).” is revised to “The  
15 discrepancy on the ERH of OA compared to that reported by Peng et al. (2001) is likely due to the  
16 effects of substrate and sample purity. The size of dry particles ranging from 10 to 20  $\mu\text{m}$  in our  
17 experiment is consistent with observation using EDB by Peng et al. (2001), which eliminates the  
18 influence of particle size. The substrate supporting droplets may promote the heterogeneous  
19 nucleation of oxalic acid while the levitated droplets in EDB study can avoid induced nucleation by  
20 the substrate. Ghorai et al. (2014) also reported the potential effects of substrate on the  
21 efflorescence transition of NaCl/dicarboxylic acid mixed particles. In addition, The OA purity in our  
22 study is 99.0% lower than that of 99.5% in study by Peng et al. (2001). Thus, trace amounts of  
23 impurities in OA droplets acting as a heterogeneous nucleus could contribute to crystallization and  
24 result in a higher ERH of OA. Due to the effects of substrate and sample purity, the heterogeneous  
25 nucleation should be responsible for the discrepancy on the observed ERH of OA.”.

26

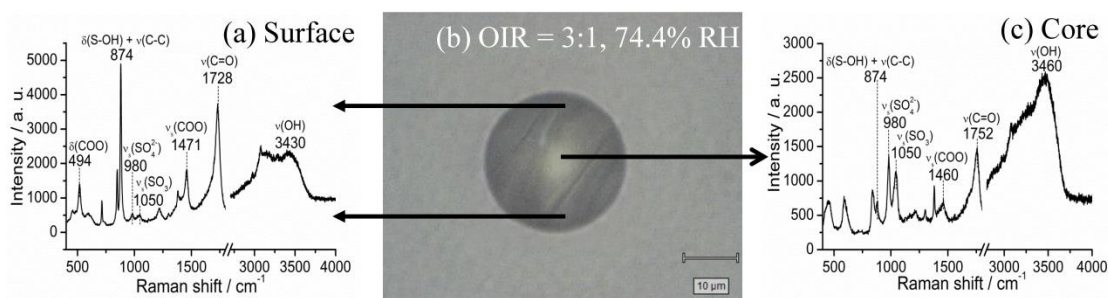
27 **10. P11, L10-12, as suggested by the previous reviewers, it may be more straightforward if the**  
28 **authors can provide optical images to show the phase transitions. For this possible evidence**  
29 **on the coating of less hygroscopic materials, it may be easy to just provide Raman spectral at**  
30 **different location of particles or compositional mapping with the imaging mode.**

1 **Reply:** We appreciate the reviewer's comments. The optical images showing the phase transitions  
 2 have been added in the text. Figure R1 presents the spatial distribution of chemicals within mixed  
 3 OA/AS (OIR = 3:1) particles at 74.4% RH. The characteristic peak of  $980\text{ cm}^{-1}$ ,  $1050\text{ cm}^{-1}$  and  $1471\text{ cm}^{-1}$   
 4  $\text{cm}^{-1}$  is assigned to  $\text{SO}_4^{2-}$ ,  $\text{HSO}_4^-$  and  $\text{HC}_2\text{O}_4^-$ , respectively. The sharp absorption at  $874\text{ cm}^{-1}$  and  
 5 obvious peak at  $1471\text{ cm}^{-1}$  indicate the abundant content of  $\text{NH}_4\text{HC}_2\text{O}_4$ . The comparison of  
 6 characteristic peaks between inner and outer phase reveals that the major component on the  
 7 surface of a mixed OA/AS (OIR = 3:1) particle is  $\text{NH}_4\text{HC}_2\text{O}_4$ . In contrast to the surface, the obvious  
 8 features of  $980\text{ cm}^{-1}$  and  $1050\text{ cm}^{-1}$  at the core of the particle suggest that  $(\text{NH}_4)_2\text{SO}_4$  and  $\text{NH}_4\text{HSO}_4$   
 9 mainly exist in the inner aqueous phase. During the dehydration process, crystalline  $\text{NH}_4\text{HC}_2\text{O}_4$  in  
 10 the outer phase acts as a heterogeneous nucleus, leading to the crystallization of oxalic acid  
 11 dihydrate,  $(\text{NH}_4)_2\text{SO}_4$  and  $\text{NH}_4\text{HSO}_4$  in the inner phase.

12 **Related changes included in the revised manuscript:**

13 Figure R1 is added into the text. **Page 11, Line 4: The sentence** “The crystallization of  $\text{NH}_4\text{HC}_2\text{O}_4$   
 14 may act as crystallization nuclei for  $\text{NH}_4^+$ ,  $\text{HSO}_4^-$  and OA in the mixed droplets to form  $\text{NH}_4\text{HSO}_4$   
 15 crystal and oxalic acid dihydrate.” **is changed into** “Figure 12 presents the spatial distribution of  
 16 chemicals within mixed OA/AS (OIR = 3:1) particles at 74.4% RH. The characteristic peak of  $980\text{ cm}^{-1}$ ,  
 17  $1050\text{ cm}^{-1}$  and  $1471\text{ cm}^{-1}$  is assigned to  $\text{SO}_4^{2-}$ ,  $\text{HSO}_4^-$  and  $\text{HC}_2\text{O}_4^-$ , respectively. The sharp  
 18 absorption at  $874\text{ cm}^{-1}$  and obvious peak at  $1471\text{ cm}^{-1}$  indicate the abundant content of  $\text{NH}_4\text{HC}_2\text{O}_4$ .  
 19 The comparison of characteristic peaks between inner and outer phase reveals that the major  
 20 component on the surface of a mixed OA/AS (OIR = 3:1) particle is  $\text{NH}_4\text{HC}_2\text{O}_4$ . In contrast to the  
 21 surface, the obvious features of  $980\text{ cm}^{-1}$  and  $1050\text{ cm}^{-1}$  at the core of the particle suggest that  
 22  $(\text{NH}_4)_2\text{SO}_4$  and  $\text{NH}_4\text{HSO}_4$  mainly exist in the inner aqueous phase. During the dehydration process,  
 23 crystalline  $\text{NH}_4\text{HC}_2\text{O}_4$  in the outer phase acts as the heterogeneous nucleus, leading to the  
 24 crystallization of oxalic acid dihydrate,  $(\text{NH}_4)_2\text{SO}_4$  and  $\text{NH}_4\text{HSO}_4$  in the inner phase.”.

25



26

27 **Figure R1.** The spatial distribution of chemicals within mixed oxalic acid/ammonium sulfate (OIR = 3:1)

1 particles at 74.4% RH upon dehydration. (a) Raman spectrum acquired on the surface showing the shell  
2 mainly consisting of  $\text{NH}_4\text{HC}_2\text{O}_4$ . (b) Optical micrograph of a partially effloresced droplet composed of oxalic  
3 acid/ammonium sulfate (OIR = 3:1) mixtures at 74.4% RH upon dehydration. (c) Raman spectrum obtained  
4 at the core of the droplet showing the liquid phase dominated by oxalic acid and ammonium sulfate.

5

6 **11. P11, L28-29, it is not clear how the RH is controlled during the 10-12h experimental period,**  
7 **stepwise or continuously? What is the variation of sample temperature during this period?**

8 **Reply:** *The RH was decreased stepwise from ~95% to ~0% over 10-12 h during the dehydration*  
9 *process. The decrease rate was typically 5-6 RH/40 min, and the rate remained 2-3 RH/40 min near*  
10 *the phase transition. The temperature of the sample was maintained at  $297 \pm 0.5$  K by using an*  
11 *automatic thermostat. In the Experimental section, we have stated that RH was decreased stepwise*  
12 *during the slow drying process.*

13 **Related changes included in the revised manuscript:**

14 **P5, L10, the sentence** “Subsequently, the RH was decreased stepwise for dehydration process, and  
15 increased from  $\text{RH} < 3\%$  to high RH for hydration process.” **is revised into** “Subsequently, the RH  
16 was decreased stepwise for a slow dehydration process, and then increased stepwise from  $\text{RH} < 3\%$   
17 to high RH for a hydration process. The decrease rate was typically 5-6 RH/40 min, and the rate  
18 remained 2-3 RH/40 min near the phase transition. The RH was decreased continuously in a few  
19 minutes for a rapid dehydration process.”.

20

21 **12. Figure 4 and 5, It is suggested to compare the experimental results with model estimation,**  
22 **such as E-AIM, ZSR, or AIOMFAC. For example, the E-AIM model**  
23 **(<http://www.aim.env.uea.ac.uk/aim/aim.php>) includes the dissociation equilibrium for some**  
24 **organic/inorganic systems. The oxalic acid is included in current E-AIM. What would E-AIM**  
25 **predict and how does that compare with your experimental data? This can not only serve as**  
26 **validation of the determined Raman growth factor but may also provide additional insides to**  
27 **the effects of reactions on particle’s hygroscopicity.**

28 **Reply:** *We thank the reviewer for the good suggestion. In fact, the Raman growth factors of pure*  
29 *ammonium sulfate and oxalic acid have been given in Fig. 9 (or Fig. 5 in ACPD) for comparisons.*  
30 *It is clear that the two species show comparable hygroscopic growth at high RH (dehydration curve,*

1 *Fig. 9(a)). According to the ZSR rule, the hygroscopic growth of mixtures of ammonium sulfate and*  
2 *oxalic acid should be close to that of pure ammonium sulfate or oxalic acid. Due to lack of Raman*  
3 *cross section data, our Raman growth factors could not be converted into ZSR-predictions. Thus,*  
4 *we used Raman growth factors of pure ammonium sulfate and oxalic acid to compare with that of*  
5 *mixtures in the original manuscript.*

6 *As for the E-AIM, our previous study by Jing et al. (2016) has shown that E-AIM could well*  
7 *describe the hygroscopic growth of equal mass mixture of ammonium sulfate and oxalic acid, which*  
8 *underwent rapid dehydration in the HTDMA system. As stated in the Discussion section, the*  
9 *HTDMA studies observed no formation of ammonium hydrogen oxalate or influence of interactions*  
10 *between ammonium sulfate and oxalic acid on water uptake of mixtures. Also, the E-AIM does not*  
11 *consider the formation of solid ammonium hydrogen oxalate. As a result, it can be expected that the*  
12 *E-AIM could not well describe water uptake of mixed ammonium sulfate/oxalic acid particles*  
13 *undergoing the slow drying process. This situation also applies to AIOMFAC model.*

14

## 15 **References**

16 Brooks, S. D., Wise, M. E., Cushing, M., and Tolbert, M. A.: Deliquescence behavior of organic/ammonium  
17 sulfate aerosol, *Geophys. Res. Lett.*, 29, 1917, doi: 10.1029/2002gl014733, 2002.

18 Ghorai, S., Wang, B., Tivanski, A., and Laskin, A.: Hygroscopic properties of internally mixed particles  
19 composed of NaCl and water-soluble organic acids, *Environ. Sci. Technol.*, 48, 2234-2241, doi:  
20 10.1021/es404727u, 2014.

21 Jing, B., Tong, S. R., Liu, Q. F., Li, K., Wang, W. G., Zhang, Y. H., and Ge, M. F.: Hygroscopic behavior of  
22 multicomponent organic aerosols and their internal mixtures with ammonium sulfate, *Atmos. Chem. Phys.*,  
23 16, 4101-4118, 2016.

24 Miñambres, L., Méndez, E., Sánchez, M. N., Castaño, F., and Basterretxea, F. J.: Water uptake of internally  
25 mixed ammonium sulfate and dicarboxylic acid particles probed by infrared spectroscopy, *Atmos. Environ.*,  
26 70, 108-116, doi: 10.1016/j.atmosenv.2013.01.007, 2013.

27 Peng, C. G., Chan, M. N., and Chan, C. K.: The hygroscopic properties of dicarboxylic and multifunctional  
28 acids: Measurements and UNIFAC predictions, *Environ. Sci. Technol.*, 35, 4495-4501, doi:  
29 10.1021/es0107531, 2001.

30 Prenni, A. J., DeMott, P. J., and Kreidenweis, S. M.: Water uptake of internally mixed particles containing



1 ammonium sulfate and dicarboxylic acids, *Atmos. Environ.*, 37, 4243–4251, doi:  
2 10.1016/S1352-2310(03)00559-4, 2003.

3 Wise, M. E., Surratt, J. D., Curtis, D. B., Shilling, J. E., and Tolbert, M. A.: Hygroscopic growth of  
4 ammonium sulfate/dicarboxylic acids, *J. Geophys. Res.*, 108, 4638, doi: 10.1029/2003jd003775, 2003.

5

6

7 |

# 1 Hygroscopic behavior and chemical composition evolution of 2 internally mixed aerosols composed of oxalic acid and ammonium 3 sulfate

4 Xiaowei Wang<sup>1,2</sup>, Bo Jing<sup>3</sup>, Fang Tan<sup>3,4</sup>, Jiabi Ma<sup>1</sup>, Yunhong Zhang<sup>1</sup> and Maofa Ge<sup>3,4,5</sup>

5 <sup>1</sup>The Institute of Chemical Physics, School of Chemistry and Chemical Engineering, Beijing Institute of  
6 Technology, Beijing 100081, P. R. China

7 <sup>2</sup>School of Chemical Engineering and Pharmaceutics, Henan University of Science and Technology, Luoyang  
8 471023, P. R. China

9 <sup>3</sup>Beijing National Laboratory for Molecular Sciences (BNLMS), State Key Laboratory for Structural Chemistry of  
10 Unstable and Stable Species, CAS Research/Education Center for Excellence in Molecular Sciences, Institute  
11 of Chemistry, Chinese Academy of Sciences, Beijing 100190, P. R. China

12 <sup>4</sup>University of Chinese Academy of Sciences, Beijing 100049, P. R. China

13 <sup>5</sup>Center for Excellence in Regional Atmospheric Environment, Institute of Urban Environment, Chinese Academy  
14 of Sciences, Xiamen 361021, P. R. China

15 *Correspondence to:* Yunhong Zhang (yhz@bit.edu.cn) and Maofa Ge (gemaofa@iccas.ac.cn)

## 16 Abstract

17 Although water uptake of aerosol particles plays an important role in the atmospheric environment,  
18 the effects of interactions between components on chemical composition and hygroscopicity of  
19 particlesaerosols are still not well constrained. The hygroscopic properties and phase transformation  
20 of oxalic acid (OA) and mixed particles composed of ammonium sulfate (AS) and OA with  
21 different organic to inorganic molar ratios (OIRs) have been investigated by using confocal Raman  
22 spectroscopy. It is found that OA droplets first crystallize to form oxalic acid dihydrate at 77%  
23 relative humidity (RH), and further lose crystalline water to convert into anhydrous oxalic acid  
24 around 5% RH during the dehydration process. The deliquescence and efflorescence point for AS is  
25 determined to be  $80.1 \pm 1.5\%$  RH and  $44.3 \pm 2.5\%$  RH, respectively. The observed efflorescence  
26 relative humidity (ERH) for mixed OA/AS droplets with OIRs of 1:3, 1:1 and 3:1 is  $34.4 \pm 2.0\%$   
27 RH,  $44.3 \pm 2.5\%$  RH and  $64.4 \pm 3.0\%$  RH, respectively, indicating the elevated OA content appears  
28 to favor the crystallization of mixed systems at higher RH. However, the deliquescence relative  
29 humidity (DRH) of AS in mixed OA/AS particles~~the partial deliquescence relative humidity (DRH)~~  
30 ~~for mixed OA/AS particles~~ with an OIR of 1:3 and 1:1 is observed to occur at  $81.1 \pm 1.5\%$  RH and  
31  $77 \pm 1.0\%$  RH, respectively. The Raman spectra of mixed OA/AS droplets indicate the formation of

1 ammonium hydrogen oxalate ( $\text{NH}_4\text{HC}_2\text{O}_4$ ) and ammonium hydrogen sulfate ( $\text{NH}_4\text{HSO}_4$ ) from  
2 interactions between OA and AS in aerosols after the slow dehydration process in the time scale of  
3 hours, which considerably influence the subsequent deliquescence behavior of internally mixed  
4 particles with different OIRs. The mixed OA/AS particles with an OIR of 3:1 exhibit no  
5 deliquescence transition over the RH range studied due to the considerable transformation of  
6  $(\text{NH}_4)_2\text{SO}_4$  into nonhygroscopic  $\text{NH}_4\text{HC}_2\text{O}_4$ . Although the hygroscopic growth of mixed OA/AS  
7 droplets is comparable to that of AS or OA at high RH during the dehydration process, Raman  
8 growth factors of mixed particles after deliquescence are substantially lower than those of mixed  
9 OA/AS droplets during the efflorescence process and further decrease with elevated OA content.  
10 The discrepancies for Raman growth factors of mixed OA/AS particles between the dehydration  
11 and hydration process at high RH can be attributed to the significant formation of  $\text{NH}_4\text{HC}_2\text{O}_4$  and  
12 residual OA, which remain solid at high RH and thus result in less water uptake of mixed particles.  
13 These findings improve the understanding of the role of reactions between dicarboxylic acid and  
14 inorganic salt in the chemical and physical properties of aerosol particles, and might have important  
15 implications for atmospheric chemistry.

## 16 **1 Introduction**

17 Atmospheric aerosols have vital impacts on the Earth's climate directly by scattering, reflecting and  
18 absorbing solar radiation, and indirectly by influencing formation of clouds and precipitation (Tang  
19 and Munkelwitz, 1994b; Jacobson et al., 2000; Penner et al., 2001; Pöschl, 2005; Martin, 2000; Von  
20 Schneidemesser et al., 2015). Direct and indirect effects depend on the chemical and physical  
21 properties of atmospheric aerosols, including size, structure, hygroscopicity and chemical  
22 composition. Field observations indicate that aerosol particles are generally internal mixtures of  
23 inorganic and organic compounds in the atmosphere (Saxena et al., 1995; Murphy et al., 1998;  
24 Murphy et al., 2006; Pratt and Prather, 2010). Ammonium sulfate (AS) is one of the most abundant  
25 inorganic constituents in the atmosphere, hygroscopicity of which has been widely investigated (Liu  
26 et al., 2008; Cziczo et al., 1997; Laskina et al., 2015).

27 Oxalic acid (OA) is ubiquitous and has been identified as the dominant dicarboxylic acid in urban  
28 and remote atmospheric aerosols (Chebbi and Carlier, 1996; Kanakidou et al., 2004; Yang and Yu,  
29 2008; Wang et al., 2012; Kawamura and Bikina, 2016). Previous studies have focused on  
30 deliquescence behavior of pure OA (Peng et al., 2001; Braban et al., 2003; Miñambres et al., 2013;

1 Ma et al., 2013a; Jing et al., 2016). It was found that due to its high deliquescence point OA  
2 exhibited no deliquescence transition or hygroscopic growth within relative humidity (RH) range  
3 studied by an electrodynamic balance (EDB) (Peng et al., 2001), vapor sorption analyzer (Ma et al.,  
4 2013a) or hygroscopicity tandem differential mobility analyzer (HTDMA) (Jing et al., 2016).  
5 Braban et al. (2003) reported that OA could deliquesce at 98% RH using aerosol flow tube Fourier  
6 transform infrared spectroscopy (AFT-FTIR). However, the study on the efflorescence behavior of  
7 OA during the dehydration process remains limited (Peng et al., 2001; Mikhailov et al., 2009). Peng  
8 et al. (2001) observed the efflorescence transition of OA using EDB while Mikhailov et al. (2009)  
9 reported continuous hygroscopic growth of OA during both hydration and dehydration process  
10 using the HTDMA.

11 The dicarboxylic acids can affect properties of internally mixed aerosol particles such as  
12 hygroscopicity, phase transition, solubility and chemical reactivity (Lightstone et al., 2000; Brooks  
13 et al., 2002; Sjogren et al., 2007; Kumar et al., 2003; Treuel et al., 2011; Laskin et al., 2012; Drozd  
14 et al., 2014; Peng et al., 2016; Jing et al., 2016; Li et al., 2017; Jing et al., 2017). Field  
15 measurements have observed the formation of low-volatility organic salts in atmospheric particles  
16 due to the reactions of organic acids with mineral salts, chloride salts, nitrate salts, ammonium and  
17 amines [\(Sullivan and Prather, 2007; Laskin et al., 2012; Wang and Laskin, 2014; Smith et al., 2010\)](#).

18 The organic salts formed typically have varying hygroscopicity compared to the corresponding  
19 organic acids. Thus, these drastic changes in aerosol composition have potential impacts on the  
20 water uptake and related physicochemical properties of particles. The effects of OA on  
21 deliquescence behaviors of AS have been extensively investigated (Brooks et al., 2002; Prenni et al.,  
22 2003; Wise et al., 2003; Miñambres et al., 2013; Jing et al., 2016). The majority of studies found  
23 that the presence of OA had no obvious impacts on the deliquescence process of OA/AS mixtures  
24 with minor OA content (Brooks et al., 2002; Prenni et al., 2003; Wise et al., 2003). To our  
25 knowledge, there is still a lack of studies on the efflorescence process of OA/AS mixed systems. In  
26 fact, the efflorescence behavior is a critical hygroscopic characteristic of atmospheric aerosols,  
27 which may favor specific chemical interactions between components within the supersaturated  
28 droplets. For example, previous studies have found that the chloride depletion could occur in the  
29 NaCl/dicarboxylic acids mixed aerosols during the dehydration or efflorescence process, which led  
30 to the formation of organic salts and in turn affected subsequent deliquescence behaviors of aerosols

1 (Laskin et al., 2012; Ghorai et al., 2014). Oxalic acid has been found to react with both mono- and  
2 di-valent cations to form low volatility and solubility compounds (Drozd et al., 2014). Miñambres  
3 et al. (2013) proposed that OA might react with AS to form ammonium hydrogen oxalate and  
4 ammonium hydrogen sulfate within OA/AS solution. Due to the lack of available thermodynamic  
5 data, the aerosol thermodynamic models typically assume that upon dehydration dicarboxylic acid  
6 could only form organic solid without the organic salt in the inorganic electrolyte/dicarboxylic acid  
7 system (Clegg and Seinfeld, 2006; Amundson et al., 2007). Thus, the incorporation of organic salts  
8 formed from interactions between inorganic salts and organic acids is crucial in the modeling of  
9 hygroscopic properties of mixed organic/inorganic particles. It merits further investigation on the  
10 interactions between OA and AS and related influence on the water uptake behaviors of aerosols  
11 during the dehydration and hydration processes.

12 Raman spectroscopy is a powerful technique to characterize aerosol compositions, water contents,  
13 molecular interactions, and particle phases especially for the efflorescence process (Ma and He,  
14 2012; Laskina et al., 2013; Zhou et al., 2014; Wang et al., 2015). In this study, the phase  
15 transformations and hygroscopic properties of OA and mixed OA/AS droplets with varying OA  
16 content were studied by confocal Raman spectroscopy in conjunction with optical microscopy.  
17 Furthermore, we explored the effects of reactions between OA and AS on the chemical  
18 compositions and hygroscopic properties of mixed OA/AS droplets.

## 19 **2 Experimental section**

### 20 **2.1 Sample preparation**

21 Ammonium sulfate (AS) and oxalic acid dihydrate were purchased from Sinopharm Chemical  
22 Reagent Co. Ltd. (99.0% purity) and used without further purification. The 0.5 mol L<sup>-1</sup> pure  
23 component AS and OA solutions were prepared by dissolving AS and oxalic acid dihydrate in  
24 ultrapure water (18.2 MΩ·cm, Barnstead Easypure II), respectively. The mixed OA/AS solutions  
25 with different organic to inorganic molar ratios (OIRs) of 1:3, 1:1 and 3:1 were obtained by  
26 dissolving a designated amount of OA into AS solutions. The sample solution was discharged from  
27 a syringe. Then, residual solution in the syringe was pushed rapidly to generate aerosol droplets  
28 spraying onto a polytetrafluorethylene (PTFE) substrate fixed to the bottom of the sample cell. Then,  
29 the sample cell was promptly sealed by a transparent polyethylene film. The RH in the sample cell  
30 was regulated by nitrogen streams consisting of a mixture of water-saturated N<sub>2</sub> and dry N<sub>2</sub> at

1 controlled flow rates. At ~ 95% RH, the droplets with a diameter of 30~40 microns detected by an  
2 optical microscope (50× objective, 0.75 numerical aperture) were selected to acquire the Raman  
3 spectra. The dry size of these particles after efflorescence ranged from 10 to 20 μm. Using a syringe,  
4 droplets from the solutions were injected onto the polytetrafluorethylene (PTFE) film fixed to the  
5 bottom of the sample cell. The diameters of these droplets ranged from 30 to 40 μm at ~ 95% RH.  
6 Then, the sample cell was sealed by a transparent polyethylene film and the RH in the sample cell  
7 was regulated by nitrogen streams consisting of a mixture of water saturated N<sub>2</sub> and dry N<sub>2</sub> at  
8 controlled flow rates. The RH and temperature of the outflow from the sample cell was measured  
9 by a humidity/temperature meter (Centertek Center 313) with an accuracy of ± 2.5% below 90%  
10 RH and ±0.7 K placed near the exit of the sample cell. The RH and temperature of the outflow from  
11 the sample cell was measured by a humidity/temperature meter (Centertek Center 313) with an  
12 accuracy of ±2.5% and ±0.7 K placed near the exit of the sample cell. The temperature accuracy of  
13 0.7 K could result in uncertainty of 4% at RH of 95%. The temperature of the sample was  
14 maintained at 297 ±0.5 K by using an automatic thermostat.

## 15 **2.2 Apparatus and conditions for the measurements**

16 The experimental setup used in this study was described in detail in previous work (Wang et al.,  
17 2008; Dong et al., 2009; Zhou et al., 2014). Briefly, the Renishaw InVia confocal Raman  
18 spectrometer equipped with a Leica DMLM microscope was used to acquire the Raman spectra. An  
19 argon-ion laser (wavelength 514.5 nm, model Stellar-REN, Modu-Laser) was used as an excitation  
20 source with an output power of 20 mW, and a 514.5 nm notch filter was adopted to remove the  
21 strong Rayleigh scattering. An 1800 g mm<sup>-1</sup> grating was used to obtain the spectra in the range of  
22 200-4000 cm<sup>-1</sup> with a resolution of about 1 cm<sup>-1</sup>. Spectral calibration was made using the 520 ±0.05  
23 cm<sup>-1</sup> Stokes shift of silicon band before performing measurements. Then, spectroscopic  
24 measurements were made on droplets observed by using the Leica DMLM microscope with a 50×  
25 objective lens (0.75 numerical aperture). The spectra were obtained with three spectral scans, and  
26 each time with an accumulation time of 10 s. The sample droplets were injected onto the substrate  
27 at high RH (~ 95% RH). Subsequently, the RH was decreased stepwise for a slow dehydration  
28 process, and then increased stepwise from RH < 3% to high RH for a hydration process. The  
29 decrease rate was typically 5-6 RH/40 min, and the rate remained 2-3 RH/40 min near the phase  
30 transition. The RH was decreased continuously in a few minutes for a rapid dehydration

1 ~~process. Subsequently, the RH was decreased stepwise for dehydration process, and increased from~~  
2 ~~RH < 3% to high RH for hydration process.~~ The particles were equilibrated with water vapor at a  
3 given RH for about 40 min, during which the intensity ratios of the water peak (3430 cm<sup>-1</sup>) to the  
4 sulfate peak (980 cm<sup>-1</sup>) remained constant. The spectra of AS, OA and mixed OA/AS droplets were  
5 monitored and measured through a full humidity cycle. Multiple particles (three or four) were  
6 selected to acquire the Raman spectra through each humidity cycle. Each humidity cycle  
7 experiment was repeated at least three times. All the measurements were taken at ambient  
8 temperature of about 297 K.

9 Raman growth factor ( $g(RH)$ ) is defined as the ratio of integrated area of OH stretching mode of  
10 water (3350–3700 cm<sup>-1</sup>) at each RH ( $A_{RH}$ ) normalized to that of a dry particle ( $A_{RH0}$ ) according to  
11 Eq. (1) (Laskina et al., 2015).

$$g(RH) = A_{RH}/A_{RH0} \quad (1)$$

12 where  $A_{RH}$  is integrated area of OH stretching mode from water (3350-3700 cm<sup>-1</sup>) at a specific RH  
13 and  $A_{RH0}$  is that of a dry particle. Hygroscopic growth curves are acquired by plotting the average  
14 Raman growth factor of duplicate particles as a function of RH. ~~Hygroscopic growth curves are~~  
15 ~~acquired by plotting the Raman growth factor as a function of RH.~~

## 17 3 Results and discussion

### 18 3.1 Raman spectra of pure AS and OA droplets

19 The Raman spectra of AS droplets during the dehydration and hydration process can be found in Fig.  
20 1a and 1b, as a function of RH can be found in Fig. S1 (a) and (b) in the Supplement, respectively.

21 AS droplets effloresce at  $44.3 \pm 2.5\%$  RH, as indicated by the disappearance of the water peak  
22 centered at 3437 cm<sup>-1</sup> and a red-shift in  $\nu_s(\text{SO}_4^{2-})$  peak position from 979 to 974 cm<sup>-1</sup> during the  
23 dehydration process. For the hydration process, the deliquescence of AS particles is observed to  
24 occur at  $80.1 \pm 1.5\%$  RH, resulting in an abrupt increase in the absorbance of the water peak  
25 centered at 3437 cm<sup>-1</sup> and a blue-shift in  $\nu_s(\text{SO}_4^{2-})$  peak position from 974 to 979 cm<sup>-1</sup>.

26 The Raman spectra of OA droplets with varying RH during the dehydration and hydration  
27 process are shown in Fig. 2, and the assignments of the peaks for OA are presented in Table 1  
28 according to previous studies (Hibben, 1935; Ebisuzaki and Angel, 1981; Chang and Huang, 1997;  
29 Mohaček-Grošev et al., 2009). As seen in Fig. 2a, the feature bands for OA droplets are observed at  
30 1460, 1750 and 3433 cm<sup>-1</sup> at 92.5% RH. At lower RH around 77% (Fig. 2a, magenta line), these

1 bands shift to 1490, 1737, 3433 and 3474  $\text{cm}^{-1}$ , and a new band at 1689  $\text{cm}^{-1}$  occurs, which is  
2 entirely consistent with the spectrum of oxalic acid dihydrate (Fig. 2a, black dashed line).~~As seen in~~  
3 ~~Fig. 1a, the feature bands for OA droplets are observed at 457, 845, 1460, 1636, 1750 and 3433  $\text{cm}^{-1}$~~   
4 ~~at 92.5% RH. At lower RH around 77% (Fig. 1a, magenta line), these bands shift to 477, 855, 1490,~~  
5 ~~1627, 1737, 3433 and 3474  $\text{cm}^{-1}$ , and a new band at 1689  $\text{cm}^{-1}$  occurs, which is entirely consistent~~  
6 ~~with the spectrum of oxalic acid dihydrate (Fig. 1a, black line).~~ It indicates OA droplets crystallize  
7 to form oxalic acid dihydrate. Oxalic acid particles after efflorescence exist in the form of dihydrate  
8 until 6.6% RH, at which the Raman spectrum of dihydrate remains unchanged for 40 min. Once RH  
9 decreases to ~5.0%, the peaks promptly shift to 1477, 1710, 2587, 2760 and 2909  $\text{cm}^{-1}$ .~~As RH~~  
10 ~~further decreases to ~5.0%, the peaks shift to 482, 828, 845, 1477, 1710, 2587, 2760 and 2909  $\text{cm}^{-1}$ ,~~  
11 and peaks at 3433 and 3474  $\text{cm}^{-1}$  assigned to  $\nu(\text{OH})$  vanish, which is the spectral feature of  
12 anhydrous oxalic acid. This result implies that oxalic acid dihydrate is converted to anhydrous  
13 oxalic acid in the RH around 5.0%. The Raman spectra of anhydrous oxalic acid particles during the  
14 hydration process as a function of RH are shown in Fig. ~~1b~~2b. It can be found that the Raman  
15 spectra feature for anhydrous oxalic acid particles occurs at  $\text{RH} < 19.6\%$ . At 19.6% RH, the peaks  
16 observed at 1490, 1737, 3433 and 3474  $\text{cm}^{-1}$  are identical to that of oxalic acid dihydrate (Fig. ~~1a~~2a,  
17 black line), indicating the formation of oxalic acid dihydrate. The observation of no spectral change  
18 until 94% RH suggests that oxalic acid dihydrate shows no deliquescence transition in the 0-94 %  
19 RH range studied, consistent with previous studies (Peng et al., 2001; Braban et al., 2003; Ma et al.,  
20 2013a; Jing et al., 2016). The transition point of anhydrous oxalic acid to oxalic acid dihydrate upon  
21 hydration is 17.9-19.6% (Fig. 2b), in agreement with the results reported by Braban et al. (2003)  
22 and Ma et al. (2013a).

### 23 **3.2 Raman spectra of OA/AS mixtures**

24 The Raman spectra of mixed OA/AS droplets with OIRs of 1:3, 1:1 and 3:1 at various RHs during  
25 the dehydration and hydration process are depicted in Fig. 3 and 4, respectively. ~~The corresponding~~  
26 ~~spectra for hydration process are given in Fig. S2 in the Supplement.~~ Since spectral features upon  
27 hydration are identical to the dehydration process, here we only analysed spectral evolution of  
28 efflorescence process in detail. The detailed assignments are summarized in Table 2. For the mixed  
29 OA/AS droplets (OIR = 1:3) at 96.2% RH (seen in Fig. 3a), the bands at 450 and 979  $\text{cm}^{-1}$  are  
30 characteristic peaks of the sulfate ion, and peak at 1049  $\text{cm}^{-1}$  are due to vibrating mode of ( $\nu_s(\text{SO}_3)$ )



1 of  $\text{HSO}_4^-$  ion. In addition, the peak at  $1741\text{ cm}^{-1}$  can be assigned to vibrating mode of OA, and peak  
 2 at  $1446\text{ cm}^{-1}$  can be attributed to vibrating mode of  $\text{HC}_2\text{O}_4^-$  ion. With decreasing RH, only small  
 3 changes are observed in the spectra until the RH reaches 34.4% RH. At 34.4% RH, the shift of  
 4  $\nu_s(\text{SO}_4^{2-})$  peak from  $979\text{ cm}^{-1}$  to  $974\text{ cm}^{-1}$  indicates the crystallization of AS, as also seen in Fig.  
 5 10b. A new band centered at  $874\text{ cm}^{-1}$  corresponds to combination bands of the vibrational mode  
 6 ( $\delta(\text{S-OH})$ ) of  $\text{HSO}_4^-$  ion from  $\text{NH}_4\text{HSO}_4$  (Dawson et al., 1986) and  $\text{HC}_2\text{O}_4^-$  ion vibrating (Shippey,  
 7 1979) A new band centered at  $874\text{ cm}^{-1}$  corresponds to the vibrational mode ( $\delta(\text{S-OH})$ ) of  $\text{HSO}_4^-$  ion  
 8 from  $\text{NH}_4\text{HSO}_4$  and the  $\text{HC}_2\text{O}_4^-$  ion vibrating (Irish and Chen, 1970; Dawson et al., 1986; Villepin  
 9 and Novak, 1971; Shippey, 1979), suggesting the formation of crystalline  $\text{NH}_4\text{HSO}_4$  and  
 10  $\text{NH}_4\text{HC}_2\text{O}_4$ . Moreover, the several new peaks at  $1416$ ,  $1469$  and  $1660\text{ cm}^{-1}$  can be attributed to the  
 11  $\text{HC}_2\text{O}_4^-$  ion vibrating of crystalline  $\text{NH}_4\text{HC}_2\text{O}_4$ . Therefore, the evolution of Raman spectra of the  
 12 mixed OA/AS droplets (OIR = 1:3) during the dehydration process confirms that OA could react  
 13 with AS to form  $\text{NH}_4\text{HSO}_4$  and  $\text{NH}_4\text{HC}_2\text{O}_4$ , which supports previous speculation for the reaction  
 14 between OA and AS (Mi ñambres et al., 2013). The reaction of OA with AS occurs via the following  
 15 pathway:



17 For the mixed OA/AS droplets (OIR = 1:1, Fig. 3b), the evolution of spectra shows resemblance  
 18 to that of mixed droplets (OIR = 1:3). At 96.1% RH, the bands at  $450$  and  $979\text{ cm}^{-1}$  are  
 19 characteristic peaks of the sulfate ion. And peaks at  $1751\text{ cm}^{-1}$ ,  $1051\text{ cm}^{-1}$  and  $1448\text{ cm}^{-1}$  can be  
 20 assigned to vibrating mode of OA,  $\text{HSO}_4^-$  ion ( $\nu_s(\text{SO}_3)$ ) and  $\text{HC}_2\text{O}_4^-$  ion, respectively. At 75.0% RH,  
 21 a new peak at  $874\text{ cm}^{-1}$  corresponding to the vibrational mode ( $\delta(\text{S-OH})$ ) of  $\text{HSO}_4^-$  and the  $\text{HC}_2\text{O}_4^-$   
 22 ion vibrating as well as the new peaks at  $494$ ,  $1469$  and  $1677\text{ cm}^{-1}$  due to the  $\text{HC}_2\text{O}_4^-$  vibrating  
 23 mode, indicates that crystalline  $\text{NH}_4\text{HC}_2\text{O}_4$  is generated from the reaction of OA with AS. As the  
 24 RH further decreases to 44.3%, the  $\nu_s(\text{SO}_4^{2-})$  band shifts from  $979\text{ cm}^{-1}$  to  $974\text{ cm}^{-1}$ , and the sharp  
 25 and narrow bands at  $450$  and  $3126\text{ cm}^{-1}$  appear, indicating the formation of crystallized AS particles.

26 For the mixed OA/AS droplets (OIR = 3:1, Fig. 3c) at 95.9% RH, the bands at  $980\text{ cm}^{-1}$ ,  $1752$   
 27  $\text{cm}^{-1}$  and  $1050\text{ cm}^{-1}$  are characteristic peak of the sulfate ion, OA and  $\text{HSO}_4^-$  ion ( $\nu_s(\text{SO}_3)$ ),  
 28 respectively. And peaks at  $1382$  and  $1460\text{ cm}^{-1}$  can be attributed to vibrating mode of  $\text{HC}_2\text{O}_4^-$  ion.  
 29 When the RH decreases to 74.4%, a new band at  $874\text{ cm}^{-1}$  could be assigned to the vibrational mode  
 30 ( $\delta(\text{S-OH})$ ) of  $\text{HSO}_4^-$  and the  $\text{HC}_2\text{O}_4^-$  ion vibrating. Meanwhile, the bands at  $494$ ,  $1471$  and  $1654$

1  $\text{cm}^{-1}$  can be attributed to  $\text{HC}_2\text{O}_4^-$  vibrating mode, suggesting OA reacts with AS to yield crystalline  
 2  $\text{NH}_4\text{HC}_2\text{O}_4$  during the dehydration process. At 64.4% RH, the peaks at 494, 874, 1471, 1654, 1718  
 3  $\text{cm}^{-1}$ , and the peak at  $3426 \text{ cm}^{-1}$  from oxalic acid dihydrate become sharp and narrow, indicating that  
 4 the OA/AS droplets (OIR = 3:1) completely crystallize to form  $\text{NH}_4\text{HSO}_4$ ,  $\text{NH}_4\text{HC}_2\text{O}_4$  and  
 5  $\text{H}_2\text{C}_2\text{O}_4 \cdot 2\text{H}_2\text{O}$  concurrently. No change in the position and shape of the bands is observed with RH  
 6 decreasing from 64.4% to 1.1%. Besides the formation of crystalline  $\text{NH}_4\text{HSO}_4$  and  $\text{NH}_4\text{HC}_2\text{O}_4$   
 7 during the dehydration process, the mixed droplets crystallize to form  $\text{H}_2\text{C}_2\text{O}_4 \cdot 2\text{H}_2\text{O}$  due to a  
 8 relatively large amount of OA in the mixed OA/AS droplets (OIR = 3:1).

### 9 **3.3 Hygroscopicity of pure AS, OA and OA/AS mixtures**

#### 10 **3.3.1 Phase transitions and chemical transformation of AS in mixed systems**

11 Considering that the peak position is sensitive to the chemical environment in the aerosols, the  
 12 position of the  $\nu_s(\text{SO}_4^{2-})$  mode can be used to determine the phase transitions of AS. The previous  
 13 studies have also applied the abrupt shift in characteristic peak position to indicate phase transition  
 14 of ammonium sulfate during the hygroscopic process (Braban and Abbatt, 2004; Ling and Chan,  
 15 2008; Yeung et al., 2009). Figure 5 presents the peak position of the  $\nu_s(\text{SO}_4^{2-})$  for AS droplets and  
 16 mixed OA/AS droplets during the dehydration and hydration process, respectively. During the  
 17 dehydration process, a red shift from  $979$  to  $974 \text{ cm}^{-1}$  can be observed for AS and OA/AS mixed  
 18 particles with OIRs of 1:3 and 1:1, indicating crystallization of AS from droplets. During the  
 19 hydration process, the observations of blue shift from  $974$  to  $979 \text{ cm}^{-1}$  for AS and OA/AS mixed  
 20 particles with OIRs of 1:3 and 1:1 suggest the deliquescence transition of AS from crystal phase to  
 21 aqueous solution. For OA/AS mixed particles with an OIR of 3:1, the peak shift between  $\sim 966$  and  
 22  $\sim 979 \text{ cm}^{-1}$  is determined during the whole RH cycle. The DRH and ERH for pure and mixed  
 23 systems have been shown in Fig. 5 and detailed discussion is given in the following section.

24 The peaks at  $\sim 1049$  and  $\sim 979 \text{ cm}^{-1}$  for mixed OA/AS droplets (OIRs = 1:3, 1:1 and 3:1) can be  
 25 attributed to the  $\text{HSO}_4^-$  and  $\text{SO}_4^{2-}$  stretching mode, respectively. The area ratio of Raman peaks  
 26 assigned to the  $\text{HSO}_4^-$  and  $\text{SO}_4^{2-}$  is used to indicate the degree of conversion of  $\text{SO}_4^{2-}$  into  $\text{HSO}_4^-$   
 27 ( $\alpha_{\text{HSO}_4^-}$ ) in mixtures, which can be expressed as following:

$$28 \quad \alpha_{\text{HSO}_4^-} = A_{1049} / (A_{1049} + A_{979}) \quad (2)$$

29 where  $A_{1049}$  and  $A_{979}$  is the peak area of the  $\text{HSO}_4^-$  and  $\text{SO}_4^{2-}$ , respectively. The  $\sim 1049 \text{ cm}^{-1}$  for  
 30  $\text{HSO}_4^-$  at solid mixture is not obvious compared to that for solutions. Thus, the calculations are

1 based on the bands at RH approaching the full efflorescence point. The estimated  $\alpha_{\text{HSO}_4^-}$  value for  
2 OIR = 1:3 (36.1% RH), OIR = 1:1 (46.2% RH) and OIR = 3:1 (66.2% RH) is 0.048, 0.368 and  
3 0.644, respectively, indicating the enhanced conversion of  $\text{SO}_4^{2-}$  into  $\text{HSO}_4^-$  with increasing OA  
4 content in the mixed systems. Due to the effects of Raman cross section,  $\alpha_{\text{HSO}_4^-}$  could not represent  
5 the actual degree of conversion. In fact, here  $\alpha_{\text{HSO}_4^-}$  is only used for comparisons of degree of  
6 conversion of  $\text{SO}_4^{2-}$  into  $\text{HSO}_4^-$  between mixed particles with varying OIRs.

### 7 3.3.2 Hygroscopic growth of pure and mixed components

8 Hygroscopicity curves of AS and OA particles are shown in Fig. 6. The optical images of the AS  
9 particle at the phase change points can be seen in Fig. 7. The ERH of AS is determined to be  $44.3 \pm$   
10  $2.5\%$  RH, which generally falls into the range from 33 to 52% RH reported in the literature (Tang  
11 and Munkelwitz, 1994a; Cziczo et al., 1997; Dougle et al., 1998; Laskina et al., 2015). The DRH of  
12 AS particles is observed to occur at  $80.1 \pm 1.5\%$  RH, which agrees well with reported values of  
13 80% RH by EDB (Tang and Munkelwitz, 1994a) and  $82.3 \pm 2.5\%$  RH by micro-Raman  
14 spectroscopy (Laskina et al., 2015). As shown in Fig. 6b and Fig. 8As shown in Fig. 4b, the  
15 measured ERH of OA is  $77 \pm 2.5\%$  RH, which deviates much from the reported value of  
16 51.8-56.7% RH by Peng et al. (2001) using the EDB technology. It is worthwhile to point out that  
17 the conversion of OA droplets to oxalic acid dihydrate at 77% RH is inconsistent with the  
18 observation of Peng et al. (2001). They observed that OA droplets crystallized to form anhydrous  
19 oxalic acid rather than oxalic acid dihydrate at 51.8-56.7% RH. The discrepancy on the ERH of OA  
20 compared to that reported by Peng et al. (2001) is likely due to the effects of substrate and sample  
21 purity. The size of dry particles ranging from 10 to 20  $\mu\text{m}$  in our experiment is consistent with  
22 observation using EDB by Peng et al. (2001), which eliminates the influence of particle size. The  
23 substrate supporting droplets may promote the heterogeneous nucleation of oxalic acid while the  
24 levitated droplets in EDB study can avoid induced nucleation by the substrate. Ghorai et al. (2014)  
25 also reported the potential effects of substrate on the efflorescence transition of NaCl/dicarboxylic  
26 acid mixed particles. In addition, The OA purity in our study is 99.0% lower than that of 99.5% in  
27 study by Peng et al. (2001). Thus, trace amounts of impurities in OA droplets acting as a  
28 heterogeneous nucleus could contribute to crystallization and result in a higher ERH of OA. Due to  
29 the effects of substrate and sample purity, the heterogeneous nucleation should be responsible for  
30 the discrepancy on the observed ERH of OA. The discrepancies between this study and that by Peng

1 ~~et al. (2001) is likely due to the effects of droplet size, substrate and experimental method.~~  
2 ~~According to classical nucleation theory, the probability of the formation of the critical nucleus is~~  
3 ~~proportional to the particle volume (Martin, 2000; Parsons et al., 2006). Considering that the droplet~~  
4 ~~size in our study was approximately 1-2 times larger than that observed by Peng et al. (2001), the~~  
5 ~~droplets deposited on the substrate in our experiment may promote the heterogeneous nucleation~~  
6 ~~while the levitated droplets using EDB can dispel the heterogeneous nucleation. Thus, the ERH of~~  
7 ~~OA obtained in our study is higher than the observation of Peng et al. (2001).~~ The water content of  
8 the supersaturated droplet at the onset of crystallization determines the form of oxalic acid crystal  
9 generated, i. e., anhydrous OA or OA dihydrate. Due to a higher ERH, oxalic acid droplets with  
10 more water content favor the formation of a dihydrate after crystallization. It should be noted that  
11 our experiment appears to be favored in the atmospheric environment, considering that insoluble  
12 material such as mineral dust mixed with OA may play the role of substrate thus facilitating the  
13 heterogeneous nucleation of OA aerosols. The Raman growth factor of OA shows no obvious  
14 change between ~77% and 6.6% RH upon dehydration. At RH lower than 5%, the Raman growth  
15 factors drop abruptly due to the transformation of crystalline  $\text{H}_2\text{C}_2\text{O}_4 \cdot 2\text{H}_2\text{O}$  into anhydrous oxalic  
16 acid, as also indicated by Raman spectrum. It seems that the structure of anhydrous OA particle is  
17 not as compact as that of dihydrate, seen in Fig. 8. Thus, the loss of crystal water results in no  
18 obvious change in particle size. During the hydration process, the Raman growth factor of OA  
19 shows a slightly increase at 19.6% RH, which can be attributed to the conversion of anhydrous  
20 oxalic acid to dihydrate. The transition point of anhydrous oxalic acid to oxalic acid dihydrate  
21 agrees with previous studies (Braban et al., 2003; Ma et al., 2013b; Miñambres et al., 2013). No  
22 deliquescence behavior is observed for oxalic acid dihydrate even at 94% RH, consistent with early  
23 observations (Ma et al., 2013b; Miñambres et al., 2013; Jing et al., 2016).

24 Figure 9 presents hygroscopic growth of OA/AS mixtures with OIRs of 1:3, 1:1 and 3:1. As can  
25 be seen in Fig. 9a and 10b, mixed OA/AS droplets (OIR = 1:3) exhibit efflorescence transition at  
26 lower  $34.4 \pm 2.0\%$  RH relative to ERH ( $44.3 \pm 2.5\%$ ) of pure AS. During the hydration process,  
27 mixed particles start to absorb slight water before deliquescence at  $81.1 \pm 1.5\%$  RH (seen in Fig. 9  
28 and 10). It can be seen in Fig. 10 that the size of 1:3 mixed OA/AS particle at 79.4% RH prior to  
29 deliquescence appears to be larger than that after complete efflorescence. The decrease in ERH and  
30 slight water uptake before deliquescence for 1:3 mixed particles is likely due to the effects of

1  $\text{NH}_4\text{HSO}_4$  formed upon dehydration.  $\text{NH}_4\text{HSO}_4$  has a low ERH (22-0.05%) and DRH (40%) (Tang  
2 and Munkelwitz, 1994a), which may affect the nucleation and crystallization of AS upon  
3 dehydration and lead to slight water uptake prior to the deliquescence of AS. The hygroscopic  
4 growth of mixed particles upon dehydration is in fair agreement with that of pure AS or OA.  
5 However, the Raman growth factors of mixed particles upon hydration show a considerable  
6 decrease in comparison to that upon dehydration. The discrepancies for Raman growth factor at  
7 high RH between the two processes can be attributed to the formation of  $\text{NH}_4\text{HC}_2\text{O}_4$ , which has a  
8 high deliquescence point larger than 95% RH (Schroeder and Beyer, 2016). During the hydration  
9 process,  $\text{NH}_4\text{HC}_2\text{O}_4$  in the mixed aerosols remains solid even at high RH (also seen in Fig. 10d),  
10 resulting in less water uptake of mixed particles. The similar phenomenon is also observed for  
11 NaCl/OA mixed particles upon hydration due to the formation of less hygroscopic sodium oxalate  
12 (Peng et al., 2016).

13 The mixed OA/AS droplets with an OIR = 1:1 first partially effloresce at  $75.0\% \pm 1.6\%$  due to  
14 the crystallization of  $\text{NH}_4\text{HC}_2\text{O}_4$ , as indicated by Raman spectra. Then, the full efflorescence occurs  
15 at  $44.3 \pm 2.5\%$  RH with the crystallization of AS. The full ERH of 1:1 OA/AS mixed droplets is  
16 highly consistent with that of pure AS. During the hydration process, the Raman growth factor of  
17 1:1 mixed particles increases slightly at 35.5% RH, and then remains almost invariable until 77%  
18 RH, which is likely due to the formation of hydrate. The deliquescence transition occurs at  $77 \pm$   
19  $1.0\%$  RH slightly lower than DRH of AS, which agrees with literature results for AS particles  
20 containing OA (Brooks et al., 2002; Jing et al., 2016). The water contents of mixed droplets after  
21 deliquescence are significantly lower than those upon dehydration. The Raman features at  $494 \text{ cm}^{-1}$   
22 and  $874 \text{ cm}^{-1}$  have confirmed the presence of solid  $\text{NH}_4\text{HC}_2\text{O}_4$  upon hydration across all RHs  
23 studied (seen in Fig. 4), which should be responsible for the decreasing water uptake of the mixed  
24 particles at high RH.

25 For mixed OA/AS droplets with an OIR = 3:1, the partial and full efflorescence transition could  
26 be observed at  $74.4 \pm 1.0\%$  RH and  $64.4 \pm 3.0\%$  RH, respectively (seen in Fig. 9 and 11). As seen  
27 in Fig. 3c, the bands at 494, 1471 and  $1654 \text{ cm}^{-1}$  suggest the formation of crystalline  $\text{NH}_4\text{HC}_2\text{O}_4$  at  
28  $74.4 \pm 1.0\%$  RH. Figure 12 presents the spatial distribution of chemicals within mixed OA/AS (OIR  
29 = 3:1) particles at 74.4% RH. The characteristic peak of  $980 \text{ cm}^{-1}$ ,  $1050 \text{ cm}^{-1}$  and  $1471 \text{ cm}^{-1}$  is  
30 assigned to  $\text{SO}_4^{2-}$ ,  $\text{HSO}_4^-$  and  $\text{HC}_2\text{O}_4^-$ , respectively. The sharp absorption at  $874 \text{ cm}^{-1}$  and obvious

1 peak at 1471 cm<sup>-1</sup> indicate the abundant content of NH<sub>4</sub>HC<sub>2</sub>O<sub>4</sub>. The comparison of characteristic  
2 peaks between inner and outer phase reveals that the major component on the surface of a mixed  
3 OA/AS (OIR = 3:1) particle is NH<sub>4</sub>HC<sub>2</sub>O<sub>4</sub>. In contrast to the surface, the obvious features of 980  
4 cm<sup>-1</sup> and 1050 cm<sup>-1</sup> at the core of the particle suggest that (NH<sub>4</sub>)<sub>2</sub>SO<sub>4</sub> and NH<sub>4</sub>HSO<sub>4</sub> mainly exist in  
5 the inner aqueous phase. During the dehydration process, crystalline NH<sub>4</sub>HC<sub>2</sub>O<sub>4</sub> in the outer phase  
6 acts as the heterogeneous nucleus, leading to the crystallization of oxalic acid dihydrate, (NH<sub>4</sub>)<sub>2</sub>SO<sub>4</sub>  
7 and NH<sub>4</sub>HSO<sub>4</sub> in the inner phase. The crystallization of NH<sub>4</sub>HC<sub>2</sub>O<sub>4</sub> may act as crystallization nuclei  
8 for NH<sub>4</sub><sup>+</sup>, HSO<sub>4</sub><sup>-</sup> and OA in the mixed droplets to form NH<sub>4</sub>HSO<sub>4</sub> crystal and oxalic acid dihydrate.

9 Thus, the full ERH of 3:1 OA/AS mixed droplets is higher than that of pure AS (44.3 ± 2.5% RH)  
10 and NH<sub>4</sub>HSO<sub>4</sub> (22-0.05% RH). During the hydration process, Raman growth factors of mixed  
11 particles slightly increase at 34.5% RH. No deliquescence transition or significant water uptake is  
12 observed over the RH range studied. This phenomenon can be explained by the fact that the most of  
13 AS in the mixtures has been converted into NH<sub>4</sub>HC<sub>2</sub>O<sub>4</sub> and NH<sub>4</sub>HSO<sub>4</sub>. Although NH<sub>4</sub>HSO<sub>4</sub> with a  
14 low DRH may contribute to water uptake of mixed particles, the minor NH<sub>4</sub>HSO<sub>4</sub> formed in the  
15 mixtures is likely to be coated by NH<sub>4</sub>HC<sub>2</sub>O<sub>4</sub> and OA with a high DRH. Thus, the mixed OA/AS  
16 particles with OIR = 3:1 show no obvious hygroscopic growth upon hydration due to the change in  
17 aerosol composition and morphology effects. The effects of morphology on the hygroscopic growth  
18 of aerosols have been reported for AS particles containing adipic acid (Sjogren et al., 2007). The  
19 water uptake of AS particles containing relatively high content of adipic acid could be suppressed  
20 due to AS enclosed by the crust of solid adipic acid with a high DRH.

21 The observed efflorescence relative humidity (ERH) for mixed droplets was dependent on the  
22 molar ratio of oxalic acid to ammonium sulfate. The mixed OA/AS droplets with an OIR of 1:3 are  
23 observed to effloresce completely at 34.4 ± 2.0% RH relative to ERH of pure AS (44.3 ± 2.5%) or  
24 OA (77 ± 2.5%). It can be seen that AS as a major fraction of the particle does not promote the  
25 heterogeneous nucleation of OA. Meanwhile, the crystallization of AS is also influenced due to the  
26 presence of OA. The similar phenomenon was also observed for malonic acid/ammonium sulfate  
27 mixtures with minor organic content (Braban and Abbatt, 2004; Parsons et al., 2004). Braban and  
28 Abbatt (2004) found that the ERH of malonic acid/ammonium sulfate mixed particles was  
29 considerably decreased compared to that of pure ammonium sulfate for mass fractions of malonic  
30 acid less than 0.3. They concluded that the presence of ammonium sulfate in the supersaturated

1 droplet could exert the extra barrier to nucleation of malonic acid crystals rather than play the role  
2 of a heterogeneous nucleation site. As for 1:3 OA/AS mixed droplets, ammonium sulfate may also  
3 inhibit the nucleation of oxalic acid at relatively high RH. With decreasing RH, aqueous oxalic acid  
4 could enhance the viscosity of the droplet due to hydrogen bond interactions (Mikhailov et al.,  
5 2009), thus limiting the nucleation of ammonium sulfate and resulting in a lower ERH with respect  
6 to the value of pure AS (Parsons et al., 2004). In the case of mixed OA/AS droplets with an OIR of  
7 1:1 and 3:1, the  $\text{NH}_4\text{HC}_2\text{O}_4$  formed at ~75% RH upon dehydration likely acts as a heterogeneous  
8 nucleus for crystallization of other components, which increases full efflorescence point of mixed  
9 particles. One study indicated that Aldrich humic acid sodium salt (NaHA) could also promote the  
10 ERH of ammonium sulfate (Badger et al., 2006). Similar to oxalic acid, succinic acid and adipic  
11 acid have a high deliquescence point and low solubility. However, it has been found that the  
12 efflorescence point of ammonium sulfate in mixed particles is not elevated even when the content  
13 of succinic acid or adipic acid is not less than 50% by mass or mole fractions (Ling and Chan, 2008;  
14 Yeung et al., 2009; Laskina et al., 2015). In contrast to ammonium sulfate particles containing  
15 succinic acid or adipic acid, our results suggest that the addition of oxalic acid into ammonium  
16 sulfate droplets may trigger partial and full crystallisation of aerosols at relatively higher RH upon  
17 dehydration due to  $\text{NH}_4\text{HC}_2\text{O}_4$  product acting as an effective nucleus.

18 During the deliquescence process, the OA/AS mixed particles with an OIR of 1:3 and 1:1 exhibit  
19 a slightly lower deliquescence point than that of pure ammonium sulfate, consistent with previous  
20 observations of effects of crystalline oxalic acid on deliquescence transition of ammonium sulfate  
21 (Brooks et al., 2002; Wise et al., 2003; Jing et al., 2016). It should be noted that prior literature  
22 result also showed that continuous or smooth water uptake from low RH was observed for particles  
23 composed of AS and OA with a mass ratio of 1.5:1 due to the fact that after drying processing  
24 oxalic acid existing in an amorphous or liquid-like state prevented nucleation of ammonium sulfate  
25 even under dry conditions (Prenni et al., 2003). In the present study, water uptake by the OA/AS  
26 mixed particles at high RH upon hydration is dramatically lower than that upon dehydration and  
27 significantly decreased with elevated OA content. This phenomenon distinguishes from hygroscopic  
28 characteristic of typical water-soluble mixtures in literatures. It has been found that hydration  
29 growth curve and dehydration growth curve are typically merged above deliquescence point for  
30 mixed systems containing inorganic salts and water-soluble organic compounds (Choi and Chan,

1 2002; Chan and Chan, 2003; Gysel et al., 2004; Clegg and Seinfeld, 2006; Sjogren et al., 2007;  
2 Pope et al., 2010; Ghorai et al., 2014; Estillore et al., 2016). In this study, Raman spectra and  
3 micrograph suggest the presence of solid  $\text{NH}_4\text{HC}_2\text{O}_4$  and residual solid OA at high RH should be  
4 responsible for the decreased water uptake during the hydration process. In contrast, Prenni et al.  
5 (2003) reported that the hygroscopic growth of OA/AS mixed particles remained unchanged at 90%  
6 RH with OA mass fraction ranging from 0.01 to 0.4. In addition, they also found that water uptake  
7 after deliquescence was well described by the model method assuming complete dissolution of OA  
8 in aqueous phase as well as no interactions between OA and AS, which was also observed by Jing et  
9 al. (2016) using the HTDMA. The previous HTDMA studies for OA/AS mixed particles indicate no  
10 composition change and no specific interactions existing between OA and AS (Prenni et al., 2003;  
11 Jing et al., 2016). However, it should be noted that the HTDMA studies did not perform  
12 measurements for the dehydration process such that aerosols underwent rapid drying on the time  
13 scale of seconds, i.e., the total residence time for transformation of droplets into dry particles in the  
14 drying section of HTDMA is typically tens of seconds (Prenni et al., 2003; Jing et al., 2016), much  
15 shorter than that (10 ~ 12 h) in our study. In the HTDMA experiments, the combination of faster  
16 drying and smaller particles with submicron size implies that the aqueous phase obtained higher  
17 supersaturations than in our present study (Rosenoern et al., 2008), leading to less dissociation of  
18 oxalic acid and thus less  $\text{HC}_2\text{O}_4^-$  formed in the droplets as well as the inhibited formation of  
19  $\text{NH}_4\text{HC}_2\text{O}_4$ . The fast evaporation of water from the surface of an aqueous droplet upon rapid drying  
20 could result in a higher surface concentration of solutes than the slow drying process (Treuel et al.,  
21 2011). The higher surface concentration of oxalic acid corresponds to less formation and hence  
22 decreased supersaturation of  $\text{HC}_2\text{O}_4^-$ . Due to the dependence of nucleation rate on the extent of  
23 supersaturation, it can be expected that the nucleation of  $\text{NH}_4\text{HC}_2\text{O}_4$  is suppressed within OA/AS  
24 mixed droplets undergoing rapid drying.~~The effects of OA on deliquescence behavior of AS has~~  
25 ~~been widely studied. Our results are consistent with early observations that OA had no obvious~~  
26 ~~effects on the DRH of AS in the OA/AS mixtures with a low ratio of OA (Brooks et al., 2002; Wise~~  
27 ~~et al., 2003; Prenni et al., 2003). Prenni et al. (2003) and Miñambres et al. (2013) observed that the~~  
28 ~~equal mass AS/OA mixed particles exhibited a continuous hygroscopic growth through the~~  
29 ~~humidity range studied due to oxalic acid in an amorphous state at low RH. The previous HTDMA~~  
30 ~~studies for equal mass OA/AS mixed particles found that water uptake upon hydration at high RH~~



~~could be well described by the model methods based on assumption of no composition change, suggesting no specific interactions exist between oxalic acid and ammonium sulfate. However, it should be noted that the total residence time for transformation of droplets into dry particles in the drying section of HTDMA is typically tens of seconds (Kumar et al., 2003; Prenni et al., 2003; Jing et al., 2016; Peng et al., 2016), much shorter than that (10 ~ 12 h) in our study.~~

Considering the potential effects of drying time on the reactions between OA and AS, we explored the hygroscopicity of OA/AS particles with an OIR of 1:1 after rapid drying process. The mixed OA/AS droplets undergo dehydration to form dry particles in 3 ~ 5 min. We observed one-step efflorescence of rapidly-dried particles (1:1, molar ratio) occurred at 47% ± 2.5% RH, compared to the two-step efflorescence of slowly-dried particles occurring at 75% and 44.3% RH, respectively. The Raman spectra and hygroscopic curve upon hydration for OA/AS particles with an OIR of 1:1 are presented in Fig. 13. The obvious discrepancies can be observed for spectra at ~2% RH between the two drying processes. After rapid drying process, the spectra at ~2% RH show the feature of crystalline AS ( $967\text{ cm}^{-1}$ ,  $\nu_s(\text{SO}_4^{2-})$ ) and anhydrous OA ( $1710\text{ cm}^{-1}$ ,  $\nu(\text{C}=\text{O})$ ;  $1479\text{ cm}^{-1}$ ,  $\nu_s(\text{COO})$ ). Meanwhile, no characteristic peaks for  $\text{NH}_4\text{HC}_2\text{O}_4$  ( $494\text{ cm}^{-1}$ ,  $\delta(\text{COO})$ ;  $874\text{ cm}^{-1}$ ,  $\nu(\text{C}-\text{C})$ ;  $1729\text{ cm}^{-1}$ ,  $\nu(\text{C}=\text{O})$ ;  $1469\text{ cm}^{-1}$ ,  $\nu_s(\text{COO})$ ) and  $\text{NH}_4\text{HSO}_4$  ( $874\text{ cm}^{-1}$ ,  $\delta(\text{S}-\text{OH})$ ) can be identified in the spectra. It is clear that the drying time for transformation of droplets into dry particles has impacts on the reactions of OA with AS in the aerosols due to particle-phase processes under kinetic control. Previous studies found the longer drying time could lead to greater nitrate depletion between nitrates and organic acids, which results from slow reaction and diffusion in the viscous aerosols (Wang and Laskin, 2014). The Raman growth factors of mixed particles with an OIR of 1:1 also increase slightly at 36.5% RH due to the formation of OA dihydrate, as indicated by the Raman feature. The deliquescence transition of mixed particles occurs at 79.3% RH. After deliquescence, Raman growth factors of mixed particles after rapid drying process are lower than that after slow drying process, which may be caused by the fact that at high RH the hygroscopic growth of AS is slightly lower than that of  $\text{NH}_4\text{HSO}_4$  formed in the particles after slow drying process (Tang and Munkelwitz, 1977). In addition, it is found that after deliquescence OA dihydrate remains solid in the mixed particles after rapid drying process.

#### 4 Conclusions and atmospheric implications~~4 Conclusions~~

In this work, confocal Raman spectroscopy is used to investigate the hygroscopic properties and

1 phase transformations of OA and internally mixed OA/AS droplets (OIRs = 1:3, 1:1 and 3:1). OA  
2 droplets effloresce to form oxalic acid dihydrate at  $77 \pm 2.5\%$  RH, and then oxalic acid dihydrate  
3 further loses crystalline water to form anhydrous oxalic acid at  $\sim 5.0\%$  RH during the dehydration  
4 process. The Raman spectra of mixed OA/AS droplets reveal the formation of  $\text{NH}_4\text{HC}_2\text{O}_4$  and  
5  $\text{NH}_4\text{HSO}_4$  from the reaction of OA with AS in aerosols after slow dehydration process. The  
6 deliquescence and efflorescence point for AS is observed to occur at  $80.1 \pm 1.5\%$  and  $44.3 \pm 2.5\%$   
7 RH, respectively. The ERH of the mixed OA/AS droplets with 1:3, 1:1 and 3:1 ratio is determined  
8 to be  $34.4 \pm 2.0\%$ ,  $44.3 \pm 2.5\%$  and  $64.4 \pm 3.0\%$  RH, respectively, indicating significant effects of  
9 OA content on the efflorescence transition of AS. The mixed OA/AS particles with 1:3 and 1:1 ratio  
10 show deliquescence transition at  $81.1 \pm 1.5\%$  and  $77 \pm 1.0\%$  RH, respectively, which is close to the  
11 DRH of AS. The mixed OA/AS particles with 3:1 ratio exhibit no deliquescence transition over the  
12 RH range studied due to the transformation of  $(\text{NH}_4)_2\text{SO}_4$  into nonhygroscopic  $\text{NH}_4\text{HC}_2\text{O}_4$ . The  
13 hygroscopic growth of mixed particles at high RH upon hydration is substantially lower than that of  
14 corresponding dehydration process and further decreases with increasing OA content. The  
15 discrepancies for water content of mixed particles between the two processes at high RH can be  
16 explained by the significant formation of low hygroscopic  $\text{NH}_4\text{HC}_2\text{O}_4$  and residual OA, which still  
17 remain solid and thus result in less water uptake of mixed particles.

18 The prior hygroscopic studies suggest that crystallization of internally mixed ammonium  
19 sulfate/dicarboxylic acid particles may lead to the formation of trace organic salt. Lightstone et al.  
20 (2000) estimated that approximately 2% of the initial succinic acid may form ammoniated succinate  
21 within mixed ammonium nitrate/succinic acid particles during the efflorescence process. Ling and  
22 Chan (2008) inferred that crystallization of ammonium sulfate/succinic acid droplets likely  
23 generated metastable organic salt based on change in the Raman peak form of succinic acid. Braban  
24 and Abbatt (2004) reported that  $\text{NH}_4\text{HSO}_4$  and ammoniated malonate were likely generated upon  
25 crystallization of mixed ammonium sulfate/malonic acid particles. However, due to the trace  
26 amount of organic salt below Raman or infrared detection limit, they found no apparent influence of  
27 organic salt formed upon dehydration on the water uptake or phase change of mixed particles. In  
28 contrast, our results indicate that the chemical processing upon drying of droplets containing OA  
29 and AS influences efflorescence transition and water uptake of mixed aerosols during the humidity  
30 cycle by modifying particulate component.

1 Our results highlight the atmospheric importance of dicarboxylic acid–ammonium sulfate  
2 interactions in aerosol aqueous chemistry. Such chemical processing upon drying of aerosols  
3 comprised of organic acid/(NH<sub>4</sub>)<sub>2</sub>SO<sub>4</sub> mixtures may enhance the acidity of aqueous phase in the  
4 intermediate RH due to the transformation of (NH<sub>4</sub>)<sub>2</sub>SO<sub>4</sub> into NH<sub>4</sub>HSO<sub>4</sub>. These experiments also  
5 imply that the chemical reaction between aqueous (NH<sub>4</sub>)<sub>2</sub>SO<sub>4</sub> and oxalic acid upon slow  
6 dehydration is a possible formation pathway for the low-volatility oxalate in ambient particles,  
7 which could enhance partitioning of dicarboxylic acids to aqueous particles with the presence of  
8 ammonium sulfate (Yli-Juuti et al., 2013; Hakkinen et al., 2014). It has been reported that the  
9 aerosol aqueous processing within organic acid/AS mixtures partly contributes to enhanced  
10 loadings of secondary organic aerosol (SOA) from biogenic precursors (Hoyle et al., 2011).  
11 Compared to aqueous processing such as condensed phase acid-catalyzed reactions relevant to  
12 formation of organosulfates, the contribution of other aerosol processing containing organic salt  
13 formation to SOA burden likely becomes important under less acidic condition. Formation of  
14 low-solubility organic salts from aqueous processing within aerosols alters particle-phase  
15 component and thus modifies aerosol’s hygroscopicity, optical properties and chemical reactivity.  
16 Our findings provide fundamental insight into effects of drying conditions (drying rate or time) on  
17 formation of organic salt from reactions of organic acids with inorganic salts in particle phase under  
18 ambient RH conditions. Overall, a better understanding of the chemical interactions between  
19 species in a multicomponent system during the humidity cycle is critical for the accurate modeling  
20 efforts of aerosol phase behavior in thermodynamic models.~~Field and laboratory observations have~~  
21 ~~shown that organic acids can react with inorganic salts within aerosols (Kerminen et al., 1998;~~  
22 ~~Laskin et al., 2012; Laskina et al., 2013; Ma et al., 2013b; Wang and Laskin, 2014; Ghorai et al.,~~  
23 ~~2014; Peng et al., 2016). Ma et al. (2013b) observed that reactions of OA with NaCl upon~~  
24 ~~dehydration resulted in the formation of less hygroscopic disodium oxalate driven by the high~~  
25 ~~volatility of gaseous HCl. Wang and Laskin (2014) reported that the water-soluble organic acids~~  
26 ~~could react with nitrates due to the release of HNO<sub>3</sub> during the dehydration process. Despite no~~  
27 ~~release of high volatile gas (such as HCl and HNO<sub>3</sub>), our results reveal that OA can react with AS to~~  
28 ~~form low hygroscopic organic salts in aerosols undergoing slow dehydration process. Our finds~~  
29 ~~highlight the role of drying rate in formation of organic salts from reactions of organic acids with~~  
30 ~~inorganic salts in aerosols under ambient RH conditions. Thus, the drying conditions have potential~~

1 ~~effects on reactions and composition in aerosols, which have important implications for~~  
2 ~~atmospheric chemistry.~~

3 **Data availability.** All data are available upon request from the corresponding authors.

4 **Acknowledgments.** This project was supported by the National Natural Science Foundation of  
5 China (Contract No. 91544223, 21473009, and 21373026).

6 ~~The Supplement related to this article is available online at supplement.~~

## 7 **References**

8 Amundson, N. R., Caboussat, A., He, J. W., Martynenko, A. V., and Seinfeld, J. H.: A phase  
9 equilibrium model for atmospheric aerosols containing inorganic electrolytes and organic  
10 compounds (UHAERO), with application to dicarboxylic acids, J. Geophys. Res.: Atmos., 112,  
11 D24S13, 2007.

12 Badger, C. L., George, I., Griffiths, P. T., Braban, C. F., Cox, R. A., and Abbatt, J. P. D.: Phase  
13 transitions and hygroscopic growth of aerosol particles containing humic acid and mixtures of  
14 humic acid and ammonium sulphate, Atmos. Chem. Phys., 6, 755-768, 2006.

15 Braban, C. F., Carroll, M. F., Styler, S. A., and Abbatt, J. P. D.: Phase transitions of malonic and  
16 oxalic acid aerosols, J. Phys. Chem. A, 107, 6594-6602, doi: 10.1021/jp034483f, 2003.

17 Braban, C. F., and Abbatt, J. P. D.: A study of the phase transition behavior of internally mixed  
18 ammonium sulfate-malonic acid aerosols, Atmos. Chem. Phys., 4, 1451-1459, 2004.

19 Brooks, S. D., Wise, M. E., Cushing, M., and Tolbert, M. A.: Deliquescence behavior of  
20 organic/ammonium sulfate aerosol, Geophys. Res. Lett., 29, 1917, doi: 10.1029/2002gl014733,  
21 2002.

22 Chan, M. N., and Chan, C. K.: Hygroscopic properties of two model humic-like substances and  
23 their mixtures with inorganics of atmospheric importance, Environ. Sci. Technol., 37, 5109-5115,  
24 10.1021/es034272o, 2003.

25 Chang, H., and Huang, P. J.: Thermal decomposition of  $\text{CaC}_2\text{O}_4 \cdot \text{H}_2\text{O}$  studied by thermo-Raman  
26 spectroscopy with TGA/DTA, Anal. Chem., 69, 1485-1491, doi: 10.1021/ac960881i, 1997.

27 Chebbi, A., and Carlier, P.: Carboxylic acids in the troposphere, occurrence, sources, and sinks: A  
28 review, Atmos. Environ., 30, 4233-4249, doi: 10.1016/1352-2310(96)00102-1, 1996.

29 Choi, M. Y., and Chan, C. K.: The effects of organic species on the hygroscopic behaviors of

- 1 [inorganic aerosols, Environ. Sci. Technol., 36, 2422-2428, 10.1021/es0113293, 2002.](#)
- 2 [Clegg, S. L., and Seinfeld, J. H.: Thermodynamic models of aqueous solutions containing inorganic](#)
- 3 [electrolytes and dicarboxylic acids at 298.15 K. 1. The acids as nondissociating components, J.](#)
- 4 [Phys. Chem. A, 110, 5692-5717, 10.1021/jp056149k, 2006.](#)
- 5 ~~[Colberg, C. A.: Experimente an levitierten H<sub>2</sub>SO<sub>4</sub>/NH<sub>3</sub>/H<sub>2</sub>O Aerosolteilchen: Atmosphärische](#)~~
- 6 ~~[Relevanz von Letovizit, Ph.D. Dissertation, Swiss federal institute of technology \(ETH\) Zuerich,](#)~~
- 7 ~~[2001.](#)~~
- 8 Cziczo, D. J., Nowak, J. B., Hu, J. H., and Abbatt, J. P. D.: Infrared spectroscopy of model
- 9 tropospheric aerosols as a function of relative humidity: Observation of deliquescence and
- 10 crystallization, J. Geophys. Res., 102, 18843-18850, doi: 10.1029/97jd01361, 1997.
- 11 Dawson, B. S. W., Irish, D. E., and Toogood, G. E.: Vibrational spectral studies of solutions at
- 12 elevated temperatures and pressures. 8. A Raman spectral study of ammonium hydrogen sulfate
- 13 solutions and the HSO<sub>4</sub><sup>-</sup>-SO<sub>4</sub><sup>2-</sup> equilibrium, J. Phys. Chem., 90, 334-341, doi:
- 14 10.1021/j100274a027, 1986.
- 15 Dong, J. L., Xiao, H. S., Zhao, L. J., and Zhang, Y. H.: Spatially resolved Raman investigation on
- 16 phase separations of mixed Na<sub>2</sub>SO<sub>4</sub>/MgSO<sub>4</sub> droplets, J. Raman Spectrosc., 40, 338-343, doi:
- 17 10.1002/jrs.2132, 2009.
- 18 Dougle, P. G., Veefkind, J. P., and ten Brink, H. M.: Crystallisation of mixtures of ammonium
- 19 nitrate, ammonium sulphate and soot, J. Aerosol Sci., 29, 375-386, doi:
- 20 10.1016/S0021-8502(97)10003-9, 1998.
- 21 Drozd, G., Woo, J., Häkkinen, S. A. K., Nenes, A., and McNeill, V. F.: Inorganic salts interact with
- 22 oxalic acid in submicron particles to form material with low hygroscopicity and volatility, Atmos.
- 23 Chem. Phys., 14, 5205-5215, doi: 10.5194/acp-14-5205-2014, 2014.
- 24 Ebisuzaki, Y., and Angel, S. M.: Raman study of hydrogen bonding in  $\alpha$  and  $\beta$ -oxalic acid
- 25 dihydrate, J. Raman Spectrosc., 11, 306-311, doi: 10.1002/jrs.1250110416, 1981.
- 26 [Estillore, A. D., Hettiyadura, A. P. S., Qin, Z., Leckrone, E., Wombacher, B., Humphry, T., Stone, E.](#)
- 27 [A., and Grassian, V. H.: Water uptake and hygroscopic growth of organosulfate aerosol, Environ.](#)
- 28 [Sci. Technol., 50, 4259-4268, 10.1021/acs.est.5b05014, 2016.](#)
- 29 Ghorai, S., Wang, B., Tivanski, A., and Laskin, A.: Hygroscopic properties of internally mixed
- 30 particles composed of NaCl and water-soluble organic acids, Environ. Sci. Technol., 48,

1 2234-2241, doi: 10.1021/es404727u, 2014.

2 Gysel, M., Weingartner, E., Nyeki, S., Paulsen, D., Baltensperger, U., Galambos, I., and Kiss, G.:  
3 Hygroscopic properties of water-soluble matter and humic-like organics in atmospheric fine  
4 aerosol, Atmos. Chem. Phys., 4, 35-50, 2004.

5 Hakkinen, S. A. K., McNeill, V. F., and Riipinen, I.: Effect of Inorganic Salts on the Volatility of  
6 Organic Acids, Environ. Sci. Technol., 48, 13718-13726, 10.1021/es5033103, 2014.

7 Hibben, J. H.: The Raman Spectra of Oxalic Acid, J. Chem. Phys., 3, 675-679, doi:  
8 10.1063/1.1749575, 1935.

9 Hoyle, C. R., Boy, M., Donahue, N. M., Fry, J. L., Glasius, M., Guenther, A., Hallar, A. G., Hartz,  
10 K. H., Petters, M. D., Petaja, T., Rosenoern, T., and Sullivan, A. P.: A review of the anthropogenic  
11 influence on biogenic secondary organic aerosol, Atmos. Chem. Phys., 11, 321-343,  
12 10.5194/acp-11-321-2011, 2011.

13 ~~Irish, D. E., and Chen, H.: Equilibriums and proton transfer in the bisulfate-sulfate system, J. Phys.~~  
14 ~~Chem., 74, 3796-3801, doi: 10.1021/j100715a014, 1970.~~

15 Jacobson, M. C., Hansson, H. C., Noone, K. J., and Charlson, R. J.: Organic atmospheric aerosols:  
16 Review and state of the science, Rev. Geophys., 38, 267-294, doi: 10.1029/1998RG000045,  
17 2000.

18 Jing, B., Tong, S. R., Liu, Q. F., Li, K., Wang, W. G., Zhang, Y. H., and Ge, M. F.: Hygroscopic  
19 behavior of multicomponent organic aerosols and their internal mixtures with ammonium sulfate,  
20 Atmos. Chem. Phys., 16, 4101-4118, 2016.

21 Jing, B., Peng, C., Wang, Y., Liu, Q. F., Tong, S. R., Zhang, Y. H., and Ge, M. F.: Hygroscopic  
22 properties of potassium chloride and its internal mixtures with organic compounds relevant to  
23 biomass burning aerosol particles, Sci. Rep., 7, 43572, doi: 10.1038/srep43572, 2017.

24 Kanakidou, M., Seinfeld, J. H., Pandis, S. N., Barnes, I., Dentener, F. J., Facchini, M. C., Van  
25 Dingenen, R., Ervens, B., Nenes, A., Nielsen, C. J., Swietlicki, E., Putaud, J. P., Balkanski, Y.,  
26 Fuzzi, S., Horth, J., Moortgat, G. K., Winterhalter, R., Myhre, C. E. L., Tsigaridis, K., Vignati, E.,  
27 Stephanou, E. G., and Wilson, J.: Organic aerosol and global climate modelling: a review, Atmos.  
28 Chem. Phys., 5, 1053-1123, doi: 10.5194/acp-5-1053-2005, 2004.

29 Kawamura, K., and Bikkina, S.: A review of dicarboxylic acids and related compounds in  
30 atmospheric aerosols: Molecular distributions, sources and transformation, Atmos. Res., 170,

- 1 140-160, doi: 10.1016/j.atmosres.2015.11.018, 2016.
- 2 ~~Kerminen, V. M., Teinilä K., Hillamo, R., and Pakkanen, T.: Substitution of chloride in sea salt~~  
3 ~~particles by inorganic and organic anions, J. Aerosol Sci., 29, 929-942, doi:~~  
4 ~~10.1016/S0021-8502(98)00002-0, 1998.~~
- 5 ~~Kruus, P., Hayes, A. C., and Adams, W. A.: Determination of ratios of sulfate to bisulfate ions in~~  
6 ~~aqueous solutions by raman spectroscopy, J. Solution Chem., 14, 117-128, doi:~~  
7 ~~10.1007/BF00648900, 1985.~~
- 8 Kumar, P. P., Broekhuizen, K., and Abbatt, J. P. D.: Organic acids as cloud condensation nuclei:  
9 Laboratory studies of highly soluble and insoluble species, Atmos. Chem. Phys., 3, 509–520, doi:  
10 10.5194/acp-3-509-2003, 2003.
- 11 Laskin, A., Moffet, R. C., Gilles, M. K., Fast, J. D., Zaveri, R. A., Wang, B., Nigge, P., and  
12 Shutthanandan, J.: Tropospheric chemistry of internally mixed sea salt and organic particles:  
13 Surprising reactivity of NaCl with weak organic acids, J. Geophys. Res., 117, D15302, doi:  
14 10.1029/2012jd017743, 2012.
- 15 Laskina, O., Young, M. A., Kleiber, P. D., and Grassian, V. H.: Infrared extinction spectroscopy and  
16 micro-Raman spectroscopy of select components of mineral dust mixed with organic compounds,  
17 J. Geophys. Res., 118, 6593-6606, doi: 10.1002/jgrd.50494, 2013.
- 18 Laskina, O., Morris, H. S., Grandquist, J. R., Qin, Z., Stone, E. A., Tivanski, A. V., and Grassian, V.  
19 H.: Size matters in the water uptake and hygroscopic growth of atmospherically relevant  
20 multicomponent aerosol particles, J. Phys. Chem. A, 119, 4489-4497, doi: 10.1021/jp510268p,  
21 2015.
- 22 Li, X., Gupta, D., Lee, J., Park, G., and Ro, C. U.: Real-time investigation of chemical compositions  
23 and hygroscopic properties of aerosols generated from NaCl and malonic acid mixture solutions  
24 using in situ Raman microspectrometry, Environ. Sci. Technol., 51, 263–270, doi:  
25 10.1021/acs.est.6b04356, 2017.
- 26 Lightstone, J. M., Onasch, T. B., Imre, D., and Oatis, S.: Deliquescence, efflorescence, and water  
27 activity in ammonium nitrate and mixed ammonium nitrate/succinic acid microparticles, J. Phys.  
28 Chem. A, 104, 9337-9346, doi: 10.1021/jp002137h, 2000.
- 29 Ling, T. Y., and Chan, C. K.: Partial crystallization and deliquescence of particles containing  
30 ammonium sulfate and dicarboxylic acids, Journal of Geophysical Research: Atmospheres, 113,

- 1 | [1-15, doi: 10.1029/2008JD009779, 2008.](https://doi.org/10.1029/2008JD009779)
- 2 | Liu, Y., Yang, Z. W., Desyaterik, Y., Gassman, P. L., Wang, H., and Laskin, A.: Hygroscopic  
3 | behavior of substrate-deposited particles studied by micro-FT-IR spectroscopy and  
4 | complementary methods of particle analysis, *Anal. Chem.*, 80, 633–642, doi: 10.1021/ac701638r,  
5 | 2008.
- 6 | Ma, Q., and He, H.: Synergistic effect in the humidifying process of atmospheric relevant calcium  
7 | nitrate, calcite and oxalic acid mixtures, *Atmos. Environ.*, 50, 97-102, doi:  
8 | 10.1016/j.atmosenv.2011.12.057, 2012.
- 9 | Ma, Q., He, H., and Liu, C.: Hygroscopic properties of oxalic acid and atmospherically relevant  
10 | oxalates, *Atmos. Environ.*, 69, 281-288, doi: 10.1016/j.atmosenv.2012.12.011, 2013a.
- 11 | Ma, Q., Ma, J., Liu, C., Lai, C., and He, H.: Laboratory study on the hygroscopic behavior of  
12 | external and internal C<sub>2</sub>-C<sub>4</sub> dicarboxylic acid-NaCl mixtures, *Environ. Sci. Technol.*, 47,  
13 | 10381-10388, doi: 10.1021/es4023267, 2013b.
- 14 | ~~Martin, S. T.: Phase transitions of aqueous atmospheric particles, *Chem. Rev.*, 100, 3403-3454, doi:~~  
15 | ~~10.1021/cr990034t, 2000.~~
- 16 | Miñambres, L., Méndez, E., Sánchez, M. N., Castaño, F., and Basterretxea, F. J.: Water uptake of  
17 | internally mixed ammonium sulfate and dicarboxylic acid particles probed by infrared  
18 | spectroscopy, *Atmos. Environ.*, 70, 108-116, doi: 10.1016/j.atmosenv.2013.01.007, 2013.
- 19 | Mikhailov, E., Vlasenko, S., Martin, S. T., Koop, T., and Pöschl, U.: Amorphous and crystalline  
20 | aerosol particles interacting with water vapor: conceptual framework and experimental evidence  
21 | for restructuring, phase transitions and kinetic limitations, *Atmos. Chem. Phys.*, 9 9491–9522,  
22 | 2009.
- 23 | Mohaček-Grošev, V., Grdadolnik, J., Stare, J., and Hadži, D.: Identification of hydrogen bond  
24 | modes in polarized Raman spectra of single crystals of  $\alpha$ -oxalic acid dihydrate, *J. Raman*  
25 | *Spectrosc.*, 40, 1605-1614, doi: 10.1002/jrs.2308, 2009.
- 26 | Murphy, D. M., Thomson, D. S., and Mahoney, M. J.: In situ measurements of organics, meteoritic  
27 | material, mercury, and other elements in aerosols at 5 to 19 kilometers, *Science*, 282, 1664-1669,  
28 | doi: 10.1126/science.282.5394.1664, 1998.
- 29 | Murphy, D. M., Cziczo, D. J., Froyd, K. D., Hudson, P. K., Matthew, B. M., Middlebrook, A. M.,  
30 | Peltier, R. E., Sullivan, A., Thomson, D. S., and Weber, R. J.: Single-particle mass spectrometry



1 of tropospheric aerosol particles, *J. Geophys. Res.*, 111, D23S32, doi: 10.1029/2006JD007340,  
2 2006.

3 Pöschl, U.: Atmospheric aerosols: composition, transformation, climate and health effects, *Angew.*  
4 *Chem. Int. Ed.*, 44, 7520-7540, 2005.

5 [Parsons, M. T., Knopf, D. A., and Bertram, A. K.: Deliquescence and crystallization of ammonium](#)  
6 [sulfate particles internally mixed with water-soluble organic compounds, \*J. Phys. Chem. A\*, 108,](#)  
7 [11600-11608, 10.1021/jp0462862, 2004.](#)

8 ~~Parsons, M. T., Riffell, J. L., and Bertram, A. K.: Crystallization of aqueous inorganic malonic acid~~  
9 ~~particles: Nucleation rates, dependence on size, and dependence on the ammonium-to-sulfate~~  
10 ~~ratio, *J. Phys. Chem. A*, 110, 8108-8115, doi: 10.1021/jp057074n, 2006.~~

11 Peng, C., Jing, B., Guo, Y. C., Zhang, Y. H., and Ge, M. F.: Hygroscopic Behavior of  
12 Multicomponent Aerosols Involving NaCl and Dicarboxylic Acids, *J. Phys. Chem. A*, 120,  
13 1029-1038, doi: 10.1021/acs.jpca.5b09373, 2016.

14 Peng, C. G., Chan, M. N., and Chan, C. K.: The hygroscopic properties of dicarboxylic and  
15 multifunctional acids: Measurements and UNIFAC predictions, *Environ. Sci. Technol.*, 35,  
16 4495-4501, doi: 10.1021/es0107531, 2001.

17 Penner, J. E., Andreae, M. O., Annegarn, H., Barrie, L., Feichter, J., Hegg, D., Jayaraman, A.,  
18 Leaitch, R., Murphy, D., Nganga, J., and Pitari, G.: Aerosols, their direct and indirect effects, in:  
19 *Climate Change 2001: The Scientific Basis. Contribution of Working Group I to the Third*  
20 *Assessment Report of the Intergovernmental Panel on Climate Change*, Cambridge University  
21 Press, 289-348, 2001.

22 [Pope, F. D., Dennis-Smith, B. J., Griffiths, P. T., Clegg, S. L., and Cox, R. A.: Studies of Single](#)  
23 [Aerosol Particles Containing Malonic Acid, Glutaric Acid, and Their Mixtures with Sodium](#)  
24 [Chloride. I. Hygroscopic Growth, \*J. Phys. Chem. A\*, 114, 5335-5341, 10.1021/jp100059k, 2010.](#)

25 Pratt, K. A., and Prather, K. A.: Aircraft measurements of vertical profiles of aerosol mixing states,  
26 *J. Geophys. Res.*, 115, D11305, doi: 10.1029/2009JD013150, 2010.

27 Prenni, A. J., DeMott, P. J., and Kreidenweis, S. M.: Water uptake of internally mixed particles  
28 containing ammonium sulfate and dicarboxylic acids, *Atmos. Environ.*, 37, 4243-4251, doi:  
29 10.1016/S1352-2310(03)00559-4, 2003.

30 [Rosenoern, T., Schlenker, J. C., and Martin, S. T.: Hygroscopic growth of multicomponent aerosol](#)

1 [particles influenced by several cycles of relative humidity, J. Phys. Chem. A, 112, 2378-2385,](#)  
2 [10.1021/jp0771825, 2008.](#)

3 Saxena, P., Hildemann, L. M., McMurry, P. H., and Seinfeld, J. H.: Organics alter hygroscopic  
4 behavior of atmospheric particles, J. Geophys. Res., 100, 18755-18770, doi: 10.1029/95JD01835,  
5 1995.

6 Schroeder, J. R., and Beyer, K. D.: Deliquescence relative humidities of organic and inorganic salts  
7 important in the atmosphere, J. Phys. Chem. A, 120, 9948–9957, doi: 10.1021/acs.jpca.6b08725,  
8 2016.

9 Shippey, T. A.: Very strong hydrogen bonding: single crystal raman studies of potassium hydrogen  
10 oxalate and sodium hydrogen oxalate monohydrate, J. Mol. Struct., 57, 1-11, doi:  
11 10.1016/0022-2860(79)80227-6, 1979.

12 Sjogren, S., Gysel, M., Weingartner, E., Baltensperger, U., Cubison, M. J., Coe, H., Zardini, A. A.,  
13 Marcolli, C., Krieger, U. K., and Peter, T.: Hygroscopic growth and water uptake kinetics of  
14 two-phase aerosol particles consisting of ammonium sulfate, adipic and humic acid mixtures, J.  
15 Aerosol Sci., 38, 157-171, doi: 10.1016/j.jaerosci.2006.11.005, 2007.

16 [Smith, J. N., Barsanti, K. C., Friedli, H. R., Ehn, M., Kulmala, M., Collins, D. R., Scheckman, J. H.,](#)  
17 [Williams, B. J., and McMurry, P. H.: Observations of ammonium salts in atmospheric nanoparticles](#)  
18 [and possible climatic implications, Proc. Nat. Acad. Sci. U. S. A, 107, 6634-6639,](#)  
19 [10.1073/pnas.0912127107, 2010.](#)

20 Spinner, E.: Raman-spectral depolarisation ratios of ions in concentrated aqueous solution. The  
21 next-to-negligible effect of highly asymmetric ion surroundings on the symmetry properties of  
22 polarisability changes during vibrations of symmetric ions. Ammonium sulphate and  
23 tetramethylammonium bromide, Spectrochim. Acta, Part A, 59, 1441-1456, doi:  
24 10.1016/s1386-1425(02)00293-7, 2003.

25 [Sullivan, R. C., and Prather, K. A.: Investigations of the diurnal cycle and mixing state of oxalic](#)  
26 [acid in individual particles in Asian aerosol outflow, Environ. Sci. Technol., 41, 8062-8069,](#)  
27 [10.1021/es071134g, 2007.](#)

28 Tang, I. N., and Munkelwitz, H. R.: Aerosol growth studies—III ammonium bisulfate aerosols in a  
29 moist atmosphere, J. Aerosol Sci., 8, 321-330, 1977.

30 Tang, I. N., and Munkelwitz, H. R.: Water activities, densities, and refractive indices of aqueous

1 sulfates and sodium nitrate droplets of atmospheric importance, *J. Geophys. Res.*, 99,  
2 18801-18808, doi: 10.1029/94JD01345, 1994a.

3 Tang, I. N., and Munkelwitz, H. R.: Aerosol phase-transformation and growth in the atmosphere, *J.*  
4 *Appl. Meteorol.*, 33, 791-796, doi: 10.1175/1520-0450(1994)033<0791:Aptagi>2.0.Co;2, 1994b.

5 Treuel, L., Sandmann, A., and Zellner, R.: Spatial separation of individual substances in effloresced  
6 crystals of ternary ammonium sulphate/dicarboxylic acid/water aerosols, *ChemPhysChem*, 12,  
7 1109-1117, doi: 10.1002/cphc.201000738, 2011.

8 ~~Villepin, J. D., and Novak, A.: Vibrational spectra of and isotope effect in hydrogen bonded~~  
9 ~~potassium hydrogen oxalate, *Spectrosc. Lett.*, 4, 1-8, doi: 10.1080/00387017108078634, 1971.~~

10 Von Schneidmesser, E., Monks, P. S., Allan, J. D., Bruhwiler, L., Forster, P., Fowler, D., Lauer, A.,  
11 Morgan, W. T., Paasonen, P., Righi, M., Sindelarova, K., and Sutton, M. A.: Chemistry and the  
12 linkages between air quality and climate change, *Chem. Rev.*, 115, 3856-3897, 2015.

13 Wang, B., and Laskin, A.: Reactions between water-soluble organic acids and nitrates in  
14 atmospheric aerosols: Recycling of nitric acid and formation of organic salts, *J. Geophys. Res.*,  
15 119, 3335-3351, doi: 10.1002/2013jd021169, 2014.

16 Wang, F., Zhang, Y. H., Zhao, L. J., Zhang, H., Cheng, H., and Shou, J. J.: Micro-Raman study on  
17 the conformation behavior of succinate in supersaturated sodium succinate aerosols, *Phys. Chem.*  
18 *Chem. Phys.*, 10, 4154-4158, doi: 10.1039/b719457a, 2008.

19 Wang, G. H., Kawamura, K., Cheng, C. L., Li, J. J., Cao, J. J., Zhang, R. J., Zhang, T., Liu, S. X.,  
20 and Zhao, Z. Z.: Molecular distribution and stable carbon isotopic composition of dicarboxylic  
21 acids, ketocarboxylic acids, and  $\alpha$ -dicarbonyls in size-resolved atmospheric particles from Xi'an  
22 City, China, *Environ. Sci. Technol.*, 46, 4783-4791, doi: 10.1021/es204322c, 2012.

23 Wang, Y., Ma, J. B., Zhou, Q., Pang, S. F., and Zhang, Y. H.: Hygroscopicity of mixed  
24 glycerol/Mg(NO<sub>3</sub>)<sub>2</sub>/water droplets affected by the interaction between magnesium ions and  
25 glycerol molecules, *J. Phys. Chem. B*, 119, 5558-5566, doi: 10.1021/acs.jpcc.5b00458, 2015.

26 Wise, M. E., Surratt, J. D., Curtis, D. B., Shilling, J. E., and Tolbert, M. A.: Hygroscopic growth of  
27 ammonium sulfate/dicarboxylic acids, *J. Geophys. Res.*, 108, 4638, doi: 10.1029/2003jd003775,  
28 2003.

29 Yang, L., and Yu, L. E.: Measurements of oxalic acid, oxalates, malonic acid, and malonates in  
30 atmospheric particulates, *Environ. Sci. Technol.*, 42, 9268-9275, 2008.

1 [Yeung, M. C., Lee, A. K. Y., and Chan, C. K.: Phase transition and hygroscopic properties of](#)  
2 [internally mixed ammonium sulfate and adipic acid \(AS-AA\) particles by optical microscopic](#)  
3 [imaging and Raman spectroscopy, Aerosol Sci. Technol., 43, 387–399, doi:](#)  
4 [10.1080/02786820802672904, 2009.](#)

5 [Yli-Juuti, T., Zardini, A. A., Eriksson, A. C., Hansen, A. M. K., Pagels, J. H., Swietlicki, E.,](#)  
6 [Svenningsson, B., Glasius, M., Worsnop, D. R., Riipinen, I., and Bilde, M.: Volatility of Organic](#)  
7 [Aerosol: Evaporation of Ammonium Sulfate/Succinic Acid Aqueous Solution Droplets, Environ.](#)  
8 [Sci. Technol., 47, 12123-12130, 10.1021/es401233c, 2013.](#)

9 Zhou, Q., Pang, S. F., Wang, Y., Ma, J. B., and Zhang, Y. H.: Confocal Raman studies of the  
10 evolution of the physical state of mixed phthalic acid/ammonium sulfate aerosol droplets and the  
11 effect of substrates, J. Phys. Chem. B, 118, 6198-6205, doi: 10.1021/jp5004598, 2014.

12

13

**Table 1.** Molecular vibration assignments of pure oxalic acid and ammonium sulfate.

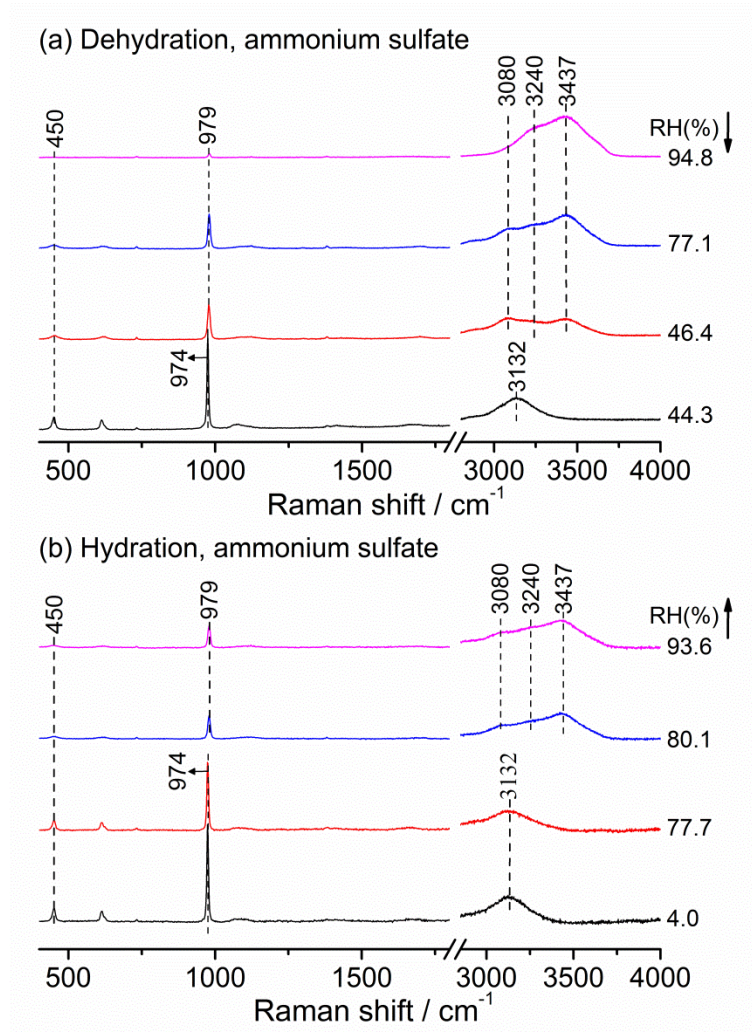
| Solid H <sub>2</sub> C <sub>2</sub> O <sub>4</sub> |            | H <sub>2</sub> C <sub>2</sub> O <sub>4</sub> | (NH <sub>4</sub> ) <sub>2</sub> SO <sub>4</sub> | Refs                                       | Assignments                  |
|--|------------|--|---|--|------------------------------|
| Anhydrous  | Dihydrate  | Droplets<br>(92.5% RH)                       | Droplets<br>(94.8% RH)                          |  |                              |
|  |            |  | 450   | (Spinner, 2003)                            | $\delta_s(\text{SO}_4^{2-})$ |
| 482  | 477        | 457  |   | (Hibben, 1935)                             | $\delta(\text{OCO})$         |
| 828  |            |  |   | (Ebisuzaki and Angel, 1981)                | $r(\text{OCO})$              |
| 845  | 855        | 845  |   | (Ebisuzaki and Angel, 1981)                | $\nu(\text{C-C})$            |
|  |            |  | 979   | (Spinner, 2003)                            | $\nu_s(\text{SO}_4^{2-})$    |
| 1477   | 1490       | 1460   |   | (Ebisuzaki and Angel, 1981)                | $\nu_s(\text{COO})$          |
|  | 1627       | 1636   |   | (Ebisuzaki and Angel, 1981)                | $\delta(\text{HOH})$         |
|  | 1689       |  |   | (Ebisuzaki and Angel, 1981)                | $\nu(\text{C=O})$            |
| 1710   | 1737       | 1750   |   | (Hibben, 1935)                             | $\nu(\text{C=O})$            |
| 2587, 2760   |            |  |   | (Mohaček-Grošev et al., 2009)              | Combinations                 |
| 2909   |            |  | 3080  | (Spinner, 2003)                            | Combinations                 |
|  |            |  | 3240  | (Spinner, 2003)                            | $\nu(\text{OH})$             |
|  | 3433, 3474 | 3433   | 3437  | (Spinner, 2003; Ebisuzaki and Angel, 1981) | $\nu(\text{OH})$             |

$\nu$ : stretching;  $\delta$ : bending;  $r$ : rocking;  $s$ : symmetric mode.

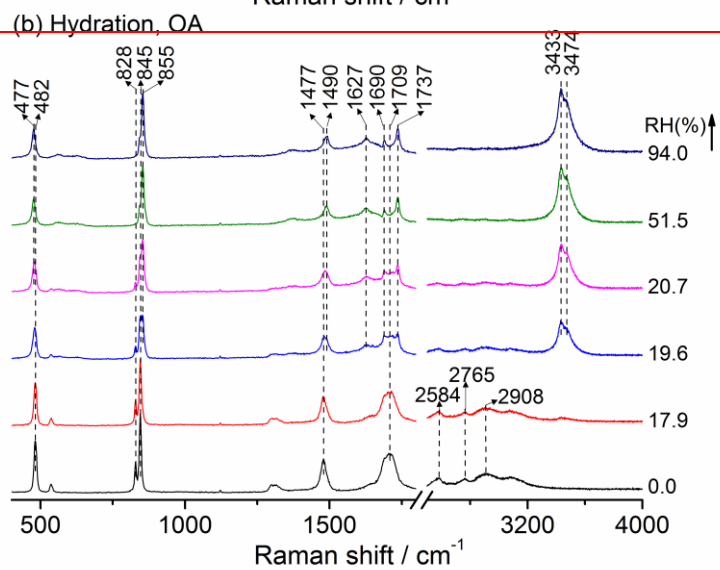
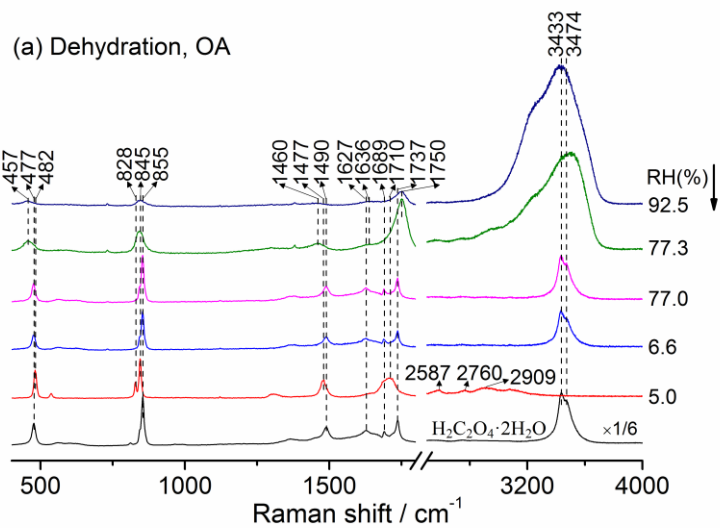
**Table 2.** Molecular vibration assignments of mixed OA/AS systems

| $\text{H}_2\text{C}_2\text{O}_4\text{-(NH}_4\text{)}_2\text{SO}_4$<br>(1:3), RH = 96.2% | $\text{H}_2\text{C}_2\text{O}_4\text{-(NH}_4\text{)}_2\text{SO}_4$<br>(1:1), RH = 96.1% | $\text{H}_2\text{C}_2\text{O}_4\text{-(NH}_4\text{)}_2\text{SO}_4$<br>(3:1), RH = 95.9% | Refs                        | Assignments                  |
|---|---|---|-----------------------------|------------------------------|
| 450   | 450   | 461   | (Spinner, 2003)             | $\delta_s(\text{SO}_4^{2-})$ |
|   | 852   | 850   | (Ebisuzaki and Angel, 1981) | $\nu(\text{C-C})$            |
| 979   | 979   | 980   | (Spinner, 2003)             | $\nu_s(\text{SO}_4^{2-})$    |
| 1049  | 1051  | 1050  | (Dawson et al., 1986)       | $\nu_s(\text{SO}_3)$         |
|   | 1382  | 1382  | (Chang and Huang, 1997)     | $\omega(\text{OCO})$         |
| 1446  | 1448  | 1460  | (Ebisuzaki and Angel, 1981) | $\nu_s(\text{COO})$          |
| 1694  |   |   | (Ebisuzaki and Angel, 1981) | $\nu(\text{C=O})$            |
| 1741  | 1751  | 1752  | (Ebisuzaki and Angel, 1981) | $\nu(\text{C=O})$            |
| 3430  | 3427  | 3426  | (Spinner, 2003)             | $\nu(\text{OH})$             |

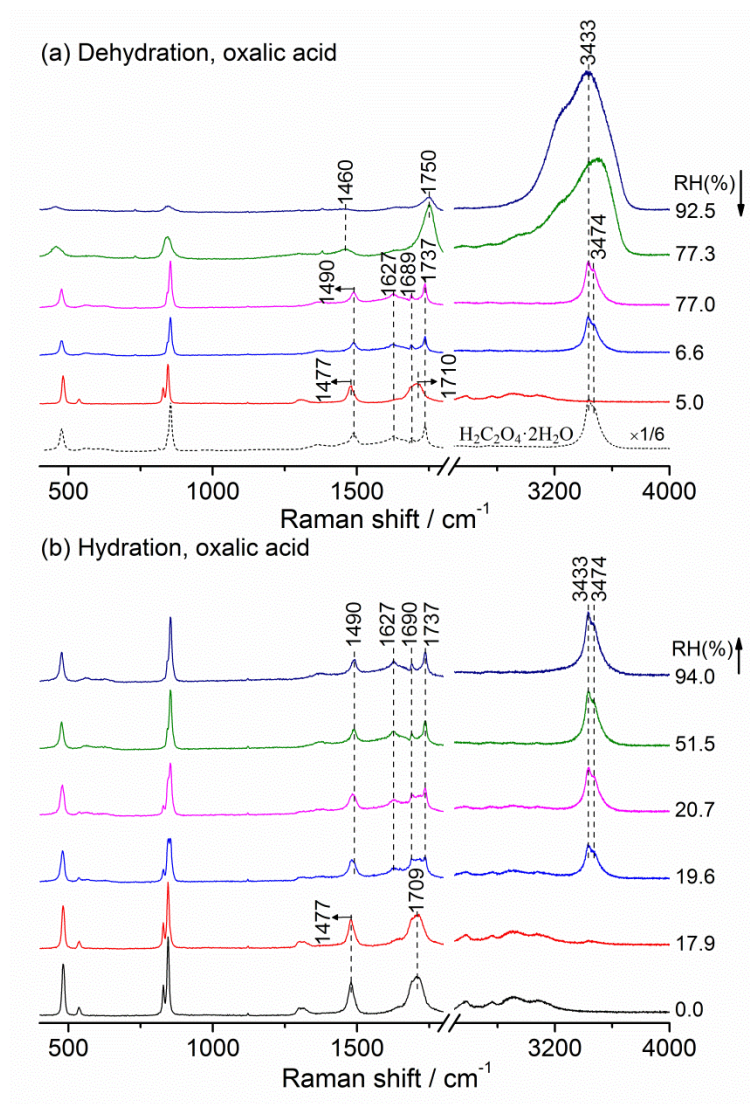
$\nu$ : stretching;  $\delta$ : bending;  $\omega$ : wagging; s: symmetric mode.



**Figure 1.** Raman spectra of ammonium sulfate droplets at various RH values during the (a) dehydration process and (b) hydration process.



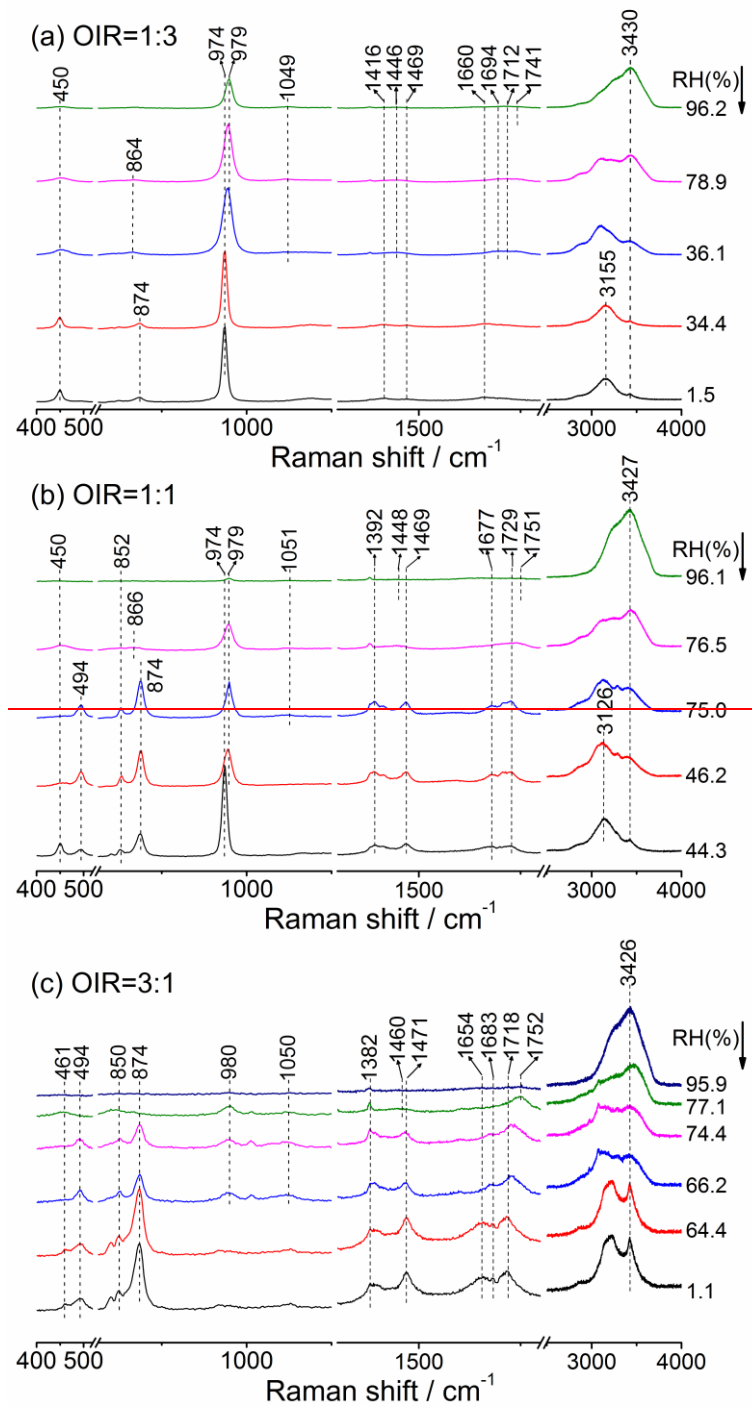


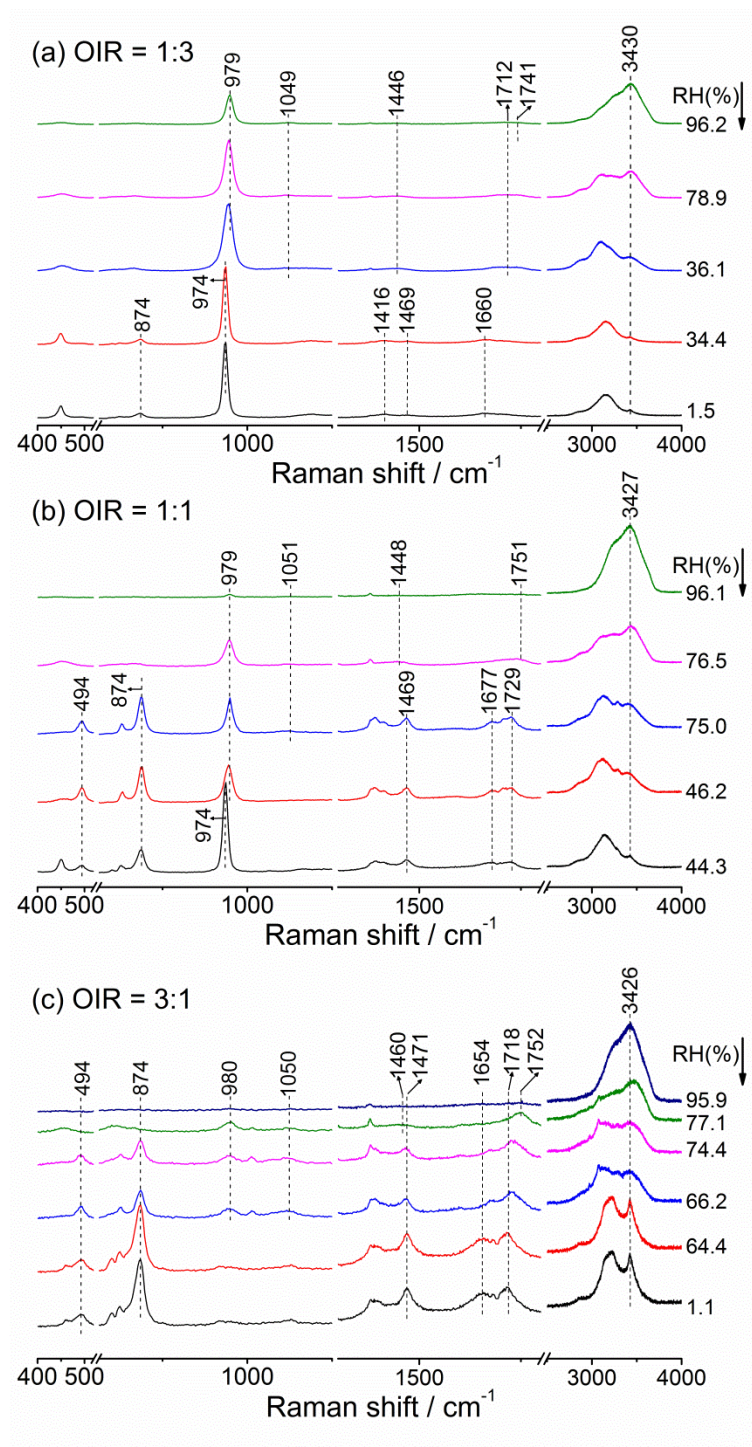


1

2 **Figure 2.** Raman spectra of oxalic acid droplets during the (a) dehydration process and (b)  
 3 hydration process. In panel (a), the black dashed line indicates the spectrum of pure  $\text{H}_2\text{C}_2\text{O}_4 \cdot 2\text{H}_2\text{O}$   
 4 particles with the peak height of  $\nu(\text{OH})$  located at  $3433 \text{ cm}^{-1}$  scaled by a factor of  $1/6$ .

5 Raman spectra of OA droplets during the (a) dehydration process and (b) hydration process. In  
 6 panel (a), the peak height of  $\nu(\text{OH})$  of  $\text{H}_2\text{C}_2\text{O}_4 \cdot 2\text{H}_2\text{O}$  particles located at  $3433 \text{ cm}^{-1}$  is scaled by a  
 7 factor of  $1/6$ .



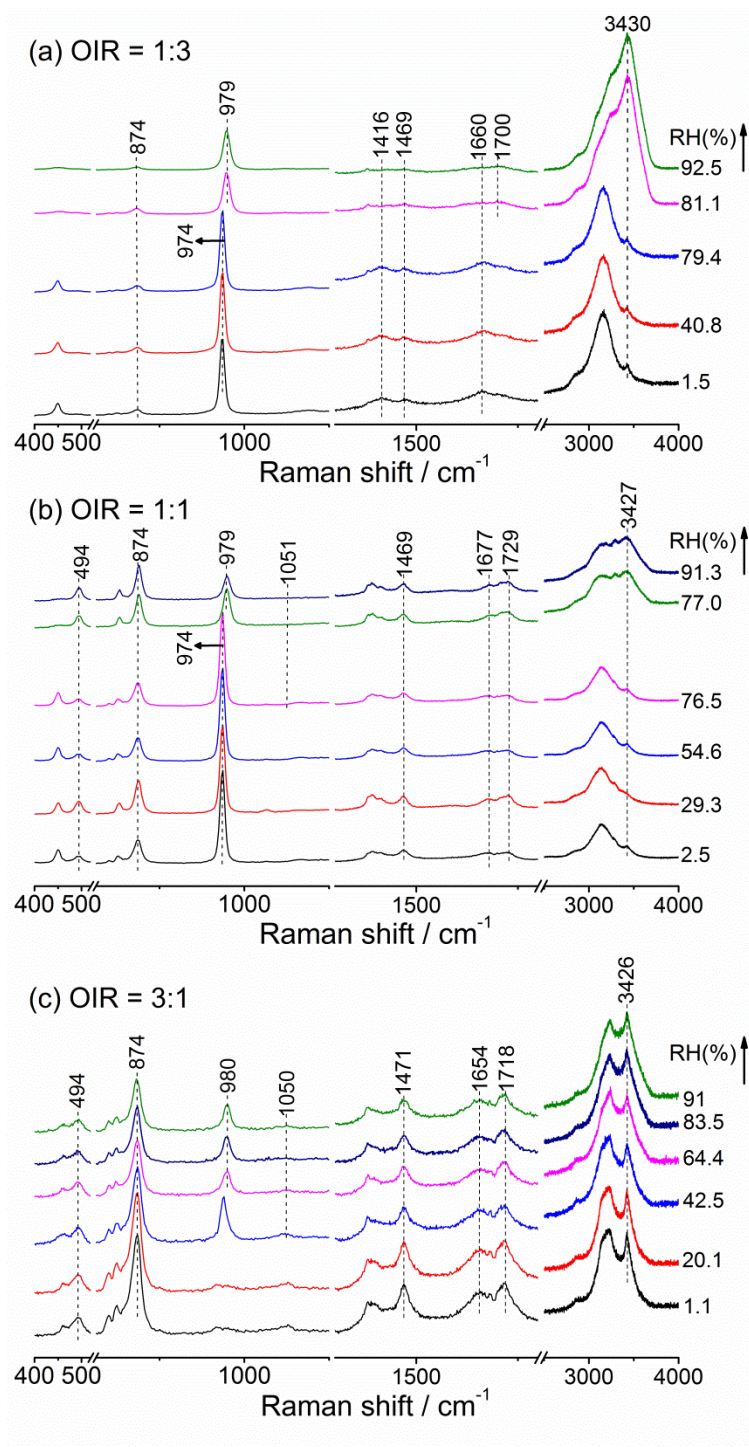


1

2 **Figure 3.** Raman spectra of mixed oxalic acid/ammonium sulfate droplets with OIRs of (a) 1:3, (b)

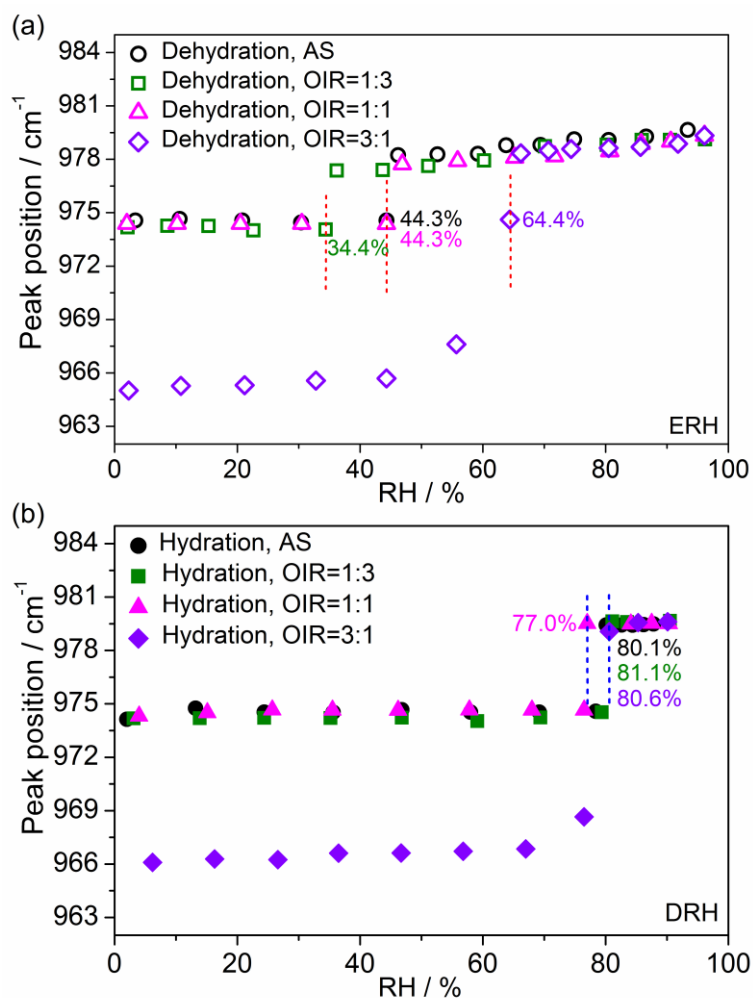
3 1:1 and (c) 3:1 at various RH values during the dehydration process.

4



1  
2  
3

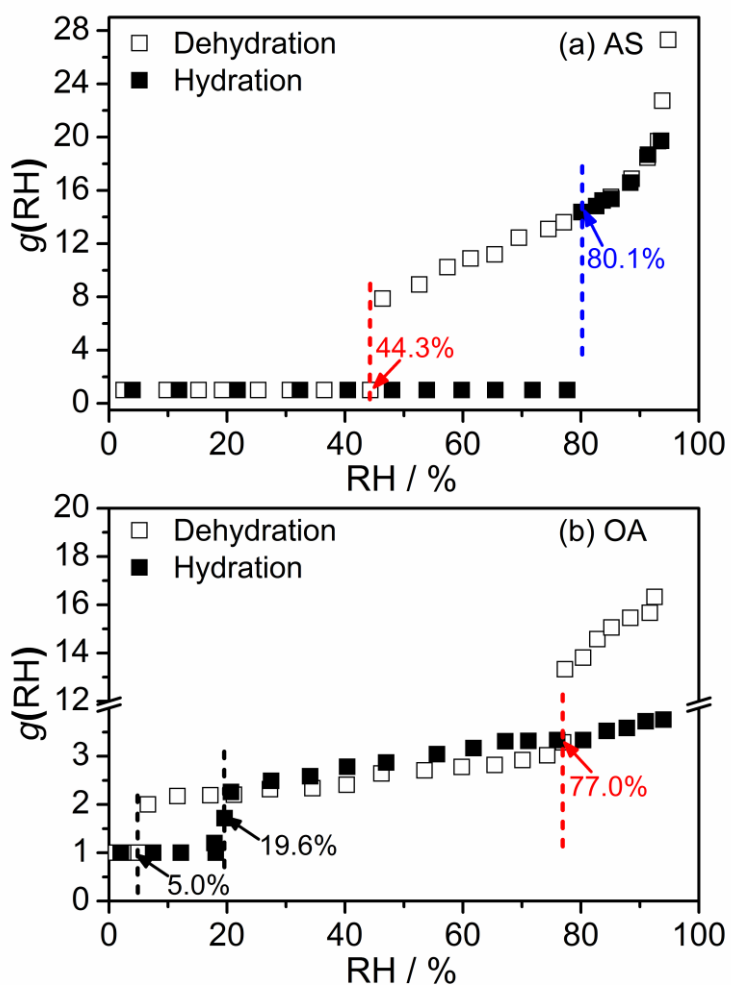
**Figure 4.** Raman spectra of mixed oxalic acid/ammonium sulfate droplets with OIRs of (a) 1:3, (b) 1:1 and (c) 3:1 at various RH values during the hydration process.



1

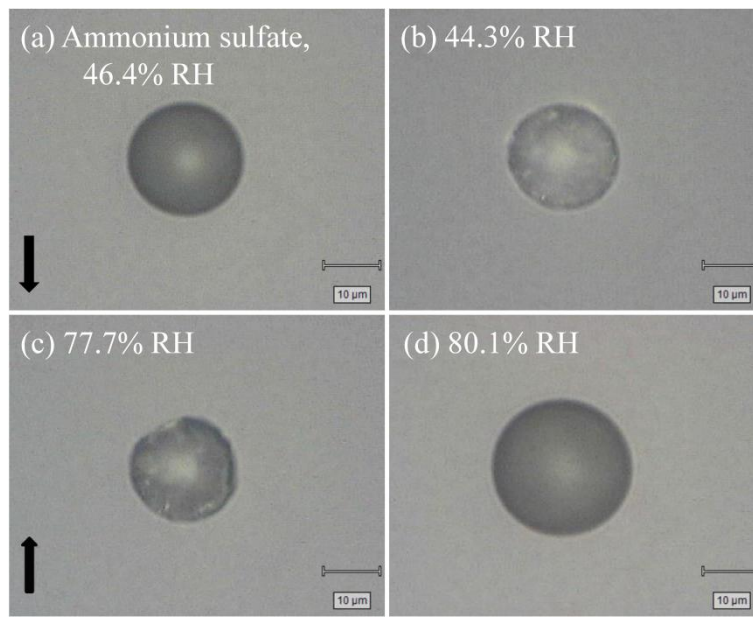
2 **Figure 5.** The peak position of the  $\nu_1\text{-SO}_4^{2-}$  peak of mixed OA/AS particles and pure AS particles at  
 3 various RHs during the (a) dehydration and (b) hydration process. The red and blue dashed lines  
 4 indicate the ERH and DRH, respectively.

5



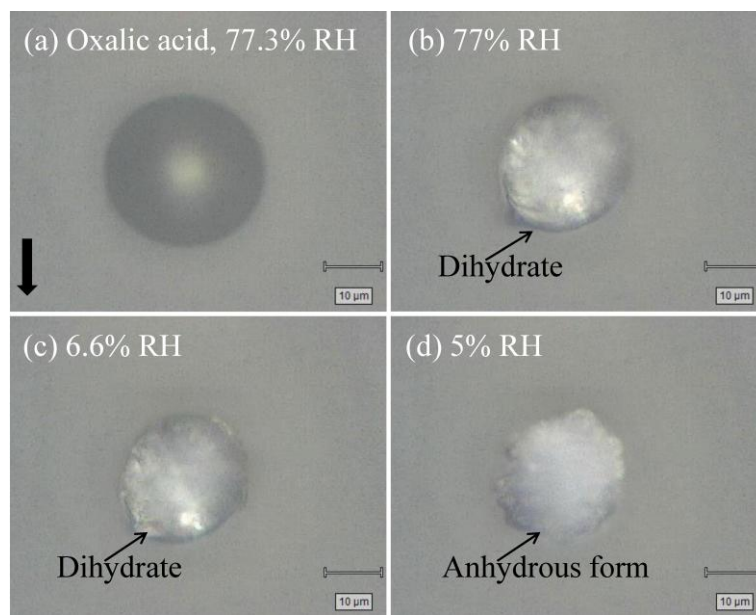
1  
2  
3  
4  
5  
6

**Figure 6.** Hygroscopicity of (a) AS and (b) OA as a function of RH by Raman spectroscopy. The red and blue dashed lines indicate the ERH and DRH, respectively. The black lines show phase transition point for the transformation between oxalic acid dihydrate and anhydrous oxalic acid.



1  
2  
3  
4  
5  
6

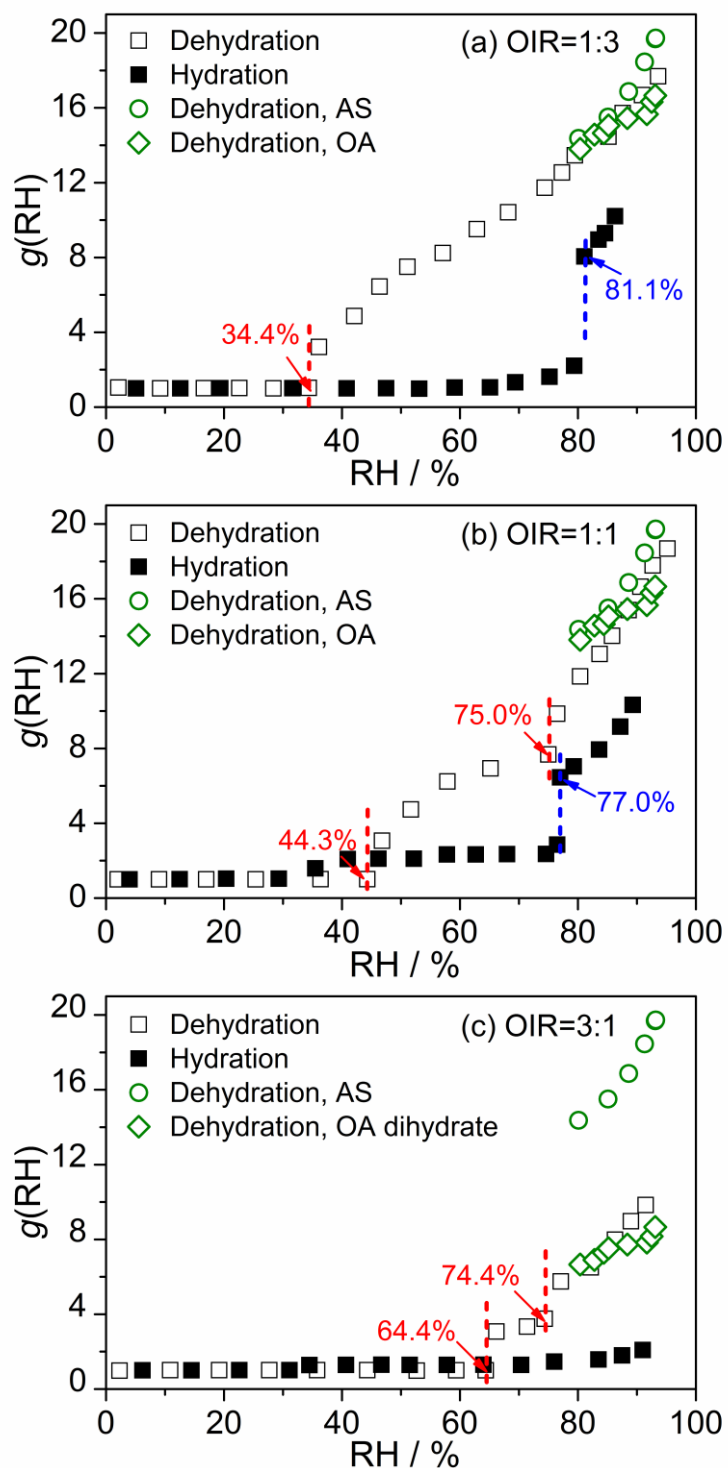
**Figure 7.** Optical micrographs of the ammonium sulfate particle at the phase change points.  
Dehydration process: (a) 46.4% RH and (b) 44.3% RH. Hydration process: (c) 77.7% RH and (d)  
80.1% RH.



1  
2  
3  
4  
5

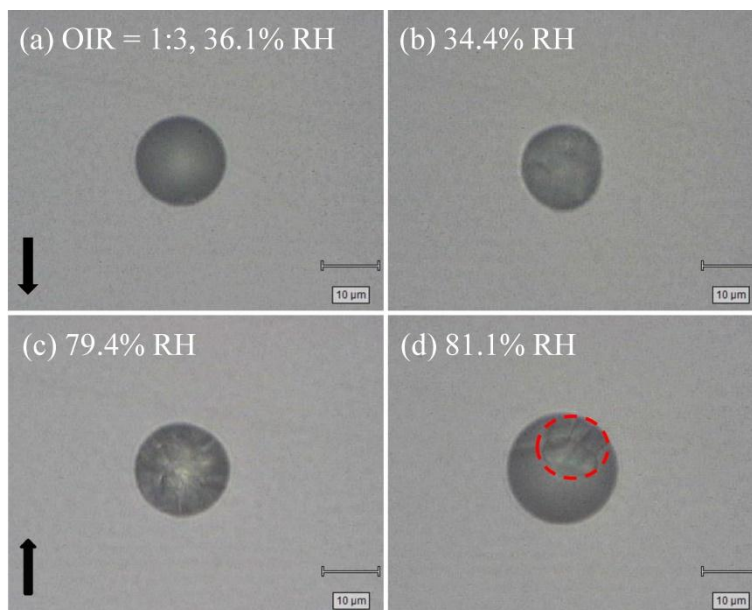
**Figure 8.** Optical micrographs of the oxalic acid particle at (a) 77.3% RH, (b) 77% RH, (c) 6.6% RH and (d) 5% RH during the dehydration process, respectively.





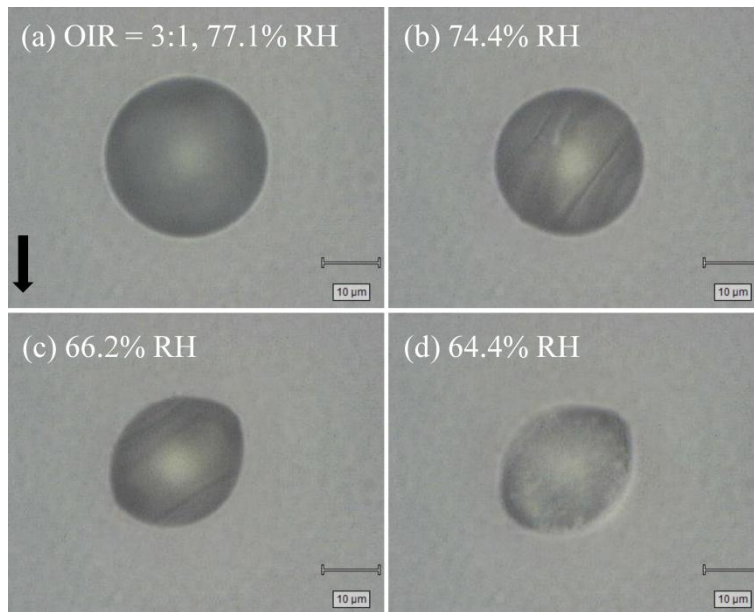
1

2 **Figure 9.** Hygroscopicity of OA/AS mixtures with OIRs of (a) 1:3, (b) 1:1 and (c) 3:1 as a function  
 3 of RH. The red and blue dashed lines indicate the ERH and DRH, respectively. In panel (a) and (b),  
 4 Raman growth factors of pure AS and OA above 80% RH in the dehydration process are also  
 5 included for comparisons. In the panel (c), Raman growth factors of pure AS and OA dihydrate  
 6 above 80% RH during the dehydration process are also given for comparisons.



1  
2  
3  
4  
5  
6  
7

**Figure 10.** Optical micrographs of the mixed oxalic acid/ammonium sulfate particle (OIR = 1:3) at phase change points. Dehydration: (a) 36.1% RH and (b) 34.4% RH. Hydration: (c) 79.4% RH and (d) 81.1% RH. In the image (d), the visual solid in aqueous phase is marked with a red dashed circle.



1  
2  
3  
4  
5  
6

**Figure 11.** Optical micrographs of the mixed oxalic acid/ammonium sulfate particle (OIR = 3:1) at (a) 77.1% RH, (b) 74.4% RH, (c) 66.2% RH and (d) 64.4% RH during the dehydration process, respectively.

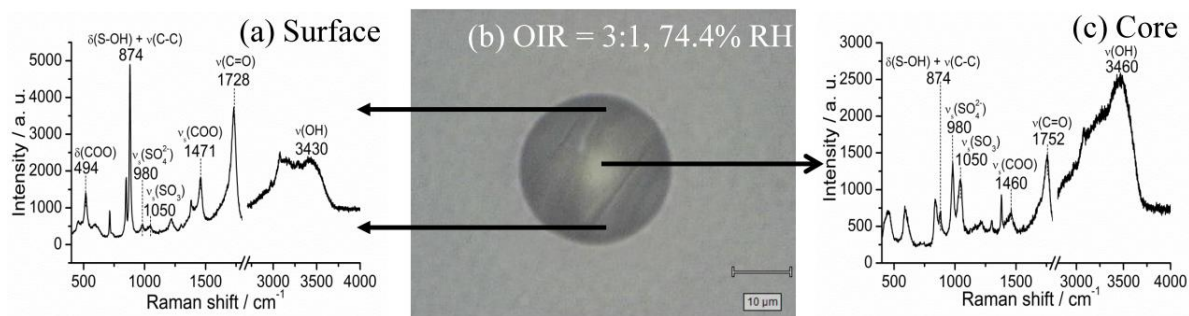
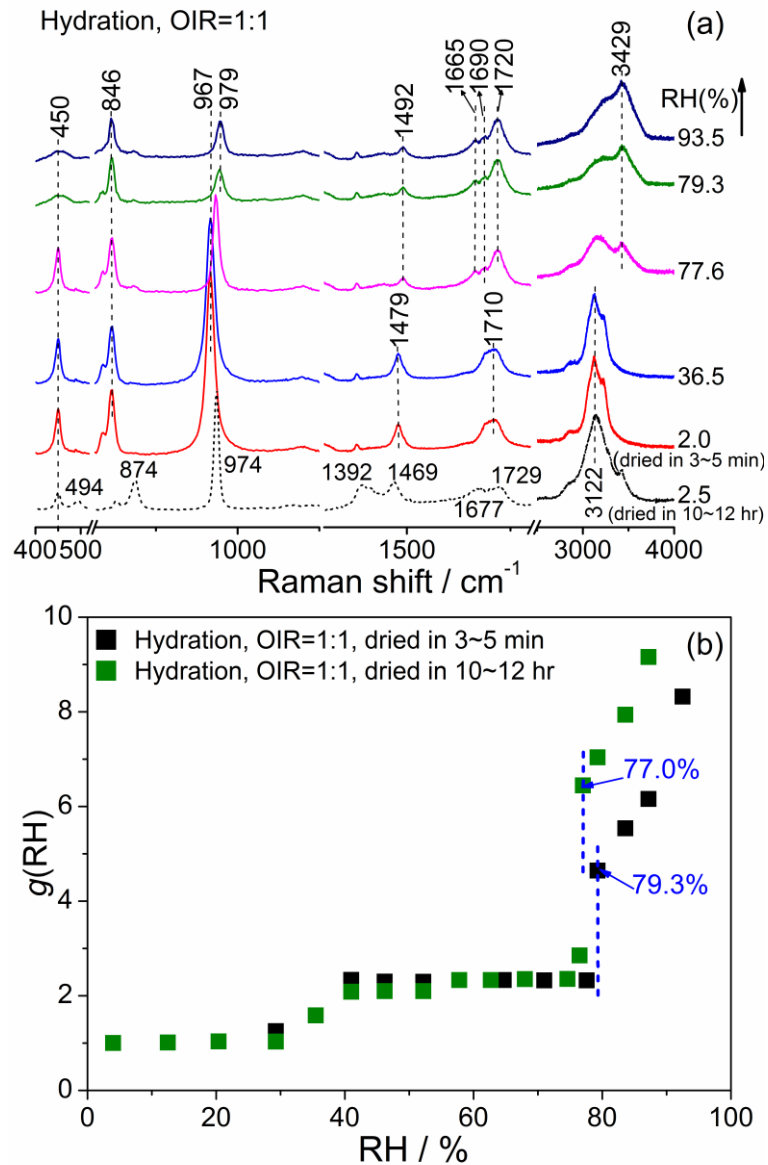


**Figure 12.** The spatial distribution of chemicals within mixed oxalic acid/ammonium sulfate (OIR = 3:1) particles at 74.4% RH upon dehydration. (a) Raman spectrum acquired on the surface showing the shell mainly consisting of  $\text{NH}_4\text{HC}_2\text{O}_4$ . (b) Optical micrograph of a partially effloresced droplet composed of oxalic acid/ammonium sulfate (OIR = 3:1) mixtures at 74.4% RH upon dehydration. (c) Raman spectrum obtained at the core of the droplet showing the liquid phase dominated by oxalic acid and ammonium sulfate.

1



2

3 **Figure 13.** (a) Raman spectra of equal molar mixed OA/AS particles after rapid drying process at  
4 various RH values upon hydration. The Raman spectrum (black short dash) at 2.5% RH obtained  
5 from the slow drying process is also given for comparisons. (b) Deliquescence curve of OA/AS  
6 mixtures with OIR of 1:1. The hygroscopic curve (olive line) of particles after slow drying process  
7 is also included for comparisons. The blue dashed lines indicate the DRH.

8